

6026

NACA-TN 2878

NATIONAL ADVISORY COMMITTEE FOR AERONAUTICS

TECHNICAL NOTE 2878

COMBINED EFFECT OF DAMPING SCREENS AND STREAM CONVERGENCE ON TURBULENCE

By Maurice Tucker

Lewis Flight Propulsion Laboratory
Cleveland, Ohio



Washington

January 1953

AFMCC
TECHNICAL LIBRARY
AFL 2811



TECH LIBRARY KAFB, NM



	Page
SUMMARY	1
INTRODUCTION	1
ANALYSIS FOR NEGLIGIBLE DECAY	3
Spectral Representation of Turbulence	3
Plane-Wave Analysis for Damping Screens	6
Plane-Wave Analysis for Contraction Section	8
Spectral Tensors for Multiple-Screen-Contraction Configurations	11
Results for Negligible Decay	13
Turbulence velocity ratios	13
One-dimensional spectra	16
Scale ratios and correlation coefficients	20
ESTIMATION OF DECAY EFFECTS	23
CONCLUDING REMARKS	26
APPENDIX A - SYMBOLS	28
APPENDIX B - TURBULENCE VELOCITY AND SCALE RATIOS	33
APPENDIX C - ONE-DIMENSIONAL SPECTRA	37
TABLE	40
FIGURES	47

NATIONAL ADVISORY COMMITTEE FOR AERONAUTICS

TECHNICAL NOTE 2878

COMBINED EFFECT OF DAMPING SCREENS AND STREAM
CONVERGENCE ON TURBULENCE

By Maurice Tucker

SUMMARY

An analysis is presented of the combined effect of a series of damping screens followed by an axisymmetric-stream convergence (or divergence) upon the mean-square fluctuation-velocity intensities, scales, correlations, and one-dimensional spectra of a turbulence field convected by a main stream. The treatment is restricted to negligible turbulence decay and linearized by postulating small fluctuation velocities and velocity gradients, and absence of viscosity except as simulated by the idealized screen action. Compressibility of the main stream is allowed for during passage through the contracting section. The density fluctuations associated with the turbulence field are regarded as negligible.

Numerical results for the statistical quantities describing the turbulence field downstream of a screen-contraction configuration are obtained for the case of upstream isotropic turbulence. The action of the damping screens and the stream convergence is to distort this initially isotropic field into a field of turbulence symmetric about the longitudinal direction with the lateral fluctuation velocities greater in magnitude than the longitudinal velocities.

An approximate method of taking into account the effects of turbulence decay upon the mean-square fluctuation velocities obtained for the case of negligible decay is presented. This method of correction together with the tabulation of fluctuation-velocity ratios over an extensive range of conditions should prove useful for engineering applications.

INTRODUCTION

The use of fine-mesh or damping screens located in a low-speed settling chamber followed by a contracting passage (entrance cone) to attain a low-turbulence test-section flow is well known from the

qualitative standpoint. Dryden and Schubauer (reference 1) have presented experimental data regarding the combined effect of screens and a contraction on the intensity of turbulence. Existing theoretical studies are confined to either the effect of the screens or of the stream contraction on turbulence. Taylor and Batchelor (reference 2) have obtained the effect of a damping screen located in a constant-area passage upon a triple Fourier integral representation of a turbulent field. The effect of a contraction upon a similar representation is analyzed in reference 3. In both references 2 and 3 initial isotropy is postulated in order to obtain numerical results.

The analyses of references 2 and 3 indicate that in the absence of decay effects (dissipation and mixing) an initially isotropic turbulence field will be distorted into a field of turbulence axisymmetric about the mean flow direction upon passage through either a damping screen or an axisymmetric contraction (contraction with all cross sections similar). An analysis of axisymmetric turbulence is given in reference 4. In conventional wind-tunnel configurations, turbulence that is initially isotropic will thus have been distorted into axisymmetric turbulence after passage through the first of the several damping screens and will remain axisymmetric while traversing the remaining screens and the following contraction. Inasmuch as the expressions obtained in reference 3 for the downstream mean-square velocity fluctuations require that the turbulence upstream of the contraction be isotropic, the results of references 2 and 3 cannot be combined in any simple manner to obtain the joint effect of screens and a contraction on turbulence that is initially isotropic.

The present analysis treats the combined effect of a series of N (symbols are defined in appendix A) identical damping screens and a downstream axisymmetric contraction upon the longitudinal and lateral turbulence velocity fluctuations, scales, correlations, and spectra of a turbulence field described by a triple Fourier integral. The configuration is shown schematically in figure 1. Although compressibility of the main stream is allowed for during passage through the contraction, the density fluctuations associated with the turbulence are regarded as negligible. The assumption of small turbulent velocity fluctuations and velocity gradients together with the postulated absence of viscosity, as in references 2 and 3, implies the absence of turbulent decay processes and linearizes the governing equations for both the screen and contraction effects.

After a discussion of the spectrum concepts used in the present analysis, the preliminary portions of the analysis which borrow from the results of references 2 and 3 are concerned with the effect of a screen and of a stream contraction upon a representative wave or Fourier component. Briefly, the screen affects only the amplitude vector of the wave; the contraction acts to change both the amplitude and wave-number

vectors. In view of the linearized analysis and the resulting absence of modulation or mutual interference between the array of plane waves making up a field of turbulence, the correlation tensor is developed from the results obtained for a typical wave. The spectral tensor is obtained as the Fourier transform of the correlation tensor. Turbulence velocity and scale ratios obtained from the spectral densities (diagonal components of the spectral tensor) are then given in tabular form for the condition of upstream isotropic turbulence. The one-dimensional spectra and the correlation-coefficient curves for a special case of upstream isotropic turbulence are also determined. An approximation for taking into account decay effects is suggested. This investigation was conducted at the NACA Lewis laboratory.

ANALYSIS FOR NEGLIGIBLE DECAY

Spectral Representation of Turbulence

Turbulence is often regarded as an assembly of eddies of randomly varying size and intensity. The present analysis treats the turbulent field as a spectrum of plane sinusoidal waves with all possible wavelengths, wave-front orientations, and phases. This superposition provides the necessary three-dimensional character to the turbulence representation. Large eddies thus are represented by waves of large wavelength (small wave number). The fluctuation-velocity components q_γ ($\gamma = 1, 2, 3$) are represented at a given instant by the triple Fourier integral

$$q_\gamma(\underline{x}) = \iiint_{-\infty}^{\infty} Q_\gamma(\underline{k}) e^{\frac{i\underline{k} \cdot \underline{x}}{}} dk_1 dk_2 dk_3 \quad (1)$$

where \underline{x} is a position vector, Q_γ a wave-amplitude vector (reference 3), and \underline{k} a wave-number vector normal to the wave front. In order that the wave amplitude vector Q_γ be finite, the field of turbulence described by equation (1) is assumed to occupy a bounded region and to vanish everywhere outside this region. For the case treated herein in which the fluctuation components are related by the incompressible-flow form of the continuity equation

$$\sum_\gamma Q_\gamma k_\gamma = 0 \quad (2)$$

the plane waves of equation (1) are transverse. In the summation of equation (2) the index γ covers the range of values 1, 2, 3.

In order to obtain the spectral tensor and, in turn, the mean-square velocity fluctuations, it will be convenient to discuss first the correlation tensor and indicate its relation with the spectral tensor. The correlation tensor $R_{\gamma\delta}(\underline{r})$ is defined as the spatial mean value of the product of the velocity component q_γ at \underline{x} and the velocity component q_δ' at $\underline{x}' = \underline{x} + \underline{r}$ as \underline{x} varies and the separation vector \underline{r} of the two points remains fixed during the averaging. If it is assumed that the field of turbulence is homogeneous and statistically steady and that the field is confined to a parallelepiped of edges $2D_1$, $2D_2$, $2D_3$ and vanishes everywhere outside, the space average is derived in reference 3 as

$$R_{\gamma\delta}(\underline{r}) = \lim_{T \rightarrow \infty} \iiint_{-\infty}^{\infty} \frac{8\pi^3}{T} Q_\gamma(\underline{k}) Q_\delta^*(\underline{k}) e^{-i\underline{k} \cdot \underline{r}} dk_1 dk_2 dk_3$$

where $Q_\delta^*(\underline{k})$ is the complex conjugate of $Q_\delta(\underline{k})$ and T is the volume $8D_1 D_2 D_3$ of the parallelepiped. The expression $\lim_{T \rightarrow \infty} \frac{8\pi^3}{T} Q_\gamma(\underline{k}) Q_\delta^*(\underline{k})$ is equivalent to the spectral tensor $\Gamma_{\gamma\delta}(\underline{k})$ defined in reference 5 as the Fourier transform of the correlation tensor $R_{\gamma\delta}(\underline{r})$

$$R_{\gamma\delta}(\underline{r}) = \iiint_{-\infty}^{\infty} \Gamma_{\gamma\delta}(\underline{k}) e^{-i\underline{k} \cdot \underline{r}} dk_1 dk_2 dk_3$$

or

$$\Gamma_{\gamma\delta}(\underline{k}) = \lim_{T \rightarrow \infty} \frac{8\pi^3}{T} Q_\gamma(\underline{k}) Q_\delta^*(\underline{k}) \quad (3)$$

A knowledge of the spectral tensor permits, as will be shown, determination of the various statistical quantities describing a turbulence field. Equation (3), which relates the spectral tensor to the wave-amplitude vector obtained for a typical Fourier component in the absence of any modulation effects, is thus basic to the present analysis.

For isotropic homogeneous turbulence fields wherein the incompressible flow form of the continuity equation is satisfied, Batchelor (reference 5) has shown that the spectral tensor can be written

$$\Gamma_{\gamma\delta}(\underline{k}) = G(\underline{k}) \left(k^2 \delta_{\gamma\delta} - \frac{k_\gamma k_\delta}{k} \right) \quad (4a)$$

where $k^2 \equiv k_1^2 + k_2^2 + k_3^2$, $\delta_{\gamma\delta} = 1$ for $\gamma = \delta$, and $\delta_{\gamma\delta} = 0$ for $\gamma \neq \delta$.

In matrix form

$$\Gamma_{\gamma\delta}(\underline{k}) = G(\underline{k}) \begin{vmatrix} k_2^2 + k_3^2 & -k_1 k_2 & -k_1 k_3 \\ -k_1 k_2 & k_1^2 + k_3^2 & -k_2 k_3 \\ -k_1 k_3 & -k_2 k_3 & k_1^2 + k_2^2 \end{vmatrix} \quad (4b)$$

It is clear from the definition of the correlation tensor that for $\underline{r} = 0$ the diagonal elements of the tensor yield the mean-square velocity fluctuations. In terms of the corresponding elements of the spectral tensor (energy spectral densities)

$$\overline{q_\gamma^2} = \iiint_{-\infty}^{\infty} \Gamma_{\gamma\gamma}(\underline{k}) dk_1 dk_2 dk_3 \quad (5)$$

The mean-square velocity fluctuations of equation (5) refer to spatial averages. Hot-wire instrumentation used to obtain these fluctuations, however, provides only time averages. Taylor (reference 6) was able to show that the spectrum of the velocity fluctuations in time is the Fourier transform of the spatial correlation function. Taylor's hypothesis (reference 7) that the main stream carries along the pattern of a weak field of turbulence unchanged past the point of measurement permits analysis of the hot-wire output signal in the form of a one-dimensional spectrum defined in the equivalent of spatial terms. The relation between the one-dimensional spectral densities F_γ and the three-dimensional spectral densities $\Gamma_{\gamma\gamma}$ is easily shown by writing equation (5) as

$$\overline{q_\gamma^2} = \int_0^\infty \left[2 \iint_{-\infty}^{\infty} \Gamma_{\gamma\gamma}(\underline{k}) dk_2 dk_3 \right] dk_1 \equiv \int_0^\infty F_\gamma(k_1) dk_1 \quad (6)$$

The various statistical quantities which characterize a field of turbulence may be obtained from the one-dimensional spectral densities as discussed in reference 8. Noting that $\frac{1}{\overline{q_\gamma^2}} \int_0^\infty F_\gamma(k_1) dk_1 = 1$, the correlation coefficients are given by

$$R_\gamma(r_1) \equiv \frac{R_{\gamma\gamma}(r_1, 0, 0)}{\overline{q_\gamma^2}} = \frac{1}{\overline{q_\gamma^2}} \int_0^\infty F_\gamma(k_1) \cos k_1 r_1 dk_1 \quad (7)$$

The Fourier transform relations yield

$$F_\gamma(k_1) = \frac{2q_\gamma^2}{\pi} \int_0^\infty R_\gamma \cos k_1 r_1 dr_1 \quad (8)$$

Two sets of characteristic lengths are customarily defined for a turbulence field. The turbulence microscales λ_γ (mean lengths weighted in favor of the small eddies which are responsible for the greater part of the viscous dissipation) are given by

$$\frac{1}{\lambda_\gamma^2} \equiv - \left(\frac{\partial^2 R_\gamma}{\partial r_1^2} \right)_{r_1=0} = \frac{1}{q_\gamma^2} \int_0^\infty k_1^2 F_\gamma(k_1) dk_1 \quad (9)$$

The turbulence scales L_γ (mean lengths representative of the average size of all the eddies) are obtained as

$$L_\gamma \equiv \int_0^\infty R_\gamma dr_1 = \frac{\pi}{2q_\gamma^2} [F_\gamma(k_1)]_{k_1=0} \quad (10)$$

This physical meaning for the scale of turbulence is only applicable when $R_\gamma > 0$ as $r_1 \rightarrow \infty$.

Plane-Wave Analysis for Damping Screens

The preceding equations indicate that the statistical quantities describing a field of turbulence may be obtained from the spectral tensor of equation (3), which is presented in terms of the plane-wave amplitude vectors $Q_\gamma(\underline{k})$. The assumptions of small turbulent velocity fluctuations and of inviscid flow, with regard to both the main stream and the turbulence field convected by the main stream, linearize the equations which govern the action of the screens and of the contraction. In the resulting absence of any modulation or interaction effects between waves, the analysis is simplified by first treating the effect of a screen and a stream convergence (or divergence) upon a representative plane wave. Superposition is then used to obtain the combination of these effects upon the complete assembly of plane waves which describes the turbulent field.

The action of a fine-mesh or damping screen on a disturbance convected by a low-speed uniform stream may be characterized by two parameters K and α . The parameter K is defined in terms of the pressure drop ΔP required to drive fluid of density ρ and velocity U through the screen

$$K \equiv \Delta P / \frac{1}{2} \rho U^2$$

The parameter α which takes into account the side force per unit area was introduced by Taylor in reference 9 and relates the angles of flow incidence ψ_1 and flow emergence ψ_2 shown in figure 2. It has been shown experimentally that the ratio $\tan \psi_2 / \tan \psi_1$ tends to a finite limit α as ψ_1 , which is usually very small, tends toward zero. For incompressible flow the continuity equation requires that the longitudinal velocity component be unchanged after passage through the screen. From kinematical considerations, at the screen the ratio of downstream to upstream lateral velocity components equals α for small values of the flow incidence angle ψ_1 .

As in reference 2 the uniform stream is regarded as incompressible and inviscid throughout the constant-area settling chamber in which the screens are located (station A to station B of fig. 1). A screen will, in general, decrease turbulent motions of larger scale than the mesh size and introduce turbulence of smaller scale. In the analysis the damping screens are assumed not to generate any wake turbulence, which implies that the screen mesh size and wire diameter are very small relative to the scale of the upstream turbulence. Far upstream of the screen, at station A, a single plane wave carried along by the main stream of velocity U in the x_1 -direction will be designated

$$\tilde{q}_\gamma^A = \tilde{Q}_\gamma^A e^{i(\underline{k} \cdot \underline{x} - k_1 Ut)}$$

Coordinate axes are fixed, with the origin located at the screen and the positive x_1 -axis pointing downstream. It is shown in reference 2 on the basis of a steady-state disturbance analysis that far downstream of the screen, at station B, the wave is transformed to

$$\tilde{q}_\gamma^B = \tilde{Q}_\gamma^B e^{i(\underline{k} \cdot \underline{x} - k_1 Ut)}$$

In order to satisfy conditions at the screen, it is necessary to postulate disturbance fields upstream and downstream of the screen which are induced by the screen. These disturbance fields attenuate, vanishing at stations A and B. Taylor and Batchelor represent these induced velocities in terms of potential flows. With the velocity components u, v, w of figure 2 designating the combined effect of the turbulent velocity fluctuations and the induced velocities, the following conditions are imposed at the screen ($x_1 = 0$)

$$(u)_{x_1=0}^B = (u)_{x_1=0}^A$$

$$(v, w)_{x_1=0}^B = \alpha(v, w)_{x_1=0}^A$$

The root-mean-square fluctuation velocities are taken to be small relative to the stream velocity so that the equations of motion can be linearized. A further condition is imposed that the local pressure drop across the screen is determined by the local longitudinal velocity and the screen pressure-drop coefficient K . The basic relations describing this idealized action of a damping screen on a representative plane wave are then obtained in reference 2 as

$$\tilde{Q}_1^B = \tilde{Q}_1^A \frac{(\beta+i)(2\alpha\beta-i\nu)}{(\beta-i)(2\beta+i\mu)} \quad (11a)$$

$$\tilde{Q}_2^B = \alpha\tilde{Q}_2^A + \frac{i\tilde{Q}_1^A k_1 k_2}{\zeta^2} \left[\frac{\beta(\alpha-1)^2 + i(\nu-\alpha\mu)}{(\beta-i)(2\beta+i\mu)} \right] \quad (11b)$$

$$\tilde{Q}_3^B = \alpha\tilde{Q}_3^A + \frac{i\tilde{Q}_1^A k_1 k_3}{\zeta^2} \left[\frac{\beta(\alpha-1)^2 + i(\nu-\alpha\mu)}{(\beta-i)(2\beta+i\mu)} \right] \quad (11c)$$

where $\zeta^2 \equiv k_2^2 + k_3^2$, $\beta^2 \equiv \frac{k_1^2}{\zeta^2}$, $\mu \equiv (1+\alpha+K)$, and $\nu \equiv (1+\alpha-\alpha K)$.

Plane-Wave Analysis for Contraction Section

The main stream will be regarded as compressible and inviscid throughout the contraction section (station B to station C of fig. 1). In the case of supersonic test-section flow, the term "contraction" is retained for convenience. As before, the turbulent field is taken to be incompressible and inviscid. The contraction section has its initial breadth and height reduced by the factors l_2 and l_3 , respectively, while the velocity $U(x_1)$ at station B is increased to $l_1 U(x_1)$ at station C. A cubical fluid volume element of edge D at station B will have been distorted into a parallelepiped of edges $l_1 D$, $l_2 D$, $l_3 D$ upon reaching station C (fig. 3). The effect of a contraction upon a turbulent field arises principally from changes in vorticity following such distortion of the fluid elements passing through the contraction.

At station B (time $t=0$) in figure 3, a particle at distance x from a corner particle of a given fluid element will at station C (time $t=t$) be at a distance \underline{x} from the corner particle. The coordinate axes are taken to move with the main stream at velocity $U(x_1)$. With the assumption of a weak turbulence field, the relative displacement of adjacent particles in a given fluid element due to turbulent

mixing is taken to be very much smaller than the displacement due to the contraction. The relation between \underline{x} and \underline{x}_γ is then simply

$$x_\gamma = l_\gamma x \quad (12)$$

With equation (12) the continuity equation for the main stream in Lagrangean form provides the relation

$$\sigma l_1 l_2 l_3 = 1 \quad (13)$$

where σ is the ratio of stream density at station C to stream density at station B. The product $l_2 l_3$ represents the ratio of tunnel cross-sectional area at station C to tunnel area at station B. The parameter l_1 represents the speed ratio referred to these stations.

The equations describing the changes in vorticity following distortion of a fluid element are, from reference 9:

$$\omega_\gamma^C = \sigma \sum_{\delta} \omega_{\delta}^B \frac{\partial x_\gamma}{\partial x_{\delta}}$$

Use of equation (12) linearizes these equations relating the upstream and downstream vorticities to

$$\omega_\gamma^C = \sigma l_\gamma \omega_\gamma^B \quad (14)$$

Upstream of the contraction at station B, a single plane wave being carried along by the main stream is designated at time $t = 0$ by

$$\tilde{q}_\gamma^B = \tilde{Q}_\gamma^B e^{ik \cdot \underline{x}} \quad (15)$$

The vorticity at station B is obtained from the curl of equation (15). A velocity distribution at station C compatible with equation (14) and satisfying continuity, equation (2), is obtained in reference 3 as

$$\tilde{q}_\gamma^C = \tilde{Q}_\gamma^C e^{ik \cdot \underline{x}}$$

where the wave-amplitude vector is

$$\tilde{Q}_\gamma^C = \frac{1}{l_\gamma} \left(\tilde{Q}_\gamma^B - \sum_{\delta} \frac{\tilde{Q}_{\delta}^B k_{\delta} k_\gamma}{l_{\delta}^2 k^2} \right) \quad (16)$$

and where the new wave-number vector \underline{k} resulting from distortion of the fluid volume element is given by

$$\underline{k} \equiv \frac{\underline{k}_1}{l_1}, \frac{\underline{k}_2}{l_2}, \frac{\underline{k}_3}{l_3} \quad (17)$$

Thus both the wave-number and wave-amplitude vectors of a plane wave are altered in going through a contraction, whereas only the amplitude vector is altered in traversing a screen.

Equations (16) and (17) describe the effect of an arbitrary contraction on a representative plane wave. For an axisymmetric contraction defined by the condition $l_2 = l_3$ (all cross sections are similar but not necessarily circular), equation (16) with the aid of equation (2) simplifies, in expanded form, to

$$\tilde{Q}_1^C = \frac{\tilde{Q}_1^B}{l_1} \frac{k_1^2 + \zeta^2}{\epsilon k_1^2 + \zeta^2} \quad (18a)$$

$$\tilde{Q}_2^C = \frac{1}{l_2} \left[\tilde{Q}_2^B + \frac{\tilde{Q}_1^B k_1 k_2 (1-\epsilon)}{\epsilon k_1^2 + \zeta^2} \right] \quad (18b)$$

$$\tilde{Q}_3^C = \frac{1}{l_2} \left[\tilde{Q}_3^B + \frac{\tilde{Q}_1^B k_1 k_3 (1-\epsilon)}{\epsilon k_1^2 + \zeta^2} \right] \quad (18c)$$

where $\epsilon \equiv l_2^2/l_1^2$. For an axisymmetric contraction, the contraction parameters l_1 , l_2 , and ϵ may be expressed in terms of the Mach numbers at stations B and C as follows:

$$\left. \begin{aligned} l_1^2 &= \left(\frac{M_C}{M_B} \right)^2 \left(\frac{5+M_B^2}{5+M_C^2} \right) \\ l_2^2 &= \left(\frac{M_B}{M_C} \right) \left(\frac{5+M_C^2}{5+M_B^2} \right)^3 \\ \epsilon &= \left(\frac{M_B}{M_C} \right)^3 \left(\frac{5+M_C^2}{5+M_B^2} \right)^4 \end{aligned} \right\} \quad (19)$$

Spectral Tensors for Multiple-Screen-Contraction Configurations

Equations (11) and (18) describe the effect of a screen and an axisymmetric contraction ($l_2=l_3$), respectively, upon the amplitude vector \tilde{Q}_γ of a single plane wave typical of the assembly of waves representing the turbulence field (equation (1)). In the Fourier integral \tilde{q}_γ corresponds to dq_γ , $\tilde{Q}_\gamma(\underline{k})$ to $Q_\gamma dk_1 dk_2 dk_3$, and $\tilde{Q}_\gamma(\underline{k})$ to $Q_\gamma dk_1 dk_2 dk_3$. Since at station C (fig. 1) the distortion resulting from the contraction transforms the wave-number vector from \underline{k} to \underline{k} and that for axisymmetry $dk_1 dk_2 dk_3 = l_1 l_2^2 dk_1 dk_2 dk_3$, equations (11) and (18) yield

$$Q_1^B = Q_1^A \frac{(\beta+i)(2\alpha\beta-i\nu)}{(\beta-i)(2\beta+i\mu)} \quad (20a)$$

$$Q_2^B = \alpha Q_2^A + \frac{i Q_1^A k_1 k_2}{\zeta^2} \left[\frac{\beta(\alpha-1)^2 + i(\nu-\alpha\mu)}{(\beta-i)(2\beta+i\mu)} \right] \quad (20b)$$

$$Q_3^B = \alpha Q_3^A + \frac{i Q_1^A k_1 k_3}{\zeta^2} \left[\frac{\beta(\alpha-1)^2 + i(\nu-\alpha\mu)}{(\beta-i)(2\beta+i\mu)} \right] \quad (20c)$$

$$Q_1^C = l_2^2 Q_1^B \left(\frac{k_1^2 + \zeta^2}{\epsilon k_1^2 + \zeta^2} \right) \quad (20d)$$

$$Q_2^C = l_1 l_2 \left[Q_2^B + \frac{Q_1^B k_1 k_2 (1-\epsilon)}{\epsilon k_1^2 + \zeta^2} \right] \quad (20e)$$

$$Q_3^C = l_1 l_2 \left[Q_3^B + \frac{Q_1^B k_1 k_3 (1-\epsilon)}{\epsilon k_1^2 + \zeta^2} \right] \quad (20f)$$

If the fluid element volume τ is taken to be a cube of edge D at station A, and hence at station B, the volume will have been distorted into a parallelepiped of edges $l_1 D$, $l_2 D$, $l_2 D$ at station C for an axisymmetric contraction. The energy spectral densities which enter directly into the calculation of turbulence fluctuation velocities are obtained from equation (3) as

$$\left[\Gamma_{\gamma\gamma}(\underline{k}) \right]^{A,B} = \lim_{D \rightarrow \infty} \frac{8\pi^3}{D^3} \left[Q_\gamma(\underline{k}) Q_\gamma^*(\underline{k}) \right]^{A,B} \quad (21a)$$

$$\left[\Gamma_{\gamma\gamma}(\underline{k}) \right]^C = \lim_{D \rightarrow \infty} \frac{8\pi^3}{l_1 l_2^2 D^3} \left[Q_\gamma(\underline{k}) Q_\gamma^*(\underline{k}) \right]^C \quad (21b)$$

With the products $Q_\gamma Q_\gamma^*$ from equations (20) formed and with the use of equations (21) and the continuity relations $Q_\gamma k_\gamma = 0$ and $Q_\gamma^* k_\gamma = 0$, the energy spectral densities may be written as:

$$\Gamma_{11}^B(\underline{k}) = \left(\frac{4\alpha^2 k_1^2 + v^2 \zeta^2}{4k_1^2 + \mu^2 \zeta^2} \right) \Gamma_{11}^A(\underline{k}) \quad (22a)$$

$$\left[\Gamma_{22}(\underline{k}) + \Gamma_{33}(\underline{k}) \right]^B = \alpha^2 \left[\Gamma_{22}(\underline{k}) + \Gamma_{33}(\underline{k}) \right]^A + \frac{(v^2 - \alpha^2 \mu^2) k_1^2}{4k_1^2 + \mu^2 \zeta^2} \Gamma_{11}^A(\underline{k}) \quad (22b)$$

$$\Gamma_{11}^C(\underline{k}) = \frac{l_2^2}{l_1} \left(\frac{k_1^2 + \zeta^2}{\epsilon k_1^2 + \zeta^2} \right)^2 \Gamma_{11}^B(\underline{k}) \quad (22c)$$

$$\left[\Gamma_{22}(\underline{k}) + \Gamma_{33}(\underline{k}) \right]^C = l_1 \left\{ \left[\Gamma_{22}(\underline{k}) + \Gamma_{33}(\underline{k}) \right]^B + \left[\frac{k_1^2 (1-\epsilon)^2 \zeta^2 - 2k_1^2 (1-\epsilon) (\epsilon k_1^2 + \zeta^2)}{(\epsilon k_1^2 + \zeta^2)^2} \right] \Gamma_{11}^B(\underline{k}) \right\} \quad (22d)$$

With the use of equations (22a) and (22c), the longitudinal energy spectral density at station C for N screens in series followed by an axisymmetric contraction may be expressed in terms of the spectral density at station A as

$$\left[\Gamma_{11}^C(\underline{k}) \right]_N = \frac{l_2^2}{l_1} \left(\frac{k_1^2 + \zeta^2}{\epsilon k_1^2 + \zeta^2} \right)^2 \left(\frac{4\alpha^2 k_1^2 + v^2 \zeta^2}{4k_1^2 + \mu^2 \zeta^2} \right)^N \left[\Gamma_{11}^A(\underline{k}) \right] \quad (23)$$

For conciseness, equations (22a), (22b), and (22d) may be written as $H_1^B = \Delta H^A$, $V_1^B = \alpha^2 V_1^A + \Sigma H^A$, and $V_1^C = l_1 V_1^B + l_1 \Omega H_1^B$, respectively. Then for N screens in series, $H_N^B = \Delta H_{N-1}^B = \Delta H^A$, $V_N^B = \alpha^2 V_{N-1}^B + \Sigma H_{N-1}^B$, and $V_N^C = l_1 V_N^B + l_1 \Omega H_N^B$. The lateral energy spectral densities at station C for N screens in series followed by an axisymmetric contraction may then be grouped as

$$\left[\Gamma_{22}^C(\underline{k}) + \Gamma_{33}^C(\underline{k}) \right]_N = \alpha^2 \left[\Gamma_{22}^C(\underline{k}) + \Gamma_{33}^C(\underline{k}) \right]_{N-1} + \frac{l_1 (v^2 - \alpha^2 \mu^2) k_1^2}{4k_1^2 + \mu^2 \zeta^2} \left[1 - \frac{(1-\epsilon) \zeta^2}{\epsilon k_1^2 + \zeta^2} \right]^2 \left[\frac{4\alpha^2 k_1^2 + v^2 \zeta^2}{4k_1^2 + \mu^2 \zeta^2} \right]^{N-1} \left[\Gamma_{11}^A(\underline{k}) \right] \quad (24)$$

Equations (23) and (24) relate the energy spectral densities downstream of a multiple-screen-axisymmetric-contraction configuration to the corresponding upstream spectral densities at station A.

Results for Negligible Decay

The solutions to be given (see appendixes B and C) will now be restricted to the case of isotropic upstream turbulence. The upstream energy spectral densities $\Gamma_{\gamma\gamma}^A(k)$ may then be obtained from equations (4).

Turbulence velocity ratios. - As shown in appendix B, the turbulence velocity ratio or ratio of mean-square fluctuation velocities downstream of a series of N identical screens followed by an axisymmetric contraction to the corresponding upstream fluctuation velocities is given for initially isotropic turbulence by

$$\frac{\overline{(q_1^2)}^C}{\overline{(q_1^2)}^A} = \frac{3a^4}{4l_1^2} \int_0^\pi \frac{\Delta^N \sin^3 \theta d\theta}{(a^2 - \cos^2 \theta)^2} \quad (25)$$

$$\frac{\overline{(q_2^2)}^C}{\overline{(q_2^2)}^A} = \frac{\overline{(q_3^2)}^C}{\overline{(q_3^2)}^A} = a^2 \frac{\overline{(q_2^2)}^C_{N-1}}{\overline{(q_2^2)}^A} + \frac{3(a^2-1)^2(v^2-\alpha^2\mu^2)}{8l_2^2} \int_0^\pi \frac{\Delta^{N-1} \sin^3 \theta \cos^2 \theta d\theta}{(4 \cos^2 \theta + \mu^2 \sin^2 \theta)(a^2 - \cos^2 \theta)^2} \quad (26)$$

$$\text{where } a^2 \equiv \frac{1}{1-\epsilon} \text{ and } \Delta \equiv \frac{4\alpha^2 \cos^2 \theta + v^2 \sin^2 \theta}{4 \cos^2 \theta + \mu^2 \sin^2 \theta}$$

A convenient approximation for equation (26) is presented later (see equation (39)).

For $N = 1$, equation (25) for the longitudinal turbulence velocity ratio integrates to

$$\frac{\overline{(q_1^2)}^C_1}{\overline{(q_1^2)}^A} = \frac{3a^4 \eta^2 v^2}{4l_1^2 \mu^2 \xi^2 (a^2 - \eta^2)^2} \left[\frac{(a^2 - \eta^2)(\xi^2 - a^2)}{a^2} + A_1 \left(\frac{1}{a} \tanh^{-1} \frac{1}{a} \right) + A_2 \left(\frac{1}{\eta} \tanh^{-1} \frac{1}{\eta} \right) \right] \quad (27)$$

where

$$\xi^2 \equiv \frac{v^2}{v^2 - 4\alpha^2}$$

$$\eta^2 \equiv \frac{\mu^2}{\mu^2 - 4}$$

$$A_1 \equiv a^2(a^2+1) + \eta^2(1-3a^2) + \frac{\xi^2[(a^2-1)^2 + (a^2+1)(\eta^2-1)]}{a^2}$$

$$A_2 \equiv 2(\eta^2-1)(\eta^2-\xi^2)$$

Equation (26) for the lateral velocity ratio (see appendix B) integrates for $N = 1$ to

$$\frac{(\overline{q_2^2})_1^C}{(\overline{q_2^2})_A^A} = \frac{a^2}{l_2^2} + \frac{v^2 \eta^2}{8l_2^2 \xi^2 \mu^2} \left[B_1 + B_2 \left(\frac{1}{a} \tanh^{-1} \frac{1}{a} \right) - B_3 \left(\frac{1}{\eta} \tanh^{-1} \frac{1}{\eta} \right) \right] \quad (28)$$

where

$$B_1 \equiv \frac{\mu^2}{2\eta^2} (\xi^2 - \eta^2)(2 - 3\eta^2) + 6(\xi^2 - \eta^2) - 2 + \frac{3(a^2 - 1)(a^2 - \xi^2)}{(a^2 - \eta^2)}$$

$$B_2 \equiv \frac{3(a^2 - 1)^2}{(a^2 - \eta^2)^2} [a^2(3\eta^2 - a^2) - \xi^2(a^2 + \eta^2)]$$

$$B_3 \equiv \frac{3(\eta^2 - 1)(\xi^2 - \eta^2)}{2} \left[(4 - \mu^2) - \frac{4(a^4 - \eta^2)}{(a^2 - \eta^2)^2} \right]$$

For the case of axisymmetric contraction with the screen absent ($a^2 = 1$, $K \rightarrow 0$), equations (27) and (28) reduce, respectively, to

$$\frac{(\overline{q_1^2})_0^C}{(\overline{q_1^2})_A^A} = \frac{(\overline{q_1^2})_0^C}{(\overline{q_1^2})_B^B} = - \frac{3a^2}{4l_1^2} \left[1 - (a^2 + 1) \left(\frac{1}{a} \tanh^{-1} \frac{1}{a} \right) \right]$$

and

$$\frac{(\overline{q_2^2})_0^C}{(\overline{q_2^2})_A^A} = \frac{(\overline{q_2^2})_0^C}{(\overline{q_2^2})_B^B} = \frac{3}{8l_2^2} \left[(a^2 + 1) - (a^2 - 1)^2 \left(\frac{1}{a} \tanh^{-1} \frac{1}{a} \right) \right]$$

which, in the present notation, are identical with the corresponding results of reference 3. Similarly, for the case of a screen and no contraction ($a^2 \rightarrow \infty$), the results of reference 2 are recovered in the form

$$\frac{\left(\frac{q_1^2}{q_2^2}\right)_1^C}{\left(\frac{q_1^2}{q_2^2}\right)_A^A} = \frac{\left(\frac{q_1^2}{q_2^2}\right)_1^B}{\left(\frac{q_1^2}{q_2^2}\right)_A^A} = \frac{v^2 \eta^2}{2 \xi^2 \mu^2} \left\{ 3\xi^2 - 1 + 3(1-\eta^2) \left[1 - (\eta^2 - \xi^2) \left(\frac{1}{\eta} \tanh^{-1} \frac{1}{\eta} \right) \right] \right\}$$

$$\frac{\left(\frac{q_2^2}{q_1^2}\right)_1^C}{\left(\frac{q_2^2}{q_1^2}\right)_A^A} = \frac{\left(\frac{q_2^2}{q_1^2}\right)_1^B}{\left(\frac{q_2^2}{q_1^2}\right)_A^A} = \alpha^2 + \frac{v^2}{8} + \frac{v^2 \eta^2}{16 \xi^2} [3(\eta^2 - \xi^2) - 2] - \frac{3v^2 \eta^2 (\eta^2 - 1)(\eta^2 - \xi^2)}{16 \xi^2} \left(\frac{1}{\eta} \tanh^{-1} \frac{1}{\eta} \right)$$

Punched-card equipment was used to obtain the turbulence-velocity ratios listed in table I. For the cases $N = 2, 3$, and 4 , the integrations required for equations (25) and (26) were performed numerically by use of Simpson's rule after changing the variable of integration from θ to x by applying the transformation $x = \cos \theta$. Intervals $\Delta x = 0.01$ were used in the range $0 \leq x \leq 0.9$; intervals $\Delta x = 0.001$ were used in the range $0.9 \leq x \leq 1.0$. In all computations the Mach number M_B upstream of the contraction was taken equal to 0.05. The turbulence velocity ratios listed in table I may be corrected for values of M_B other than 0.05 as follows: Values of the parameters l_1^2 , l_2^2 , and $a^2 \equiv \frac{1}{1-\epsilon}$ for $M_B = 0.05$ and for the desired value of M_B are obtained from equations (19). Noting that the quantities

$$l_1^2 \frac{\left(\frac{q_1^2}{q_2^2}\right)_N^C}{\left(\frac{q_1^2}{q_2^2}\right)_A^A} \text{ and } l_2^2 \frac{\left(\frac{q_2^2}{q_1^2}\right)_N^C}{\left(\frac{q_2^2}{q_1^2}\right)_A^A} \text{ depend only upon } a^2 \text{ and } K, \text{ the values}$$

of these quantities for the a^2 corresponding to the desired M_B are obtained from table I. With l_1^2 and l_2^2 known for $M_B = 0.05$ and the desired M_B , the corrected velocity ratios are obtained by simple computation. The following empirical relations (reference 1) were utilized in obtaining numerical results:

$$\alpha^2 = \left(\frac{8-K}{8+K} \right)^2 \text{ for } K \leq 1$$

$$\alpha^2 = \left(\frac{1.21}{1+K} \right) \text{ for } K > 1$$

For design purposes, the screen pressure-drop coefficient K may be estimated; according to reference 10, from the solidity ratio b , where b is the area of the holes in a unit area of screen, as

$$K \approx \frac{1 - b}{b^2}$$

For square-mesh screen with wire diameter d and mesh designation m , the solidity ratio as defined is

$$b = (1-md)^2$$

A better agreement with the screen data given in reference 1 is obtained from

$$b \approx (1-md)^{7/4}$$

The variation of the longitudinal and lateral root-mean-square velocity ratio with speed ratio η_1 for a single screen ($N=1$) upstream of the contraction is plotted in figures 4(a) and 4(b), respectively, for selected values of the screen pressure-drop coefficient K . The results for $K = 0$, which correspond to the case of stream convergence or divergence in the absence of any screen, are, of course, identical with the results of reference 3. In general, both the longitudinal and the lateral fluctuation velocities downstream of the screen-contraction configuration are reduced as the screen parameter K is increased. The somewhat anomalous trend of the longitudinal velocity ratios for values of the speed ratio less than 2 seems to reflect the variation of the auxiliary screen parameter ξ^2 which approaches zero at $K = 2.76$, becomes infinitely large in the negative sense as K increases to 5.28, and becomes infinitely large in the positive sense as K decreases to 5.28.

The losses incurred through the use of damping screens are proportional to the product NKU_A^3 , where N denotes the number of identical screens in series (multiple screens) and NK is the over-all screen pressure-drop coefficient. The velocity ratios for a multiple-screen arrangement upstream of a contraction are compared on the basis of equal screen losses in figure 5 for the particular case $NK = 6$. The advantages of using a number of screens in series to attain a given over-all coefficient NK are obvious. An examination of table I indicates that the use of multiple screens to attenuate the downstream fluctuation velocities becomes more effective as the over-all coefficient NK is increased. The screen losses can be reduced by decreasing the settling-chamber stream velocity U_A . Low-turbulence wind tunnels are generally characterized by their many damping screens and large-cross-sectional-area settling chambers.

One-dimensional spectra. - In accordance with equation (6), the one-dimensional spectra at stations A and B are given by

$$F_{\gamma}^A = 2 \iint_{-\infty}^{\infty} \Gamma_{\gamma\gamma}^A(k) dk_2 dk_3 \quad (29)$$

and

$$F_{\gamma}^C = 2 \iint_{-\infty}^{\infty} \Gamma_{\gamma\gamma}^C(k) dk_2 dk_3$$

As pointed out in reference 3, a comparison of the upstream and downstream spectra on the basis of the upstream longitudinal wave number k_1 is equivalent to a comparison of the time spectra indicated by fixed hot-wire probes located at the corresponding stations. Defining the downstream spectra $F_{\gamma}^C(k_1) \equiv l^{-1} F_{\gamma}^C$ such that

$\int_0^{\infty} F_{\gamma}^C(k_1) dk_1 = \int_0^{\infty} F_{\gamma}^C(k_1) dk_1$, the one-dimensional spectra at station C are given by

$$\left[F_{\gamma}^C(k_1) \right]_N = \frac{2}{l_1 l_2^2} \iint_{-\infty}^{\infty} \left[\Gamma_{\gamma\gamma}^C \left(\frac{k_1}{l_1}, \frac{k_2}{l_2}, \frac{k_3}{l_2} \right) \right]_N dk_2 dk_3 \quad (30)$$

Evaluation of equations (29) and (30) requires that the amplitude function $G(k)$ in equation (4) be specified. Compatible with the empirical relation for isotropic turbulence obtained in reference 8, this function is taken to be

$$G(k) = \frac{H}{(k_1^2 + n^2 + \zeta^2)^3} \quad (31)$$

where the constants n and H are defined as $n \equiv \frac{1}{(L_1)^A}$ and $H \equiv \frac{2n}{\pi^2} \left(\frac{q_1}{2} \right)^A$.

As shown in appendix C, the one-dimensional spectra obtained from equations (4) and (31) may be expressed in terms of a dimensionless wave number k_1/n as incorporated in the following parameters:

$$\left. \begin{aligned} s &\equiv 1 + k_1^2/n^2 \\ f &\equiv s/\eta^2 + 4/\mu^2 \\ g &\equiv s/\zeta^2 + 4\alpha^2/v^2 \\ h &\equiv \frac{1 - a^2 - s^2}{a^2} \end{aligned} \right\} \quad (32)$$

Thus the upstream one-dimensional spectra for this special case of isotropic turbulence are, in dimensionless form,

$$\frac{F_1^A(k_1/n)}{F_1^A(0)} = \frac{1}{s} \quad (33)$$

$$\frac{F_2^A(k_1/n)}{F_2^A(0)} = \frac{3s-2}{s^2} \quad (34)$$

Also, the longitudinal one-dimensional spectrum downstream of a single-screen-axisymmetric-contraction configuration may be written (see appendix C) in dimensionless form as

$$\frac{F_1^C(k_1/n)}{F_1^A(0)} = \frac{2v^2}{l_1^2 \mu^2} \left[C_1 + C_2 \log_e \frac{s+h}{s} + C_3 \log_e \frac{4(s-1)}{\mu^2 s} \right] \quad (35)$$

where

$$C_1 \equiv \frac{1}{h^3} \left\{ \frac{g(2f-h)}{f^2} + \frac{gh}{2fs} + \frac{h(1+2g)}{f} + \frac{(1+h)^2 \mu^2}{v^2} \left[\frac{a^2(v^2 - 4\alpha^2) - v^2}{a^2(\mu^2 - 4) - \mu^2} \right] \right\}$$

$$C_2 \equiv \frac{\mu^2}{h^2 [a^2(\mu^2 - 4) - \mu^2]} \left\{ \frac{3sg}{h^2} + \frac{g(s+2)}{h} + 1 - h - \frac{\mu^2(s+h)(g+h)}{h[a^2(\mu^2 - 4) - \mu^2]} \right\}$$

$$C_3 \equiv \frac{(s-f)(f-g)(\mu^2 - 4)^2 a^4}{f^3 [a^2(\mu^2 - 4) - \mu^2]^2}$$

The corresponding lateral one-dimensional spectrum is

$$\frac{F_2^C(k_1/n)}{F_2^A(0)} = \frac{2(s-1)}{l_2^2} \left[E_1 + E_2 \log_e \frac{s+h}{s} + E_3 \log_e \frac{4(s-1)}{\mu^2 s} \right] \quad (36)$$

where

$$\begin{aligned}
 E_1 &\equiv \frac{\alpha^2(3s-2)}{2s^2(s-1)} + \frac{(v^2 - \alpha^2\mu^2)(2s-f)}{2\mu^2f^2s} + \frac{2v^2}{a^2fh} \left[\frac{g(h-f)}{fh} - \frac{g}{2s} - 1 \right] \\
 &\quad \frac{-v^2}{2a^4\mu^2h} \left[2(s+h) \left\{ \frac{f(g+h)-g(h-f)}{f^2h^2} + \frac{\mu^2[a^2(v^2-4\alpha^2) - v^2]}{v^2h^2[a^2(\mu^2-4) - \mu^2]} \right\} + \frac{2h(g-f)-fg}{f^2h} \right] \\
 E_2 &\equiv \frac{(s+h)[a^2(v^2-4\alpha^2) - v^2]}{a^2h^4[a^2(\mu^2-4) - \mu^2]} \left\{ 2h + \frac{3s+h}{a^2} + \frac{4(a^2-1)(v^2-\alpha^2\mu^2)h}{[a^2(\mu^2-4) - \mu^2][a^2(v^2-4\alpha^2) - v^2]} \right\} \\
 E_3 &\equiv \frac{4(s-1)(v^2-\alpha^2\mu^2)}{\mu^4f^3} \left[1 + \frac{4}{a^2(\mu^2-4) - \mu^2} \right]^2
 \end{aligned}$$

The one-dimensional spectra given by equations (33) to (36) are applicable when the amplitude function $G(k)$ has the particular form of equation (31). Although these spectra are not expected to be valid for the very high wave numbers because of the neglect of viscosity, various experiments on isotropic turbulence have indicated that equations (33) and (34) provide a very good approximation to that portion of the actual isotropic spectrum containing the largest part of the turbulent energy. Equations (35) and (36) should furnish a similar approximation for axisymmetric turbulence. The restrictions given for equations (33) to (36) do not apply to the expressions for turbulence velocity ratios, equations (25) and (26), for which there is no need to particularize the spectrum amplitude function $G(k)$.

The downstream longitudinal and lateral one-dimensional spectra, equations (35) and (36), are compared with the corresponding upstream isotropic spectra, equations (33) and (34), in figures 6(a) and 6(b), respectively, for the following typical case: $M_B = 0.05$, $M_C = 2.0$, $K = 2$, $N = 1$. The case $K = 0$, as obtained in reference 3, has also been included for comparison. The scaling factors indicated by equations (B5) and (B6) of appendix B have been incorporated in the downstream spectral ordinates so that the zero-wave-number intercept gives the turbulence scale ratio (appendix B).

The distortion in shape of the longitudinal spectrum noted in reference 3 as a consequence of the stream convergence is accentuated (fig. 6(a)) by the presence of a damping screen upstream of the contraction. This distortion is accompanied by a reduction in the ordinate values by the factors $(\overline{q_1^2})^C / (\overline{q_1^2})^A$ and $(\overline{q_1^2})^C / (\overline{q_1^2})^B$ for $K = 2$ and $K = 0$, respectively. The downstream lateral spectrum ordinates

(fig. 6(b)) are increased by the factors $(\overline{q_2^2})^C / (\overline{q_2^2})^A$ and $(\overline{q_2^2})^C / (\overline{q_2^2})^B$ for $K = 2$ and $K = 0$, respectively. The distortion in shape is relatively slight compared with the distortion noted for the longitudinal spectrum.

As may be seen from equations (33) and (34) for the upstream isotropic spectra, the longitudinal and lateral spectral ordinates have maximum values at $k_1/n = 0$ and $k_1/n = 1/\sqrt{3}$, respectively. The situation is reversed for the downstream spectra. Here the lateral spectral ordinates have maximum values at $k_1/n = 0$ and the longitudinal spectral ordinates at $k_1/n \approx 1.4$. Occurrence of a peak in the spectrum curve at some wave number other than zero is an indication that the correlation coefficient may take on negative values.¹

Scale ratios and correlation coefficients. - For the scales of turbulence defined by equation (10), the longitudinal and lateral turbulence scale ratios (ratios of downstream to corresponding upstream scales) for a screen-contraction configuration are obtained in appendix B as

$$\frac{(L_1)_N^C}{(L_1)_A^A} = \left(\frac{v^2}{\mu^2}\right)^N \left[l_1^2 \frac{(\overline{q_1^2})_N^C}{(\overline{q_1^2})^A} \right]^{-1} \quad (37)$$

$$\frac{(L_2)_N^C}{(L_2)_A^A} = \alpha^{2N} \left[l_2^2 \frac{(\overline{q_2^2})_N^C}{(\overline{q_2^2})^A} \right]^{-1} \quad (38)$$

The scale ratios obtained from equations (37) and (38) which do not require that the amplitude function $G(k)$ of equation (31) be specified are listed in table I for the case of isotropic turbulence at station A. Typical results are plotted in figure 7.

The lateral scale ratio (see fig. 7(a)) approaches a constant value of approximately $4/3$ for values of the speed ratio l_1 greater than 3. Measurements of the lateral correlation curve at a speed ratio near unity which are reported in reference 11 indicate that the lateral scale is substantially unchanged by damping screens. This is in qualitative agreement with the present result which indicates that for l_1 slightly greater than unity the downstream lateral scale will not exceed the

¹For example, when $F_\gamma(k_1) = k_1^{P-1} e^{-k_1/n}$, the correlation coefficient is obtained by using equation (7) as

$\left[\left(\frac{1}{n}\right)^2 + r_1^2\right]^{-P/2} \Gamma(P) \cos(P \tan^{-1} nr_1)$ where Γ designates the gamma function. For $P = 1$, $R_\gamma(r_1)$ is always positive; for $P > 1$, $R_\gamma(r_1)$ will take on negative values for particular values of r_1 .

corresponding upstream scale by more than about 20 percent. Taking the lateral scale ratio equal to $4/3$ leads to the following convenient approximation for the lateral turbulence velocity ratio from equation (38):

$$\frac{\left(\frac{q_2^2}{2}\right)^C_N}{\left(\frac{q_2^2}{2}\right)^A} \approx \frac{3\alpha^{2N}}{4l_2^2} \quad (39)$$

For a given value of the screen pressure-drop coefficient NK , the longitudinal scale ratio (see fig. 7(b)) decreases with increasing speed ratio l_1 to a minimum value at $l_1 = 27.4$ (corresponding to $M_B = 0.05$, $M_C = \sqrt{3}$) where the contraction parameter α^2 has its minimum value. As shown in table I, the longitudinal scale ratio attains a zero value when the screen parameter $v^2 = 0$ ($K \approx 2.76$). This and the occurrence of maximums in the downstream longitudinal spectrum curves at nonzero wave numbers suggest that the downstream longitudinal correlation coefficients are negative for extensive ranges of the separation distance r_1 . Under these conditions interpretation of the conventionally defined scales as lengths characteristic of the average size of the turbulence eddies is open to question, and consideration of the correlation coefficient curves is advisable.

The correlation coefficients at station A for isotropic turbulence with the spectrum amplitude function $G(k)$ given by equation (31) are obtained from equation (7) as

$$R_1^A = e^{-r_1 n} \quad (40)$$

$$R_2^A = \left(1 - \frac{r_1 n}{2}\right) e^{-r_1 n} \quad (41)$$

The contour integrations used to obtain equations (40) and (41) are not valid when $r_1 = 0$; hence the microscales λ_γ are evaluated from the integral relation of equation (9). Such evaluations indicate that $\lambda_1^A = \lambda_2^A = 0$, which is to be expected in view of the neglect of viscosity effects in the analysis. The longitudinal correlation coefficient curve of equation (40) is plotted in figure 8(a) and is always positive; the lateral correlation coefficient curve of equation (41) plotted in figure 8(b) reaches its zero value at $r_1 n = 2$ ($r_1 = 2L_1^A$) and its minimum value at $r_1 n = 3$ ($r_1 = 3L_1^A$).

The downstream correlation coefficient curves (at station C) have been obtained numerically for the case $N = 1$ from the following rearrangement of equations (7):

$$R_1^C(r_1n) = \frac{2}{\pi} \int_0^\infty \frac{F_1^C\left(\frac{k_1}{n}\right)}{F_1^A(0)} \frac{\left(\frac{q_1^2}{r_1^2}\right)_1^C}{\left(\frac{q_1^2}{r_1^2}\right)^A} \cos k_1 r_1 d\left(\frac{k_1}{n}\right) \quad (42)$$

$$R_2^C(r_1n) = \frac{1}{\pi} \int_0^\infty \frac{F_2^C\left(\frac{k_1}{n}\right)}{F_2^A(0)} \frac{\left(\frac{q_2^2}{r_1^2}\right)_1^C}{\left(\frac{q_2^2}{r_1^2}\right)^A} \cos k_1 r_1 d\left(\frac{k_1}{n}\right) \quad (43)$$

In evaluating equations (42) and (43), values of the integrand were obtained for k_1/n ranging from 0 to 50; and for k_1/n greater than 50, in view of the asymptotic behavior of the functions $\frac{F_Y^C(k_1/n)}{F_Y^A(0)} \frac{(\frac{q_Y^2}{r_1^2})_1^C}{(\frac{q_Y^2}{r_1^2})^A}$, the integrand was approximated as $\frac{\cos k_1 r_1}{(k_1/n)^2}$. Typical downstream longitudinal and lateral correlation coefficient curves (for the case $M_B = 0.05$, $M_C = 2.00$, $K = 2$, $N = 1$) are also plotted in figures 8(a) and 8(b), respectively, to indicate the changes resulting from passage of initially isotropic turbulence through a given screen and contraction. Although the downstream lateral correlation coefficient is shown in figure 8(b) to reach slightly negative values, it is believed that these are the result of unavoidable "round-off" errors in computation of the Fourier transforms and that the coefficient is actually always positive, consistent with the corresponding spectrum curve of figure 6(b), which has its maximum value at zero wave number.

The correlation between simultaneous fluctuation velocities at two points a distance r_1 apart will decrease more rapidly with increasing values of r_1 when the eddies comprising the turbulent field are small than when the eddies are large. Figure 8(a) thus indicates that the longitudinal scale of an initially isotropic field of turbulence is decreased by passage through the particular screen-contraction configuration chosen. Figure 8(b) indicates that the corresponding lateral scale is increased.

In view of the negative values attained by the downstream longitudinal correlation coefficient, no physical meaning can be assigned to the longitudinal scale ratio defined in the conventional manner by equation (10). For example, the longitudinal scale ratio reaches a zero value even though the longitudinal turbulence velocity ratios are finite when the screen pressure-drop coefficient NK has the value 2.76. The negative values attained by the upstream lateral correlation coefficient do not present a similar anomaly because of the relation between the longitudinal and lateral scales in the case of isotropic turbulence, namely, $L_1^A = 2L_2^A$.

The difficulty is removed if an effective longitudinal scale L_1' is defined as the positive area under the corresponding correlation curve. Effective longitudinal scale ratios are plotted in figure 9 and show a qualitative similarity with the conventional ratios shown in figure 7(b). For a given value of the screen pressure-drop coefficient NK , the effective scale ratio decreases with increasing speed ratio l_1 to a minimum value at $l_1 = 27.4$ for which the contraction parameter a^2 has its minimum value. For a given contraction the effective scale ratio reaches its minimum value when $NK \approx 2.76$.

ESTIMATION OF DECAY EFFECTS

In view of the assumptions of inviscid flow and small fluctuation velocities relative to the main stream, the preceding analysis is strictly applicable only in the absence of the turbulent decay processes (viscous dissipation and turbulent mixing). For many wind-tunnel configurations, effects of decay upon turbulence are of the same order of magnitude as the screen-contraction effects. Correction of the theoretical turbulence velocity ratios may therefore prove necessary for practical applications of the theory.

Selection of the appropriate decay correction presents certain difficulties inasmuch as there is a lack of experimental investigations of axisymmetric turbulence decay. Some guidance may be obtained from the theoretical studies of Batchelor (reference 4) and Chandrasekhar (reference 12) on axisymmetric turbulence. The time rates of change of the mean-square velocity components are, in the notation of reference 4:

$$\frac{d}{dt} (\overline{u_1^2}) = -4m_0 + 2v(-10a - 2b - 2c - 14d)$$

$$\frac{d}{dt} (\overline{u_2^2}) = 2m_0 + 2v(-10a + b - 3d)$$

In these equations and in equations (44) and (45), the symbol v represents the kinematic viscosity coefficient. The corresponding expression for the mean-square resultant velocity is

$$\frac{d}{dt} (\overline{u_1^2 + 2u_2^2}) = -2v(30a + 2c + 20d) \quad (44)$$

For isotropic turbulence, $c = d = 0$ and equation (44) becomes

$$\frac{d}{dt} (\overline{u_1^2 + 2u_2^2}) = \frac{d}{dt} (3\overline{u_1^2}) = -2v(30a) \quad (45)$$

The velocity components $\overline{u_1^2}$ and $\overline{u_2^2}$ of reference 4 are identical with $\overline{q_1^2}$ and $\overline{q_2^2}$ in the present notation. The quantities a , b , c , and d in appropriate groupings represent the coefficients in the series expansions in r_1 for the longitudinal and lateral velocity correlation coefficients. The quantity m_0 depends on the two-point velocity-pressure correlation which tends to zero as isotropy is approached. For the decay of isotropic turbulence in a constant-area channel during the initial period wherein both inertia and viscous forces are of importance, equation (45) leads to the semiempirical relation (reference 13)

$$\frac{1}{3} \left[\frac{\overline{q_1^2}}{(\overline{q_1^2})^A} + 2 \frac{\overline{q_2^2}}{(\overline{q_2^2})^A} \right] = \left\{ 1 + \frac{0.58t(l_1)}{L_2^A} \left[(\overline{q_1^2})^A \right]^{1/2} \right\}^{-1} \equiv J \quad (46)$$

where $\overline{q_1^2}$ and $\overline{q_2^2}$ represent the mean-square velocity components at any station downstream of the reference station A and $t(l_1)$ represents the appropriate decay time.

The absence of the velocity-pressure correlation term m_0 in both equations (44) and (45) suggests that, provided the quantity $(2c + 20d)$ is much smaller than the quantity $30a$, equation (46) may yield a satisfactory approximation for the decay of the mean-square resultant turbulent velocity in axisymmetric turbulence. The data of references 1 and 14 tend to support such an approximation. The assumption that the effects of the screen-contraction combination and the decay upon the turbulent velocity ratios proceed independently (see reference 3) leads to the relation

$$\frac{1}{3} \left[\frac{(\overline{q_1^2})_N^C}{(\overline{q_1^2})^A} + 2 \frac{(\overline{q_2^2})_N^C}{(\overline{q_2^2})^A} \right]_{scd} = \frac{J}{3} \left[\frac{(\overline{q_1^2})_N^C}{(\overline{q_1^2})^A} + 2 \frac{(\overline{q_2^2})_N^C}{(\overline{q_2^2})^A} \right]_{sc} \quad (47)$$

where the subscript sc refers to the turbulence velocity ratios obtained in the absence of decay, computed from equations (25) and (26) and listed in table I, and the subscript scd implies that the effects of initial period decay have been included. In computing J from equation (46), the decay time $t(l_1)$ is taken as the time required for a particle at local main-stream velocity to pass through the screens and the contraction starting from station A. This implies that the contraction affects only the decay time. Some question exists as to the applicability of equation (46) and hence equation (47) for damping screens in which the wire diameters are usually very small.

A comparison of the theoretical mean-square resultant turbulence velocity ratio corrected for decay by the use of equation (47) with the experimental ratios obtained from reference 1 is shown in figure 10. The mean-square resultant velocity in the absence of decay for the case of a single-screen-contraction configuration ($N=1$) is also included to show the magnitude of the correction involved for the configuration of reference 1. The following data were used in applying the decay correction: $U_A = 62.8$ feet per second, $[(\bar{q}_1^2)^A]^{1/2} = 0.15$ foot per second; and $L_2^A = 0.05$ foot (estimated). The screen pressure-drop coefficients were corrected as suggested in reference 14

$$K = K_e + \frac{U_A}{2} \frac{dK_e}{dU_A}$$

where K_e designates the screen pressure-drop coefficient measured at a given speed U_A . Although the single experimental points obtained for each multiscreen arrangement do not check the decay correction as well as do those for the single-screen arrangement, the limited data do not warrant any refinement of the correction method for multiscreen-contraction configurations.

In order to obtain the resolution of the resultant turbulence velocity ratio into longitudinal and lateral components, some knowledge of the velocity-pressure correlation is required. As shown in reference 4 the effect of this correlation as represented by the term m_0 is to transfer energy from the larger to the smaller of the velocity components, thus providing a drive towards isotropy. As shown in table I, the longitudinal component will, in general, be much smaller than the lateral component so that adjustment of the longitudinal component is more critical than adjustment of the lateral component. The magnitude of the longitudinal component is governed by two opposing effects. Turbulent decay processes reduce this component; the drive towards isotropy tends to increase it. In the absence of any quantitative knowledge concerning the velocity-pressure term m_0 , the simplest assumption to be made is that the longitudinal turbulence velocity ratio may be corrected for decay and isotropy drive by taking an average of the values for zero decay and isotropic decay or

$$\left[\frac{(\bar{q}_1^2)^C_N}{(\bar{q}_1^2)^A} \right]_{scd} = \left(\frac{J+1}{2} \right) \left[\frac{(\bar{q}_1^2)^C_N}{(\bar{q}_1^2)^A} \right]_{sc} \quad (48)$$

Consistent values of the lateral turbulence velocity ratio are then obtained from the longitudinal velocity ratio of equation (48) and the resultant velocity ratio of equation (47).

The comparison shown in figure 11 provides some estimate as to the agreement that might be expected between the predicted turbulence-velocity-ratio components (corrected for decay) and the experimental values. The agreement shown is considered satisfactory for most engineering applications. The theoretical velocity ratios obtained in the absence of decay are included for the case $N = 1$ to indicate the magnitude of the correction.

The turbulence scales are also affected by the turbulence decay process, tending to increase as the decay time is increased. Under the action of the viscous forces the smallest eddies are dissipated so that the average eddy size (scale) would be expected to increase. For isotropic turbulence, the change in scale during the initial period analogous to the relation given for the fluctuation velocity, equation (46), is

$$\left(\frac{L_2}{A}\right)^2 = J^{-1}$$

Presumably the effect of decay upon the scales of turbulence could thus be obtained by a procedure similar to the one suggested for the fluctuation velocities. In the absence of any experimental data such development does not appear warranted.

CONCLUDING REMARKS

The present analysis treats, in the absence of turbulent decay processes, the combined effect of a series of identical damping screens followed by a stream convergence (or divergence) upon the mean-square fluctuation velocities, scales, correlation coefficients, and one-dimensional spectra of a field of turbulence convected by a main stream. Numerical results are presented for the case of upstream isotropic turbulence.

The limited experimental data available confirm at least qualitatively some of the theoretical results obtained such as the distortion of an initially isotropic field of turbulence by the damping screens and stream convergence into a field axisymmetric about the main-stream direction with the lateral components of the resultant fluctuation velocity larger in magnitude than the longitudinal component, and the relative insensitivity of the lateral scale of turbulence to damping-screen and stream-convergence effects. The beneficial effects of using several screens in series to attain a given over-all screen pressure-drop coefficient in attenuating the fluctuation velocities are also substantiated. This attenuation is accentuated as the screen coefficient NK is increased.

The theory predicts certain marked changes in the ordinates of the downstream one-dimensional spectra and, in the case of the longitudinal spectra, a noticeable distortion of shape which should be confirmable by experiment. The longitudinal downstream correlation coefficients attain negative values over a large range of the separation distance r_1 . Under these conditions, the scales of turbulence as conventionally defined cannot be regarded as representative of the average eddy size. Accordingly, the longitudinal scales have been redefined. The effect of the damping screens and stream convergence is to decrease the longitudinal scale and to increase the lateral scale.

An approximate method of correcting the predicted turbulent fluctuation velocities for the effects of turbulent decay is presented. Tabulations of the fluctuation velocities over a wide range of conditions are provided for convenience in engineering applications.

Lewis Flight Propulsion Laboratory
National Advisory Committee for Aeronautics
Cleveland, Ohio, October 28, 1952

APPENDIX A

SYMBOLS

The following symbols are used in this report:

$A_{1,2}$	parameter groupings defined after equation (27)
a^2	auxiliary contraction parameter, $a^2 \equiv l/l - \epsilon$
$B_{1,2,3}$	parameter groupings defined after equation (28)
b	solidity ratio of damping screen
$C_{1,2,3}$	parameter groupings defined after equation (35)
$D_{1,2,3}$	edge lengths of volume within which the turbulence field is defined
d	wire diameter of damping screen
$E_{1,2,3}$	parameter groupings defined after equation (36)
F_γ	F_1 , F_2 , or F_3
F_1	one-dimensional longitudinal spectral density (see equation (6))
$F_{2,3}$	one-dimensional lateral spectral densities (see equation (6))
f	auxiliary wave-number parameter, $f \equiv s/\eta^2 + 4/\mu^2$
$G(k)$	amplitude function in isotropic spectrum tensor (see equations (4) and (31))
g	auxiliary wave-number parameter, $g \equiv s/\xi^2 + 4\alpha^2/\nu^2$
H	constant appearing in amplitude function of special isotropic spectrum tensor, $H \equiv \frac{2n}{\pi^2} (\overline{q_1^2})^A$ (see equation (31))
h	auxiliary wave-number parameter, $h \equiv \frac{l - a^2 - s^2}{a^2}$
i	$\sqrt{-1}$

J	turbulence decay factor (see equation (46))
K	screen pressure-drop coefficient, $K \equiv \frac{\Delta p}{\frac{1}{2} \rho U^2}$
k	amplitude of vector \underline{k} : $k^2 = k_1^2 + k_2^2 + k_3^2$
\underline{k}_γ	$k_\gamma = k_1, k_2$, or k_3 ; wave-number vector
L_γ	L_1, L_2 , or L_3
L_1	longitudinal scale of turbulence (see equation (10))
L_1'	effective longitudinal scale of turbulence
L_2, L_3	lateral scales of turbulence (see equation (10))
l_1	stream velocity at station C divided by stream velocity at station B (see equation (19))
l_2	stream breadth at station C divided by stream breadth at station B (see equation (19))
l_3	stream height at station C divided by stream height at station B
$M_{B,C}$	stream Mach number at station B, C
m	mesh designation of damping screen (reciprocal of center-to-center distance between neighboring wires)
N	number of screens in series (cascade)
n	constant appearing in amplitude function of special isotropic spectral tensor, $n \equiv \frac{1}{(L_1)^A}$
P	constant
p	static pressure
\underline{Q}_γ	Q_1, Q_2 , or Q_3 ; wave-amplitude vector

\underline{q}	$q_\gamma = q_1, q_2, \text{ or } q_3$; turbulence-velocity-fluctuation vector
$R_\gamma(r_1)$	correlation coefficient (see equation (7))
$R_{\gamma\delta}(\underline{r})$	correlation tensor, $R_{\gamma\delta}(\underline{r}) \equiv \overline{q_\gamma(\underline{x})q_\delta(\underline{x+r})}$
\underline{r}	$r_\gamma = r_1, r_2, \text{ or } r_3$; separation vector
s	wave-number parameter, $s \equiv k_1^2/\gamma^2 + 1$
t	time
$t(\tau_1)$	decay time
U	main-stream velocity
u	longitudinal component of combined turbulent velocity fluctuations and potential-flow velocities induced by screen
V_1	longitudinal root-mean-square turbulence velocity ratio (used in table I)
V_2	lateral root-mean-square turbulence velocity ratio (used in table I)
v, w	lateral components of combined turbulent velocity fluctuations and potential-flow velocities induced by screen
\underline{x}	$x_\gamma = x_1, x_2, \text{ or } x_3$; position vector
α	screen deflection parameter, $\alpha \equiv \lim_{\psi_1 \rightarrow 0} \frac{\tan \psi_2}{\tan \psi_1}$
β^2	$k_1^2 (k_2^2 + k_3^2)^{-1}$
$\Gamma_{\gamma\delta}(\underline{k})$	three-dimensional spectral tensor
Δ	$\frac{4\alpha^2 \cos^2 \theta + v^2 \sin^2 \theta}{4 \cos^2 \theta + \mu^2 \sin^2 \theta}$

$\delta_{\gamma\delta}$	Kronecker delta; $\delta_{\gamma\delta} = 1$ for $\gamma = \delta$ and $\delta_{\gamma\delta} = 0$ for $\gamma \neq \delta$
ϵ	axisymmetric contraction parameter, $\epsilon \equiv l_2^2/l_1^2$
ζ^2	$k_2^2 + k_3^2$
η^2	auxiliary screen parameter, $\eta^2 \equiv \frac{\mu^2}{\mu^2 - 4}$
θ	polar angle (see appendix B)
κ	amplitude of vector \underline{k} ; $\kappa^2 = k_1^2 + k_2^2 + k_3^2$
\underline{k}	$k_\gamma = k_1, k_2$, or k_3 : wave-number vector at station C
Λ	$\frac{4\alpha^2 k_1^2 + v^2 \zeta^2}{4k_1^2 + \mu^2 \zeta^2} \quad (\text{see equation (22a)})$
λ_γ	λ_1, λ_2 , or λ_3
λ_1	longitudinal microscale of turbulence (see equation (9))
$\lambda_{2,3}$	lateral microscales of turbulence (see equation (9))
μ	auxiliary screen parameter, $\mu \equiv 1 + \alpha + K$
v	auxiliary screen parameter, $v \equiv 1 + \alpha - \alpha K$
ξ^2	auxiliary screen parameter, $\xi^2 \equiv \frac{v^2}{v^2 - 4\alpha^2}$
ρ	stream density
Σ	$\frac{(v^2 - \alpha^2 \mu^2) k_1^2}{4k_1^2 + \mu^2 \zeta^2} \quad (\text{see equation (22b)})$
σ	main-stream density at station C divided by main-stream density at station B
τ	volume

φ	azimuth angle (see appendix B)
\underline{x}	$x_\gamma = x_1, x_2,$ or $x_3;$ position vector (see equation (12))
ψ_1	angle to screen normal of flow incidence upstream of screen
ψ_2	angle to screen normal of flow emergence downstream of screen
Ω	$\frac{k_1^2(1-\epsilon)^2 \zeta^2 - 2k_1^2(1-\epsilon)(\epsilon k_1^2 + \zeta^2)}{(\epsilon k_1^2 + \zeta^2)^2} \quad (\text{see equation (22d)})$
$\underline{\omega}$	$\omega_\gamma = \omega_1, \omega_2,$ or $\omega_3;$ vorticity vector

Superscripts:

A	station upstream of screens
B	station downstream of screens and upstream of contraction
C	station downstream of contraction
*	complex conjugate

Subscripts:

A	station upstream of screens
B	station downstream of screens and upstream of contraction
C	station downstream of contraction
N	number of like screens in series
sc	only effects of screens and contraction present
scd	effects of screen and contraction corrected for initial period of decay
1	longitudinal component
2,3	lateral components

APPENDIX B

TURBULENCE VELOCITY AND SCALE RATIOS

Velocity ratios. - Using spherical polar coordinates

$$k_1 \equiv k \cos \theta$$

$$k_2 \equiv k \sin \theta \cos \varphi$$

$$k_3 \equiv k \sin \theta \sin \varphi$$

$$k^2 \equiv k_1^2 + k_2^2 + k_3^2$$

equations (23) and (24) may be put in the form

$$\left[\Gamma_{11}^C(\underline{k}) \right]_N = \frac{l_2^2 k^2 G(k)}{l_1} \frac{\Delta^N \sin^2 \theta}{(\epsilon \cos^2 \theta + \sin^2 \theta)^2} \quad (B1)$$

$$\left[\Gamma_{22}^C(\underline{k}) + \Gamma_{33}^C(\underline{k}) \right]_N = \alpha^2 \left[\Gamma_{22}^C(\underline{k}) + \Gamma_{33}^C(\underline{k}) \right]_{N-1} + \frac{l_1 G(k) (\nu^2 - \alpha^2 \mu^2) k^2 \Delta^{N-1} \epsilon^2 \sin^2 \theta \cos^2 \theta}{(4 \cos^2 \theta + \mu^2 \sin^2 \theta)(\epsilon \cos^2 \theta + \sin^2 \theta)^2} \quad (B2)$$

$$\text{where } \Delta \equiv \frac{4\alpha^2 \cos^2 \theta + \nu^2 \sin^2 \theta}{4 \cos^2 \theta + \mu^2 \sin^2 \theta}$$

The downstream mean-square fluctuation velocities are given by

$$(\overline{q_r^2})^C = \iint_{-\infty}^{\infty} \Gamma_{rr}^C(\underline{k}) dk_1 dk_2 dk_3$$

analogous to equation (5). Inasmuch as the function $G(k)$ appears in the expressions for the energy spectral densities, the variable of integration will be changed from \underline{k} to k so that

$$\overline{q_r^2} = \frac{1}{l_1 l_2} \iint_{-\infty}^{\infty} \Gamma_{rr}(\underline{k}) dk_1 dk_2 dk_3. \text{ Noting that}$$

$dk_1 dk_2 dk_3 = k^2 \sin \theta d\theta d\varphi dk$, the downstream mean-square velocity components of the turbulent field are obtained from equations (B1) and (B2) as

$$\left(\overline{q_1^2}\right)_N^C = \frac{1}{l_1^2} \int_0^\infty k^4 G(k) dk \int_0^{2\pi} d\varphi \int_0^\pi \frac{\Delta^N \sin^3 \theta d\theta}{(\epsilon \cos^2 \theta + \sin^2 \theta)^2}$$

and, inasmuch as the downstream turbulence will be axisymmetric when the upstream turbulence is isotropic,

$$\left(\overline{q_2^2}\right)_N^C = \left(\overline{q_3^2}\right)_N^C = \alpha^2 \left(\overline{q_2^2}\right)_{N-1}^C + \frac{\epsilon^2(v^2 - \alpha^2 \mu^2)}{2l_2^2} \int_0^\infty k^4 G(k) dk \int_0^{2\pi} d\varphi \int_0^\pi \frac{\Delta^{N-1} \sin^3 \theta \cos^2 \theta d\theta}{(4 \cos^2 \theta + \mu^2 \sin^2 \theta)(\epsilon \cos^2 \theta + \sin^2 \theta)^2}$$

The mean-square velocity components of the upstream isotropic turbulence are obtained by using equation (4) as

$$\left(\overline{q_1^2}\right)^A = \left(\overline{q_2^2}\right)^A = \left(\overline{q_3^2}\right)^A = \int_0^\infty k^4 G(k) dk \int_0^{2\pi} d\varphi \int_0^\pi \sin^3 \theta d\theta = \frac{8\pi}{3} \int_0^\infty k^4 G(k) dk$$

The turbulence velocity ratio or ratio of mean-square fluctuation velocities downstream of a series of N identical screens followed by an axisymmetric contraction to the corresponding upstream fluctuation velocities is then given for the longitudinal and lateral components, respectively, by

$$\frac{\left(\overline{q_1^2}\right)_N^C}{\left(\overline{q_1^2}\right)^A} = \frac{3a^4}{4l_1^2} \int_0^\pi \frac{\Delta^N \sin^3 \theta d\theta}{(a^2 - \cos^2 \theta)^2} \quad (B3)$$

$$\frac{\left(\overline{q_2^2}\right)_N^C}{\left(\overline{q_2^2}\right)^A} = \frac{\left(\overline{q_3^2}\right)_N^C}{\left(\overline{q_3^2}\right)^A} = \alpha^2 \frac{\left(\overline{q_2^2}\right)_{N-1}^C}{\left(\overline{q_2^2}\right)^A} + \frac{5(a^2 - 1)^2(v^2 - \alpha^2 \mu^2)}{8l_2^2} \int_0^\pi \frac{\Delta^{N-1} \sin^3 \theta \cos^2 \theta d\theta}{(4 \cos^2 \theta + \mu^2 \sin^2 \theta)(a^2 - \cos^2 \theta)^2} \quad (B4)$$

where $a^2 \equiv \frac{1}{1-\epsilon}$. The new contraction parameter a^2 is introduced for convenience in subsequent calculations. It may be noted that the velocity ratios are independent of the amplitude function $G(k)$ which appears in both the isotropic and axisymmetric spectral tensors. Equations (B3) and (B4) appear in the text as equations (25) and (26), respectively.

Turbulence scale ratios. - The turbulence scales may be obtained from the energy spectral densities as indicated by equations (6) and (10). Compatible with the formulation

$$\left(\frac{\overline{q_1^2}}{2}\right)^C = \frac{1}{l_1 l_2^2} \int_{-\infty}^{\infty} \int_{-\infty}^{\infty} \int_{-\infty}^{\infty} \Gamma_{rr}^C(k) dk_1 dk_2 dk_3$$

the longitudinal scale at station C is

$$(L_1)_N^C = \frac{\pi}{l_1 l_2^2 \left(\frac{\overline{q_1^2}}{2}\right)_N^C} \int_{-\infty}^{\infty} \int_{-\infty}^{\infty} \left\{ \left[\Gamma_{11}^C(k) \right]_N \right\}_{k_1=0} dk_2 dk_3$$

or, applying equation (24),

$$(L_1)_N^C = \frac{\pi}{l_1^2 \left(\frac{\overline{q_1^2}}{2}\right)_N^C} \left(\frac{v^2}{\mu^2} \right)^N \int_{-\infty}^{\infty} \int_{-\infty}^{\infty} \left[\Gamma_{11}^A(k) \right]_{k_1=0} dk_2 dk_3$$

The longitudinal scale at station A is

$$(L_1)_N^A = \frac{\pi}{\left(\frac{\overline{q_1^2}}{2}\right)_N^A} \int_{-\infty}^{\infty} \left[\Gamma_{11}^A(k) \right]_{k_1=0} dk_2 dk_3$$

The ratio of longitudinal scale downstream of a series of N identical screens followed by an axisymmetric contraction to the corresponding upstream scale or longitudinal scale ratio is thus.

$$\frac{(L_1)_N^C}{(L_1)_N^A} = \frac{\left[F_1(0) \right]_N^C}{\left[F_1(0) \right]_N^A} = \left(\frac{v^2}{\mu^2} \right)^N \left[l_1^2 \frac{\left(\frac{\overline{q_1^2}}{2} \right)_N^C}{\left(\frac{\overline{q_1^2}}{2} \right)_N^A} \right]^{-1} \quad (B5)$$

The corresponding ratio for the lateral scales is obtained in a similar manner as

$$\frac{(L_2)^C}{(L_2)^A} \equiv \frac{[\bar{F}_2(0)]^C_N}{[\bar{F}_2(0)]^A \frac{(\overline{q_2^2})^C}{(\overline{q_2^2})^A}} = (\alpha^2)^N \left[l_2^2 \frac{\left(\frac{(\overline{q_2^2})^C}{(\overline{q_2^2})^A}\right)}{N} \right]^{-1} \quad (B6)$$

These relations for the scale ratios do not require that the upstream turbulence be isotropic. Equations (B5) and (B6) appear in the text as equations (37) and (38), respectively.

APPENDIX C

ONE-DIMENSIONAL SPECTRA

With the use of equations (4) and (31), equations (29) can be written

$$F_1^A = 4\pi H \int_0^\infty \frac{\zeta^3 d\zeta}{(k_1^2 + n^2 + \zeta^2)^3}$$

$$F_2^A = F_3^A = 2\pi H \int_0^\infty \frac{(2k_1^2 + \zeta^2)\zeta d\zeta}{(k_1^2 + n^2 + \zeta^2)^3}$$

Integration yields, after use of equation (32),

$$F_1^A = \frac{\pi H}{n^2 s} \quad (C1)$$

$$F_2^A = F_3^A = \frac{\pi H (3s - 2)}{2n^2 s^2} \quad (C2)$$

Equations (33) and (34) follow upon dividing equations (C1) and (C2) by $(F_1^A)_{k_1/n=0}$ and $(F_2^A)_{k_1/n=0}$, respectively.

With use of equations (4) and (B1) and (B2) of appendix B, equations (30) can be written

$$(F_1^C)_N = \frac{4\pi H a^4}{l_1^2} \int_0^\infty \frac{(4\alpha^2 k_1^2 + \nu^2 \zeta^2)^N (k_1^2 + \zeta^2)^2 \zeta^3 d\zeta}{(4k_1^2 + \mu^2 \zeta^2)^N (k_1^2 + \eta^2 + \zeta^2)^3 [a^2 (k_1^2 + \zeta^2) - k_1^2]^2} \quad (C3)$$

$$(F_2^C)_N = \alpha^2 (F_2^C)_{N-1} + \frac{2\pi\alpha(a^2-1)^2(\nu^2-\alpha^2\mu^2)}{\nu^2} \int_0^\infty \frac{(4\alpha^2 k_1^2 + \nu^2 \zeta^2)^{N-1} (k_1^2 + \zeta^2)^2 k_1^2 \zeta^3 d\zeta}{(4k_1^2 + \mu^2 \zeta^2)^N (k_1^2 + \eta^2 + \zeta^2)^3 [a^2(k_1^2 + \zeta^2) - k_1^2]^2} \quad (C4)$$

For the case of a single-screen-axisymmetric-contraction configuration, integration of equations (C3) and (C4) yields equations (35) and (36) of the text, respectively. For the case $N = 1$, the quantity $(F_2^C)_{N-1}$ designates the one-dimensional lateral spectrum downstream of an axisymmetric contraction in the absence of damping screens and may be obtained from reference 3.

REFERENCES

1. Dryden, Hugh L., and Schubauer, G. B.: The Use of Damping Screens for the Reduction of Wind-Tunnel Turbulence. *Jour. Aero. Sci.*, vol. 14, no. 4, April 1947, pp. 221-228.
2. Taylor, G. I., and Batchelor, G. K.: The Effect of Wire Gauze on Small Disturbances in a Uniform Stream. *Quart. Jour. Mech. Appl. Math.*, vol. II, 1949, pp. 1-29.
3. Ribner, H. S., and Tucker, M.: Spectrum of Turbulence in a Contracting Stream. NACA TN 2606, 1952.
4. Batchelor, G. K.: The Theory of Axisymmetric Turbulence. *Proc. Roy. Soc. (London)*, ser. A., vol. 186, Sept. 24, 1946, pp. 480-502.
5. Batchelor, G. K.: The Role of Big Eddies in Homogeneous Turbulence. *Proc. Roy. Soc. (London)*, ser. A, vol. 195, Feb. 3, 1949, pp. 513-532.
6. Taylor, G. I.: The Spectrum of Turbulence. *Proc. Roy. Soc. (London)*, ser. A, vol. 164, Feb. 18, 1938, pp. 476-490.
7. Lin, C. C.: On Taylor's Hypothesis in Wind-Tunnel Turbulence. Naval Ordnance Lab. Memo. 10775, Proj. NR-061-069, Feb. 20, 1950.
8. Dryden, Hugh L.: A Review of the Statistical Theory of Turbulence. *Quart. Appl. Math.*, vol. 1, no. 1, April 1943, p. 35.
9. Lamb, Horace: Hydrodynamics. Cambridge Univ. Press. 6th ed., 1932, p. 205.
10. Simmons, L. F. G., and Cowdrey, C. F.: Measurements of the Aerodynamic Forces Acting on Porous Screens. R. & M. No. 2276, British A.R.C., Aug. 1945.
11. Schubauer, G. B., Spangenberg, W. G., and Klebanoff, P. S.: Aerodynamic Characteristics of Damping Screens. NACA TN 2001, 1950.
12. Chandrasekhar, S.: The Theory of Axisymmetric Turbulence. *Phil. Trans. Roy. Soc. (London)*, ser. A. vol. 242, 1950, pp. 557-577.
13. Dryden, Hugh L., and Abbott, Ira H.: The Design of Low-Turbulence Wind Tunnels. NACA Rep. 940, 1949. (Supersedes NACA TN 1755.)
14. Townsend, A. A.: The Passage of Turbulence Through Wire Gauzes. *Quart. Jour. Mech. Appl. Math.*, vol. IV, 1951, pp. 308-320.

TABLE I. - TURBULENCE VELOCITY AND SCALE RATIOS

$$v_1^2 = \frac{(q_1^2)^c}{(q_1)^k}, v_2^2 = \frac{(q_2^2)^c}{(q_2)^k}, n_B = 0.05$$

NACA

n	k	n_k	n_c	z_1	v_1^2	v_2^2	$\frac{1}{3}(v_1^c + v_2^2)$	v_1	v_2	$\frac{(L_1)^c}{(L_1)^k}$	$\frac{(L_2)^c}{(L_2)^k}$
1	0.00	0.00	0.023	0.464	1.675	0.9597	1.198100	1.8490	0.9796	2.7728000	0.4836
1	1.00	1.00	0.023	0.464	1.140369	0.764930	0.890076	1.0677	0.8746	2.726984	0.5491
1	1.50	1.50	0.023	0.464	0.75910	0.518013	0.670645	0.8809	0.7861	2.680870	0.6149
1	2.00	2.00	0.023	0.464	0.52876	0.360602	0.513290	0.7265	0.7113	2.683905	0.6792
1	2.50	2.50	0.023	0.464	0.40814	0.251907	0.314876	0.4907	0.5932	2.497543	0.7980
1	3.00	3.00	0.023	0.464	0.307097	0.1943305	0.191236	0.2951	0.4933	2.2118931	0.9234
1	3.50	3.50	0.023	0.464	0.29166	0.1484298	0.132587	0.1708	0.4293	1.603481	1.0159
1	4.00	4.00	0.023	0.464	0.27348	0.1040459	0.103077	0.1006	0.3667	0.388081	1.0731
1	4.50	4.50	0.023	0.464	0.257102	0.087578	0.087419	0.0843	0.3701	0.000881	1.0906
1	5.00	5.00	0.023	0.464	0.241981	0.078666	0.078666	0.1023	0.3558	3.156865	1.1007
1	6.00	6.00	0.023	0.464	0.236715	0.078858	0.070184	0.1266	0.3197	1.547161	1.1069
1	8.00	1.000	0.023	0.464	0.21690	0.058684	0.0646811	0.1916	0.2808	2.439350	1.0831
1	0.00	0.00	0.025	0.500	1.604	0.9443	1.154200	1.2660	0.9718	2.426000	0.5294
1	1.00	1.00	0.025	0.500	1.094991	0.761268	0.878259	1.0464	0.8725	2.447859	0.5943
1	1.50	1.50	0.025	0.500	0.747877	0.521796	0.663623	0.8645	0.7885	2.398713	0.6580
1	2.00	2.00	0.025	0.500	0.514258	0.361260	0.512600	0.7136	0.7171	2.344144	0.7190
1	2.50	2.50	0.025	0.500	0.347664	0.263849	0.320821	0.4845	0.6322	2.208175	0.8313
1	3.00	3.00	0.025	0.500	0.266519	0.1955676	0.199290	0.3941	0.5056	1.9285331	0.94655
1	3.50	3.50	0.025	0.500	0.230179	0.140526	0.140526	0.1737	0.4224	1.335653	1.0303
1	4.00	4.00	0.025	0.500	0.211321	0.1159640	0.110200	0.1064	0.3996	0.394894	1.0828
1	4.50	4.50	0.025	0.500	0.198412	0.100389	0.0917	0.3826	0.000664	1.0999	
1	6.00	6.00	0.025	0.500	0.0808418	0.046378	0.0400389	0.0694	0.3693	2.41984	1.1091
1	8.00	1.000	0.025	0.500	0.07986	0.036378	0.039581	0.1044	0.3470	1.280813	1.1165
1	0.00	0.00	0.025	0.500	0.070895	0.020417	0.028310	0.1265	0.3299	1.875537	1.1115
1	1.00	1.00	0.025	0.500	0.061007	0.0160862	0.01600100	0.1468	0.3164	2.144828	1.0989
1	2.00	2.00	0.025	0.500	0.021557	0.0082838	0.007028	0.1882	0.2878	2.390737	1.0433
1	4.00	4.00	0.025	0.500	0.0354508	0.020412	0.0256794	0.2886	0.2458	2.476737	1.0104
1	0.00	0.00	0.030	0.600	1.435	0.9816	1.092700	1.1980	0.9600	1.935000	0.6153
1	1.00	1.00	0.030	0.600	0.988058	0.763690	0.838479	0.9400	0.8739	1.883875	0.7109
1	1.50	1.50	0.030	0.600	0.680466	0.439937	0.535447	0.8249	0.8000	1.889381	0.7675
1	2.00	2.00	0.030	0.600	0.468559	0.341629	0.517872	0.7845	0.7360	1.769368	0.8208
1	2.50	2.50	0.030	0.600	0.321698	0.296159	0.339339	0.7080	0.6310	1.683836	0.9116
1	3.00	3.00	0.030	0.600	0.266812	0.209744	0.241900	0.7936	0.5383	1.341826	1.0023
1	3.50	3.50	0.030	0.600	0.233413	0.1826742	0.1628299	0.7682	0.4762	0.837767	1.0673
1	4.00	4.00	0.030	0.600	0.2114789	0.167084	0.149652	0.7216	0.4325	1.56593	1.1087
1	4.50	4.50	0.030	0.600	0.1910569	0.160404	0.110459	0.7028	0.4147	0.00032	1.1226
1	6.00	6.00	0.030	0.600	0.1230301	0.1414286	0.098384	0.7109	0.3761	0.787556	1.1408
1	8.00	1.000	0.030	0.600	0.0620406	0.1327282	0.090274	0.1275	0.3568	1.288402	1.1408
1	0.00	0.00	0.035	0.700	1.399	0.9209	1.1046900	1.1400	0.9596	1.570000	0.7599
1	1.00	1.00	0.035	0.700	0.901771	0.780017	0.7200602	0.9496	0.8832	1.565098	0.8120
1	1.50	1.50	0.035	0.700	0.627119	0.666404	0.553309	0.7919	0.8163	1.458333	0.8599
1	2.00	2.00	0.035	0.700	0.436591	0.573724	0.528013	0.6608	0.7574	1.195233	0.9034
1	2.50	2.50	0.035	0.700	0.321869	0.433458	0.397928	0.6167	0.6585	1.846010	0.9769
1	3.00	3.00	0.035	0.700	0.287003	0.323191	0.344462	0.5950	0.5688	0.557538	1.0994
1	3.50	3.50	0.035	0.700	0.241625	0.236881	0.235605	0.5182	0.5068	0.093078	1.1327
1	4.00	4.00	0.035	0.700	0.211359	0.1965839	0.196087	0.4437	0.4287	0.000198	1.1444
1	4.50	4.50	0.035	0.700	0.1817558	0.161985	0.162610	0.4177	0.4025	0.513518	1.1680
1	6.00	6.00	0.035	0.700	0.120777	0.106789	0.1024561	0.3297	0.3144	0.914320	1.1666
1	8.00	1.000	0.035	0.700	0.0603157	0.0520406	0.0485070	0.1736	0.1640	1.155636	1.1684
1	0.00	0.00	0.040	0.800	1.184	0.9366	1.019100	1.0880	0.9678	1.320000	0.8540
1	1.00	1.00	0.040	0.800	0.829528	0.806351	0.814077	0.9108	0.8980	2.662194	0.8977
1	1.50	1.50	0.040	0.800	0.588630	0.698934	0.660173	0.7633	0.8360	1.801743	0.9370
1	2.00	2.00	0.040	0.800	0.410177	0.609305	0.542929	0.7006	0.7139	1.136929	0.9721
1	2.50	2.50	0.040	0.800	0.308214	0.356206	0.366875	0.6970	0.6568	0.557538	1.0870
1	3.00	3.00	0.040	0.800	0.261625	0.239529	0.246894	0.6370	0.5968	0.390752	1.1275
1	3.50	3.50	0.040	0.800	0.217558	0.212080	0.153239	0.5171	0.4949	0.00012	1.1546
1	4.00	4.00	0.040	0.800	0.175745	0.206579	0.142968	0.4255	0.4545	0.474931	1.1715
1	4.50	4.50	0.040	0.800	0.1415448	0.182188	0.126608	0.3245	0.4268	0.352716	1.1807
1	6.00	6.00	0.040	0.800	0.0717465	0.163437	0.114780	0.2582	0.3043	0.671489	1.1846
1	8.00	1.000	0.040	0.800	0.0280284	0.0148556	0.0158087	0.1428	0.1654	0.890163	1.1787
1	0.00	0.00	0.045	0.900	1.086	0.9642	1.004800	1.04260	0.9519	1.177000	0.9337
1	1.00	1.00	0.045	0.900	0.767481	0.840203	0.815692	0.8762	0.8166	1.077144	0.9698
1	1.50	1.50	0.045	0.900	0.444112	0.7362145	0.722414	0.7378	0.8500	1.016219	1.0208
1	2.00	2.00	0.045	0.900	0.3298161	0.5842147	0.6020128	0.625	0.6048	0.350929	1.0208
1	2.50	2.50	0.045	0.900	0.2298557	0.3986299	0.403528	0.4447	0.5118	0.850929	1.0725
1	3.00	3.00	0.045	0.900	0.1980374	0.3680974	0.3691316	0.3991	0.5613	0.541737	1.115520
1	3.50	3.50	0.045	0.900	0.154350	0.3150464	0.3244514	0.3884	0.5613	0.886333	1.11744
1	4.00	4.00	0.045	0.900	0.1207284	0.2444885	0.2484686	0.3157	0.4949	0.616357	1.14744
1	4.50	4.50	0.045	0.900	0.091989	0.19291820	0.170031	0.28725	0.3471	0.890068	1.1688
1	6.00	6.00	0.045	0.900	0.0521957	0.148121	0.140410	0.21503	0.3496	0.653419	1.190735
1	8.00	1.000	0.045	0.900	0.0268607	0.0816489	0.0816497	0.14857	0.15997	0.5098440	1.202050
1	0.00	0.00	0.050	1.100	0.925342	0.885304	0.862824	0.9205	0.8998	1.720255	1.169655
1	1.00	1.00	0.050	1.100	0.6581118	0.9238890	0.872653	0.8155	0.9612	0.832700	1.16770
1	1.50	1.50	0.050	1.100	0.419956	0.8202928	0.708927	0.69413	0.6864	0.230283	1.16455
1	2.00	2.00	0.050	1.100	0.329256	0.605033	0.605024	0.5910	0.5847	0.350556	1.161455
1	2.50	2.50	0.050	1.100	0.217356	0.5250330	0.484367	0.4323	0.5227	0.705808	1.167336
1	3.00	3.00	0.050	1.100	0.1796284	0.3973076	0.3894666	0.3200	0.3200	0.777406	1.171328
1	3.50	3.50	0.050	1.100	0.139729	0.3164374	0.267494	0.2405	0.2326	0.179443	1.20137
1	4.00	4.00	0.050	1.100	0.1029608	0.2164689	0.150862	0.1400			

TABLE I. - Continued. TURBULENCE VELOCITY AND SCALE RATIOS

$$\left[\frac{v_1^2}{v_1^2} = \frac{(q_1^2)^C_M}{(q_1^2)^A}, v_2^2 = \frac{(q_2^2)^C_R}{(q_2^2)^A}, N_B = 0.05 \right]$$



N	K	Hx	M_0	t_1	v_1^2	v_2^2	$\frac{1}{3}(v_1^2 + v_2^2)$	v_1	v_2	$\frac{(L_1)^C_H}{(L_1)^A}$	$\frac{(L_2)^C_H}{(L_2)^A}$
1	0.00	0.000	0.060	0.1200	0.85803	1.0912	1.013500	0.9263	1.0446	0.809500	1.0990
1	.20	0.00	0.060	1.200	0.628107	0.971519	0.855048	.7887	.9857	.748178	1.1169
1	.40	0.00	0.060	1.200	0.453584	0.866683	0.728963	.6734	.9310	.686328	1.1327
1	.60	0.00	0.060	1.200	0.338594	0.774367	0.72109	.5767	.8800	.623308	1.1466
1	1.00	1.00	0.060	1.200	0.182588	0.620208	0.474335	.4273	.7875	.493021	1.1697
1	1.50	1.50	0.060	1.200	0.091568	0.486837	0.356081	.3026	.6977	.315901	1.1982
1	2.00	2.00	0.060	1.200	0.050574	0.399989	0.283517	.2249	.6324	.138408	1.2028
1	2.50	2.50	0.060	1.200	0.038011	0.319362	0.236913	.1789	.5825	.018090	1.2217
1	3.00	3.00	0.060	1.200	0.026943	0.214615	0.181724	.1461	.5609	.000003	1.2366
1	3.50	3.00	0.060	1.200	0.018397	0.164817	0.104524	.1547	.5430	.014015	1.2305
1	4.00	3.50	0.060	1.200	0.010881	0.120791	0.080814	.1445	.5107	.116004	1.2365
1	4.50	4.00	0.060	1.200	0.002026	0.093957	0.062713	.1422	.4837	.257766	1.2404
1	5.00	4.50	0.060	1.200	0.002681	0.072283	0.048426	.1438	.4607	.388097	1.2428
1	6.00	5.00	0.060	1.200	0.003686	0.046636	0.018984	.1539	.4083	.620774	1.2440
1	1.000	1.000	0.060	1.200	0.007721	0.010709	0.00639	.1665	.3273	.768832	1.2417
1	0.50	0.000	0.070	0.1000	0.74524	1.1992	1.047900	0.8033	1.0551	0.844900	1.2660
1	.20	0.000	0.070	1.400	0.548289	1.074949	0.993939	.7405	.1036	.623359	1.2767
1	.40	0.000	0.070	1.400	0.406030	0.943808	0.782666	.6378	.0503	.563359	1.2867
1	.60	0.000	0.070	1.400	0.302843	0.865844	0.678177	.5503	.0305	.403059	1.2954
1	1.00	1.00	0.070	1.400	0.172553	0.699834	0.53403	.4154	.021	.140342	1.3001
1	1.50	1.50	0.070	1.400	0.091235	0.552456	0.498722	.3021	.7433	.332951	1.3248
1	2.00	2.00	0.070	1.400	0.053305	0.461528	0.381878	.2309	.6231	.096503	1.3361
1	2.50	2.50	0.070	1.400	0.029911	0.368929	0.280593	.1876	.000009	.000009	1.3447
1	3.00	3.00	0.070	1.400	0.018656	0.290389	0.213482	.1631	.6004	.000002	1.3550
1	3.50	3.50	0.070	1.400	0.008273	0.219937	0.167161	.1507	.5472	.078333	1.3656
1	4.00	4.00	0.070	1.400	0.002128	0.166329	0.1457	.5184	.180526	1.3789	
1	4.50	4.50	0.070	1.400	0.000902	0.124389	0.1446	.4939	.282192	1.3610	
1	6.00	6.00	0.070	1.400	0.002179	0.091250	0.134893	.1489	.4373	.407050	1.3615
1	1.000	1.000	0.070	1.400	0.000458	0.072286	0.082660	.1566	.3496	.388604	1.3681
1	0.00	0.50	0.1000	0.0000	0.514514	1.12576	1.035250	0.2183	1.0550	0.485000	1.2540
1	.20	0.00	0.1000	0.0000	0.319250	1.052272	1.079321	.6265	.1198	.372391	1.2663
1	.40	0.00	0.1000	0.0000	0.203349	1.015690	0.955683	.5831	.1333	.380835	1.2714
1	.60	0.00	0.1000	0.0000	0.143456	0.952433	0.877338	.5330	.1076	.285551	1.2757
1	1.00	1.00	0.0000	0.0000	0.094553	0.852402	0.730004	.4907	.8676	.046384	1.2802
1	1.50	1.50	0.0000	0.0000	0.058701	0.754646	0.635164	.4336	.7909	.005339	1.2879
1	2.00	2.00	0.0000	0.0000	0.038701	0.671040	0.573247	.4183	.7332	.000001	1.2883
1	2.50	2.50	0.0000	0.0000	0.023349	0.584761	0.5055	.4835	.6339	.034733	1.2894
1	3.00	3.00	0.0000	0.0000	0.015135	0.514524	0.475052	.4146	.5105	.083990	1.2930
1	3.50	3.50	0.0000	0.0000	0.009159	0.437575	0.408589	.4196	.5815	.139375	1.2941
1	4.00	4.00	0.0000	0.0000	0.002113	0.346096	0.347508	.4145	.6105	.083990	1.2964
1	4.50	4.50	0.0000	0.0000	0.001910	0.264096	0.315766	.41382	.6812	.077404	1.2984
1	6.00	6.00	0.0000	0.0000	0.001595	0.214349	0.2623	.6036	.169732	1.3149	
1	1.000	1.000	0.0000	0.0000	0.001324	0.165544	0.158582	.1145	.1009	.424973	1.2972
1	0.00	0.00	0.140	0.0000	0.31795	0.346183	0.212300	0.8883	1.0550	0.169800	1.3050
1	.20	0.00	0.140	0.0000	0.2795	0.271109	0.192047	1.370679	1.3856	.161363	1.3155
1	.40	0.00	0.140	0.0000	0.214389	0.173659	0.128919	.6430	.1378	.267524	1.3264
1	.60	0.00	0.140	0.0000	0.171163	0.156998	0.110370	.4137	.1250	.223172	1.3307
1	1.00	1.00	0.140	0.0000	0.12795	0.118141	0.102451	.3434	.11321	.147913	1.3481
1	1.50	1.50	0.140	0.0000	0.090756	0.070956	0.070566	.3664	.1023	.075117	1.3593
1	2.00	2.00	0.140	0.0000	0.064889	0.048897	0.053075	.2111	.0236	.026337	1.3610
1	2.50	2.50	0.140	0.0000	0.043634	0.031984	0.030698	.1906	.0846	.002936	1.3713
1	3.00	3.00	0.140	0.0000	0.028838	0.021883	0.020397	.1688	.08246	.000001	1.3812
1	3.50	3.50	0.140	0.0000	0.014159	0.012689	0.018659	.1470	.07994	.002144	1.3827
1	4.00	4.00	0.140	0.0000	0.002113	0.001669	0.014550	.1454	.07535	.018474	1.3838
1	4.50	4.50	0.140	0.0000	0.001910	0.001409	0.013766	.1382	.06812	.045454	1.3858
1	6.00	6.00	0.140	0.0000	0.001595	0.001169	0.01263	.1263	.0636	.169732	1.3914
1	1.000	1.000	0.140	0.0000	0.001324	0.001035	0.011554	.1151	.0613	.296432	1.3964
1	0.00	0.00	0.180	0.0000	0.3489	0.349266	0.269000	0.4997	1.0571	0.310900	1.3920
1	.20	0.00	0.180	0.0000	0.2589	0.191961	0.242469	.4643	.1571	.261166	1.3996
1	.40	0.00	0.180	0.0000	0.160446	0.193293	0.151567	.4006	.1610	.216797	1.4098
1	.60	0.00	0.180	0.0000	0.130483	0.198349	0.136589	.3612	.1084	.177547	1.4200
1	1.00	1.00	0.180	0.0000	0.088592	0.160964	0.09276	.3239	.113552	.055313	1.4208
1	1.50	1.50	0.180	0.0000	0.058444	0.129587	0.083396	.2417	.1384	.018745	1.4215
1	2.00	2.00	0.180	0.0000	0.031836	0.107959	0.073364	.2043	.10590	.002033	1.4221
1	2.50	2.50	0.180	0.0000	0.020878	0.092135	0.063769	.1784	.096168	.002000	1.4226
1	3.00	3.00	0.180	0.0000	0.015549	0.080931	0.058346	.1682	.092799	.000000	1.4231
1	3.50	3.50	0.180	0.0000	0.012159	0.071924	0.054809	.1602	.09996	.001466	1.4237
1	4.00	4.00	0.180	0.0000	0.010889	0.064720	0.048669	.1470	.08491	.012535	1.4242
1	4.50	4.50	0.180	0.0000	0.008690	0.058827	0.043775	.1373	.08045	.030938	1.4252
1	6.00	6.00	0.180	0.0000	0.005948	0.046204	0.031854	.1164	.07797	.121145	1.4292
1	1.000	1.000	0.180	0.0000	0.003291	0.047087	0.021587	.1018	.07421	.220924	1.4323
1	0.00	0.00	0.340	0.0000	0.6124	0.612300	0.485800	0.4833	2.0700	0.333250	1.4320
1	.20	0.00	0.340	0.0000	0.5948	0.594740	0.450542	2.0714	1.3514	.19684	1.4320
1	.40	0.00	0.340	0.0000	0.58875	0.58875	0.436442	.4871	.1873	.153690	1.4301
1	.60	0.00	0.340	0.0000	0.570544	0.570544	0.4216	.4624	.18506	.122447	1.4301
1	1.00	1.00	0.340	0.0000	0.537040	0.537048	0.413343	.4818	.16095	.074439	1.4302
1	1.50	1.50	0.340	0.0000	0.501552	0.501552	0.405072	.4818	.14288	.034335	1.4303
1	2.00	2.00	0.340	0.0000	0.453778	0.453778	0.377423	.4817	.13775	.000000	1.4303
1	2.50	2.50	0.340	0.0000	0.408389	0.408389	0.357765	.4816	.13581	.000811	1.4303
1	3.00	3.00	0.340	0.0000	0.368285	0.368285	0.329076	.4815	.13281	.006868	1.4303
1	3.50	3.50	0.340	0.0000	0.334390	0.334390	0.297248	.4814	.12981	.012685	1.4304
1	4.00	4.00	0.340	0.0000	0.302955	0.302955	0.264931	.4813	.12681	.017079	1.4304
1	4.50</										

TABLE I. - Continued. TURBULENCE VELOCITY AND SCALE RATIOS

$$v_1^2 = \frac{(q_1^2)^c}{(q_1^2)^k}, v_2^2 = \frac{(q_2^2)^c}{(q_2^2)^k}, M_B = 0.05$$



N	K	M _K	M _C	t ₁	v ₁ ²	v ₂ ²	$\frac{1}{3}(v_1^2 + 2v_2^2)$	v ₁	v ₂	$\frac{(L_1)^c}{(L_1)^k}$	$\frac{(L_2)^c}{(L_2)^k}$
1	0.00	0.00	0.500	0.9761	0.05604	6.492	4.346700	0.3367	2.5480	0.187400	1.3380
1	.20	.20	.500	0.9761	0.046780	5.874	3.931898	0.163	2.4237	1.50331	1.3325
1	.40	.40	.500	0.9761	0.039456	5.314	4.650	0.2054	1.19189	1.3325	
1	.60	.60	.500	0.9761	0.033540	4.806	9.979	0.1572	2.1925	0.93309	1.3325
1	1.00	1.00	.500	0.9761	0.024714	3.927	4.57	0.173	1.9818	0.555034	1.3325
1	1.50	1.50	.500	0.9761	0.017857	3.142	3.310	0.1336	1.7727	0.24476	1.3325
1	2.00	2.00	.500	0.9761	0.013756	2.618	5.858	0.1054	1.6182	0.07688	1.3325
1	2.50	2.50	.500	0.9761	0.01116	2.244	4.96	0.1454	1.4982	0.00787	1.3325
1	2.76	2.76	.500	0.9761	0.010099	2.089	8.289	0.1054	1.4454	0.000000	1.3325
1	3.00	3.00	.500	0.9761	0.009314	1.963	9.30	0.0965	1.4014	0.005544	1.3325
1	3.50	3.50	.500	0.9761	0.008025	1.745	7.11	0.0896	1.3213	0.04561	1.3325
1	4.00	4.00	.500	0.9761	0.007066	1.571	1.37	0.0841	1.2534	0.111448	1.3325
1	4.50	4.50	.500	0.9761	0.006330	1.428	3.03	0.0796	1.1951	0.19158	1.3325
1	6.00	6.00	.500	0.9761	0.004892	1.122	3.23	0.0699	1.0594	0.45397	1.3325
1	10.00	1.000	.500	0.9761	0.003225	0.714	1.37	0.0568	0.8451	0.29853	1.3325
1	0.00	0.700	1.3363	0.03340	7.947	5.309100	0.1828	2.8190	0.167600	1.3320	
1	.20	.700	1.3363	0.028092	7.189	6.77	4.802488	1.676	2.6814	1.33563	1.3330
1	.40	.700	1.3363	0.023879	6.504	5.541	4.344320	1.545	2.5504	1.05078	1.3330
1	.60	.700	1.3363	0.020447	5.883	2.111	3.928956	1.430	2.4255	0.81732	1.3330
1	1.00	1.00	1.3363	0.015262	4.806	8.29	3.209640	1.235	2.1924	0.47548	1.3330
1	1.50	1.50	1.3363	0.011779	3.845	8.53	2.567628	1.057	1.9611	0.20859	1.3330
1	2.00	2.00	1.3363	0.008709	3.204	8.76	2.139487	0.933	1.7902	0.06479	1.3330
1	2.50	2.50	1.3363	0.007098	2.747	0.355	1.833723	0.843	1.6574	0.006558	1.3330
1	2.76	2.76	1.3363	0.006472	2.557	0.808	1.706877	0.804	1.5991	0.000000	1.3330
1	3.00	3.00	1.3363	0.005986	2.403	6.54	1.604431	0.774	1.5504	0.004552	1.3330
1	3.50	3.50	1.3363	0.005180	2.136	5.81	1.426114	0.720	1.4617	0.3769	1.3330
1	4.00	4.00	1.3363	0.004575	1.922	9.21	1.283472	0.676	1.3867	0.09187	1.3330
1	4.50	4.50	1.3363	0.004105	1.748	1.09	1.166774	0.641	1.2222	0.15760	1.3330
1	6.00	6.00	1.3363	0.003175	1.373	5.13	9.167334	0.563	1.1760	0.37326	1.3330
1	10.00	1.000	1.3363	0.002069	0.874	0.50	0.582299	0.455	0.9349	0.83039	1.3330
1	0.00	0.900	1.6702	0.022887	8.618	5.753000	0.1518	2.9360	0.156800	1.3330	
1	.20	.900	1.6702	0.019262	7.798	2.24	5.805837	1.388	2.7925	1.24703	1.3330
1	.40	.900	1.6702	0.016442	7.055097	4.708879	1.282	2.6561	0.97700	1.3330	
1	.60	.900	1.6702	0.014133	6.381	1.77	4.288829	1.189	2.5380	0.75702	1.3330
1	1.00	1.00	1.6702	0.010680	5.813	6.90	3.479333	1.031	2.3834	0.43743	1.3330
1	1.50	1.50	1.6702	0.007835	4.717	1.37	2.783530	0.885	2.0484	0.19054	1.3330
1	2.00	2.00	1.6702	0.006138	3.476	1.46	2.319477	0.783	1.8644	0.05865	1.3330
1	2.50	2.50	1.6702	0.005025	2.979	5.54	1.988044	0.709	1.7261	0.00595	1.3330
1	2.76	2.76	1.6702	0.004591	2.773	5.80	1.850544	0.678	1.6654	0.000000	1.3330
1	3.00	3.00	1.6702	0.004252	2.607	1.09	1.739490	0.652	1.6147	0.00407	1.3330
1	3.50	3.50	1.6702	0.003688	2.317	4.89	1.546183	0.607	1.5283	0.03389	1.3330
1	4.00	4.00	1.6702	0.003262	2.085	6.68	1.391545	0.571	1.4442	0.08247	1.3330
1	4.50	4.50	1.6702	0.002931	1.896	0.78	1.265029	0.541	1.3770	0.14134	1.3330
1	6.00	6.00	1.6702	0.002868	1.489	7.75	0.993939	0.476	1.2206	0.33448	1.3330
1	10.00	1.000	1.6702	0.001471	0.948	0.37	0.582315	0.384	0.9737	0.74750	1.3330
1	0.00	1.000	1.8262	0.019492	8.694	5.808500	0.1395	2.9490	0.154000	1.3330	
1	.20	1.000	1.8262	0.016493	7.867	1.29	5.850250	1.284	2.8048	1.21824	1.3330
1	.40	1.000	1.8262	0.014098	7.117	4.38	4.749658	1.187	2.6679	0.95315	1.3330
1	.60	1.000	1.8262	0.012133	6.437	5.63	4.995753	1.101	2.5372	0.73761	1.3330
1	1.00	1.00	1.8262	0.009137	5.825	9.59	3.509555	0.956	2.3934	0.42529	1.3330
1	1.50	1.50	1.8262	0.006756	4.208	8.36	2.807743	0.822	2.0514	0.18483	1.3330
1	2.00	2.00	1.8262	0.005303	3.506	8.88	2.339676	0.728	1.8727	0.05698	1.3330
1	2.50	2.50	1.8262	0.004348	3.005	8.88	2.005337	0.659	1.7337	0.000575	1.3330
1	2.76	2.76	1.8262	0.003974	2.798	0.26	1.866677	0.630	1.6727	0.000000	1.3330
1	3.00	3.00	1.8262	0.003682	2.633	9.07	1.559670	0.565	1.6218	0.003393	1.3330
1	3.50	3.50	1.8262	0.003197	2.041	1.16	1.403687	0.532	1.5290	0.079571	1.3330
1	4.00	4.00	1.8262	0.002829	1.912	8.33	1.276069	0.504	1.4856	0.13629	1.3330
1	4.50	4.50	1.8262	0.002542	1.619	2.93	1.008615	0.474	1.4290	0.1831	1.3330
1	6.00	6.00	1.8262	0.001968	1.502	9.39	0.928135	0.357	1.2259	0.382844	1.3330
1	10.00	1.000	1.8262	0.001275	0.956	4.15	0.520205	0.257	0.7280	0.72147	1.3330
1	0.00	1.200	2.1153	0.014942	8.436	5.889000	0.1221	2.8040	0.143600	1.3330	
1	.20	1.200	2.1153	0.012693	7.634	5.07	5.093692	1.127	2.7631	1.17929	1.3330
1	.40	1.200	2.1153	0.010869	6.905	9.78	4.608875	1.043	2.6281	0.92149	1.3330
1	.60	1.200	2.1153	0.009370	6.247	2.07	4.167928	1.011	2.4994	0.711193	1.3330
1	1.00	1.00	2.1153	0.007077	5.04	4.32	3.405180	0.841	2.3593	0.40930	1.3330
1	1.50	1.50	2.1153	0.005248	4.083	8.01	2.724283	0.724	2.2030	0.17735	1.3330
1	2.00	2.00	2.1153	0.004129	3.403	1.67	2.270154	0.643	1.8448	0.05454	1.3330
1	2.50	2.50	2.1153	0.003392	2.917	0.00	1.945797	0.582	1.7079	0.00549	1.3330
1	2.76	2.76	2.1153	0.003103	2.715	2.93	1.611830	0.557	1.6478	0.000000	1.3330
1	3.00	3.00	2.1153	0.002876	2.558	3.75	1.702342	0.536	1.5976	0.00375	1.3330
1	3.50	3.50	2.1153	0.002500	2.268	7.77	1.513351	0.500	1.5062	0.03118	1.3330
1	4.00	4.00	2.1153	0.002214	2.041	8.99	1.362004	0.471	1.4290	0.07577	1.3330
1	4.50	4.50	2.1153	0.001990	1.856	2.72	1.238178	0.446	1.3625	0.12975	1.3330
1	6.00	6.00	2.1153	0.001541	1.458	4.99	0.972846	0.393	1.2077	0.30684	1.3330
1	10.00	1.000	2.1153	0.000977	0.988	1.35	0.619089	0.316	0.9634	0.68764	1.3330
1	0.00	1.500	2.4920	0.01103	7.391	4.931000	0.1050	2.7190	0.146100	1.3330	
1	.20	1.500	2.4920	0.009358	6.688	4.63	4.462095	0.967	2.5862	1.15309	1.3330
1	.40	1.500	2.4920	0.008083	5.651	0.84	4.036737	0.896	2.4599	0.89940	1.3330
1	.60	1.500	2.4920	0.006985	5.473	0.81	3.651029	0.832	2.3395	0.69405	1.3330
1	1.00	1.000	2.4920	0.005841	4.471	7.57	2.986205	0.724	2.1146	0.3983	1.3330
1	1.50	1.500	2.4920	0.003895	3.577	7.54	2.386468	0.624	1.8915	0.17919	1.3330
1	2.00	2.00	2.4920	0.003069	2.981	4.61	1.988664	0.554	1.7867	0.05287	1.3330
1	2.50	2.50	2.4920	0.002524	2.555	5.38	1.704533	0.5			

TABLE I. - Continued. TURBULENCE VELOCITY AND SCALE RATIOS

$$v_1^2 = \frac{(q_1^2)^c}{(q_1^2)^A}, v_2^2 = \frac{(q_2^2)^c}{(q_2^2)^A}, u_B = 0.05$$



N	K	NK	η_C	t_1	v_1^2	v_2^2	$\frac{1}{3}(v_1^2 + v_2^2)$	v_1	v_2	$\frac{(L_1)^c}{(L_1)^A}$	$\frac{(L_2)^c}{(L_2)^A}$
1	0.00	0.00	2.000	2.9822	0.007701	5.158	14.57200	0.0878	22.700	0.146000	1.33330
1	.30	.30	8.000	2.9822	0.006534	4.661783	33.10093	0.0808	21.591	1.15325	1.33332
1	.40	.40	8.000	2.9822	0.005602	4.217540	28.13561	0.0748	20.537	0.89954	1.33332
1	.50	.50	2.000	2.9822	0.004835	3.814671	23.44786	0.0695	19.531	0.69416	1.33332
1	1.00	1.00	2.000	2.9822	0.003659	3.116747	2.07951	0.0605	17.654	0.39828	1.33332
1	1.50	1.50	2.000	2.9822	0.002719	2.493652	1.65341	0.0521	15.791	0.17222	1.33332
1	2.00	2.00	2.000	2.9822	0.002143	2.078043	1.386076	0.0463	14.415	0.05288	1.33332
1	2.50	2.50	2.000	2.9822	0.001762	1.781180	1.188041	0.0420	13.346	0.0532	1.33332
1	2.76	2.76	2.000	2.9822	0.001613	1.658013	1.105880	0.0402	12.876	0.05000	1.33332
1	3.00	3.00	2.000	2.9822	0.001496	1.558532	1.039520	0.0387	12.484	0.05363	1.33332
1	3.50	3.50	2.000	2.9822	0.001301	1.385368	.924008	0.0361	11.770	0.05014	1.33332
1	4.00	4.00	2.000	2.9822	0.001153	1.246826	.831603	0.0340	11.166	0.057321	1.33332
1	4.50	4.50	2.000	2.9822	0.001037	1.133478	.755598	0.0322	10.646	0.052532	1.33332
1	6.00	6.00	2.000	2.9822	0.000803	.890593	.533994	0.0283	9.437	0.029627	1.33332
1	1.000	1.000	2.000	2.9822	0.000519	.566738	.377998	0.0228	7.528	0.066455	1.33332
1	0.00	0.00	3.000	3.5866	0.004599	2.0533	1.970300	0.0707	14.330	0.155500	1.33330
1	.30	.30	3.000	3.5866	0.004227	1.857859	1.239982	0.0650	13.630	0.123244	1.33331
1	.40	.40	3.000	3.5866	0.003610	1.680815	1.121374	0.0601	12.965	0.096491	1.33331
1	.50	.50	3.000	3.5866	0.003105	1.502026	1.014543	0.0557	12.330	0.074717	1.33331
1	1.00	1.00	3.000	3.5866	0.002336	1.242116	.888856	0.0483	11.145	0.043126	1.33331
1	1.50	1.50	3.000	3.5866	0.001726	.993794	.661703	0.0415	9.969	0.028754	1.33331
1	2.00	2.00	3.000	3.5866	0.001268	.928162	.525693	0.0308	9.000	0.008796	1.33331
1	2.50	2.50	3.000	3.5866	0.001109	.709853	.473605	0.0333	8.423	0.00585	1.33331
1	2.76	2.76	3.000	3.5866	0.001013	.660767	.440849	0.0318	8.129	0.00000	1.33331
1	3.00	3.00	3.000	3.5866	0.000938	.621121	.414393	0.0306	7.881	0.000400	1.33331
1	3.50	3.50	3.000	3.5866	0.000814	.558107	.368034	0.0285	7.430	0.003329	1.33331
1	4.00	4.00	3.000	3.5866	0.000721	.496897	.331505	0.0268	7.049	0.008098	1.33332
1	4.50	4.50	3.000	3.5866	0.000647	.451172	.301365	0.0254	6.721	0.013877	1.33331
1	6.00	6.00	3.000	3.5866	0.000501	.354926	.236784	0.0224	5.958	0.032835	1.33331
1	1.000	1.000	3.000	3.5866	0.000385	.285868	.150683	0.0180	4.752	0.073423	1.33332
1	0.00	0.00	4.000	3.9046	0.003844	0.8114	0.542200	0.0620	0.9008	0.170600	1.33330
1	.30	.30	4.000	3.9046	0.003230	0.734087	.490468	0.0568	0.8568	0.136081	1.33329
1	.40	.40	4.000	3.9046	0.002742	0.664132	.443669	0.0524	0.8149	0.107185	1.33329
1	.50	.50	4.000	3.9046	0.002346	0.600693	.401244	0.0484	0.7750	0.083468	1.33329
1	1.00	1.00	4.000	3.9046	0.001747	0.490791	.327776	0.0418	0.7006	0.048648	1.33329
1	1.50	1.50	4.000	3.9046	0.001277	0.398673	.286220	0.0357	0.6266	0.021385	1.33329
1	2.00	2.00	4.000	3.9046	0.000993	0.387227	.218482	0.0315	0.5720	0.006654	1.33329
1	2.50	2.50	4.000	3.9046	0.000809	0.280480	.187256	0.0284	0.5296	0.000676	1.33329
1	2.76	2.76	4.000	3.9046	0.000737	0.261085	.174302	0.0271	0.5110	0.00000	1.33329
1	3.00	3.00	4.000	3.9046	0.000681	0.245420	.163840	0.0261	0.4954	0.000465	1.33329
1	3.50	3.50	4.000	3.9046	0.000589	0.218151	.145630	0.0243	0.4671	0.003882	1.33329
1	4.00	4.00	4.000	3.9046	0.000520	0.196336	.131064	0.0220	0.4311	0.009466	1.33329
1	4.50	4.50	4.000	3.9046	0.000467	0.178487	.119147	0.0216	0.4225	0.016843	1.33329
1	6.00	6.00	4.000	3.9046	0.000361	0.140839	.093613	0.0190	0.3745	0.038477	1.33329
1	1.000	1.000	4.000	3.9046	0.000235	0.089843	.05153	0.0153	0.2867	0.082475	1.33329
1	0.00	0.00	5.000	4.0835	0.003171	0.3480	0.333100	0.0563	0.3899	0.189200	1.33320
1	.30	.30	5.000	4.0835	0.002647	0.314847	0.210780	0.0515	0.5611	0.151795	1.33325
1	.40	.40	5.000	4.0835	0.002231	0.284843	0.190639	0.0472	0.5337	0.180437	1.33325
1	.50	.50	5.000	4.0835	0.001896	0.257634	0.172388	0.0435	0.5076	0.094422	1.33325
1	1.00	1.00	5.000	4.0835	0.001395	0.210498	0.140797	0.0374	0.4588	0.055706	1.33325
1	1.50	1.50	5.000	4.0835	0.001007	0.168415	0.12612	0.0317	0.4104	0.024805	1.33325
1	2.00	2.00	5.000	4.0835	0.000775	0.140345	0.093822	0.0278	0.3746	0.007799	1.33325
1	2.50	2.50	5.000	4.0835	0.000626	0.120896	0.08406	0.0250	0.3468	0.000799	1.33325
1	2.76	2.76	5.000	4.0835	0.000568	0.111977	0.074841	0.0238	0.3446	0.00000	1.33325
1	3.00	3.00	5.000	4.0835	0.000524	0.105258	0.070347	0.0229	0.3244	0.000553	1.33325
1	3.50	3.50	5.000	4.0835	0.000451	0.093563	0.062526	0.0212	0.3059	0.004634	1.33325
1	4.00	4.00	5.000	4.0835	0.000397	0.084206	0.056270	0.0199	0.2902	0.011331	1.33325
1	4.50	4.50	5.000	4.0835	0.000356	0.076551	0.051153	0.0189	0.2767	0.019476	1.33325
1	6.00	6.00	5.000	4.0835	0.000275	0.060147	0.040190	0.0166	0.2452	0.046148	1.33325
1	1.000	1.000	5.000	4.0835	0.000182	0.038275	0.025577	0.0135	0.1956	0.101381	1.33325
1	0.00	0.00	6.000	4.1916	0.002709	0.1653	0.110000	0.0581	0.4046	0.210500	1.33310
1	.30	.30	6.000	4.1916	0.002245	0.148107	.099486	0.0474	0.3848	0.169882	1.33316
1	.40	.40	6.000	4.1916	0.001877	0.133398	.089554	0.0433	0.3660	0.135897	1.33316
1	.50	.50	6.000	4.1916	0.001582	0.121193	.081383	0.0398	0.3481	0.107271	1.33316
1	1.00	1.00	6.000	4.1916	0.001148	0.099019	.066395	0.0339	0.3147	0.064235	1.33316
1	1.50	1.50	6.000	4.1916	0.000816	0.079282	.053087	0.0286	0.2855	0.0289036	1.33316
1	2.00	2.00	6.000	4.1916	0.000621	0.066018	.044219	0.0249	0.2569	0.009843	1.33317
1	2.50	2.50	6.000	4.1916	0.000496	0.056586	.037889	0.0223	0.2379	0.000956	1.33317
1	2.76	2.76	6.000	4.1916	0.000449	0.052673	.035265	0.0212	0.2295	0.000000	1.33317
1	3.00	3.00	6.000	4.1916	0.000413	0.049513	.033146	0.0203	0.2235	0.000666	1.33317
1	3.50	3.50	6.000	4.1916	0.000354	0.044011	.029459	0.0188	0.2098	0.005610	1.33317
1	4.00	4.00	6.000	4.1916	0.000311	0.039609	.026310	0.0176	0.1990	0.013756	1.33317
1	4.50	4.50	6.000	4.1916	0.000278	0.036008	.024098	0.0167	0.1898	0.023677	1.33317
1	6.00	6.00	6.000	4.1916	0.000215	0.028289	.018933	0.0147	0.1682	0.056087	1.33317
1	1.000	1.000	6.000	4.1916	0.000144	0.018003	.012050	0.0120	0.1342	0.121008	1.33318
1	0.00	0.00	7.000	4.2611	0.002363	0.08566	0.056600	0.0486	0.3892	0.2333200	1.33310
1	.30	.30	7.000	4.2611	0.001939	0.075716	.051124	0.0440	0.3752	0.190303	1.33301
1	.40	.40	7.000	4.2611	0.001607	0.068499	.046202	0.0401	0.3617	0.153603	1.33301
1	.50	.50	7.000	4.2611	0.001343	0.061955	.041751	0.0366	0.3489	0.124202	1.33301
1	1.00	1.00	7.000	4.2611	0.000960	0.050619	.034066	0			

TABLE I. - Continued. TURBULENCE VELOCITY AND SCALE RATIOS

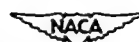
$$\left[v_1^2 = \frac{\left(\frac{q_1}{q_2}\right)^c}{\left(\frac{q_1}{q_2}\right)^A}, v_2^2 = \frac{\left(\frac{q_2}{q_1}\right)^c}{\left(\frac{q_2}{q_1}\right)^A}, M_B = 0.05 \right]$$



π	K	M_C	t_1	v_1^2	v_2^2	$\frac{1}{3}(v_1^2 + v_2^2)$	v_1	v_2	$\frac{(L_1)^C}{(L_1)^A}$	$\frac{(L_2)^C}{(L_2)^A}$	
2	0.20	0.40	0.023	0.464	0.785545	0.618041	0.673875	0.8863	0.7868	2.652738	
	0.40	0.80	0.023	0.464	371594	419605	0.403602	6096	6478	2.507957	
	1.00	1.00	0.023	0.464	178021	298374	258803	4219	5463	2.321231	
	1.20	2.00	0.023	0.464	044058	167113	128609	3099	4088	1.85393	
	1.50	3.00	0.023	0.464	010726	096034	0.675797	1036	3099	1.769190	
	2.00	4.00	0.023	0.464	004726	063441	0.43870	0687	2519	1.704544	
	3.00	6.00	0.023	0.464	002293	034304	0.836365	0479	1852	1.000472	
	6.00	12.00	0.023	0.464	001177	01177	0.07250	0387	1057	1.382594	
	0.20	0.40	0.040	0.800	0.585905	0.698921	0.661849	0.7654	0.8360	1.197477	
	0.40	0.80	0.040	0.800	294319	533812	453981	5485	7306	1.066106	
	1.00	1.20	0.040	0.800	150619	414747	326704	3883	924086	1.00574	
	1.50	2.00	0.040	0.800	024680	107781	106673	3065	5886	1.000000	
	2.00	3.00	0.040	0.800	011343	107781	109093	1663	3974	1.239743	
	3.00	6.00	0.040	0.800	004356	106705	072593	0661	036348	1.186599	
	6.00	12.00	0.040	0.800	001534	058374	039487	0393	2416	1.000238	
	0.20	0.40	0.060	0.1200	0.454888	0.868674	0.729245	0.6747	0.9310	0.585653	
	0.40	0.80	0.060	0.1200	347860	693157	544584	4973	8386	564129	
	1.00	1.20	0.060	0.1200	138272	556944	417587	3718	7463	1.15804	
	1.50	2.00	0.060	0.1200	047655	362462	257579	2183	6080	0.844613	
	2.00	3.00	0.060	0.1200	015875	837308	156850	1260	4766	0.578826	
	3.00	6.00	0.060	0.1200	006911	155745	106134	0831	3946	0.010807	
	6.00	12.00	0.060	0.1200	002885	086250	058824	0478	1935	0.000071	
	0.20	0.40	0.080	0.1200	0.008684	0.1200	0.02247	0224	14866	0.522445	
	0.40	0.80	0.080	0.1200	0.008684	0.1200	0.02247	0224	14866	0.522445	
	1.00	1.20	0.080	0.1200	0.008684	0.1200	0.02247	0224	14866	0.522445	
	1.50	2.00	0.080	0.1200	0.008684	0.1200	0.02247	0224	14866	0.522445	
	2.00	3.00	0.080	0.1200	0.008684	0.1200	0.02247	0224	14866	0.522445	
	3.00	6.00	0.080	0.1200	0.008684	0.1200	0.02247	0224	14866	0.522445	
	6.00	12.00	0.080	0.1200	0.008684	0.1200	0.02247	0224	14866	0.522445	
	0.20	0.40	0.100	0.2000	0.008684	0.1200	0.02247	0224	14866	0.522445	
	0.40	0.80	0.100	0.2000	0.008684	0.1200	0.02247	0224	14866	0.522445	
	1.00	1.20	0.100	0.2000	0.008684	0.1200	0.02247	0224	14866	0.522445	
	1.50	2.00	0.100	0.2000	0.008684	0.1200	0.02247	0224	14866	0.522445	
	2.00	3.00	0.100	0.2000	0.008684	0.1200	0.02247	0224	14866	0.522445	
	3.00	6.00	0.100	0.2000	0.008684	0.1200	0.02247	0224	14866	0.522445	
	6.00	12.00	0.100	0.2000	0.008684	0.1200	0.02247	0224	14866	0.522445	
	0.20	0.40	0.120	0.2000	0.008684	0.1200	0.02247	0224	14866	0.522445	
	0.40	0.80	0.120	0.2000	0.008684	0.1200	0.02247	0224	14866	0.522445	
	1.00	1.20	0.120	0.2000	0.008684	0.1200	0.02247	0224	14866	0.522445	
	1.50	2.00	0.120	0.2000	0.008684	0.1200	0.02247	0224	14866	0.522445	
	2.00	3.00	0.120	0.2000	0.008684	0.1200	0.02247	0224	14866	0.522445	
	3.00	6.00	0.120	0.2000	0.008684	0.1200	0.02247	0224	14866	0.522445	
	6.00	12.00	0.120	0.2000	0.008684	0.1200	0.02247	0224	14866	0.522445	
	0.20	0.40	0.140	0.2795	0.014613	1736805	1829408	04633	13179	0.867684	
	0.40	0.80	0.140	0.2795	138113	1420288	099892	3716	1919	1.160929	
	1.00	1.20	0.140	0.2795	091947	116094	080465	1023	1515	1.000000	
	1.50	2.00	0.140	0.2795	020974	114637	075871	1028	9798	0.548510	
	2.00	3.00	0.140	0.2795	016160	1343229	232866	1077	5859	0.000181	
	3.00	6.00	0.140	0.2795	004733	198728	130063	0688	4390	0.000006	
	6.00	12.00	0.140	0.2795	001081	0.68744	0.08190	0329	2884	0.530217	
	0.20	0.40	0.160	0.3400	0.160583	2193587	1515966	04007	4813	0.211060	
	0.40	0.80	0.160	0.3400	3589	107189	1794905	3274	13397	1.145452	
	1.00	1.20	0.160	0.3400	073890	1468001	1003897	8718	18116	0.993577	
	1.50	2.00	0.160	0.3400	037837	979547	656564	1945	9897	0.344457	
	2.00	3.00	0.160	0.3400	019006	626747	481463	1379	7920	0.070893	
	3.00	6.00	0.160	0.3400	004998	135086	20700	1168	1484	0.000047	
	6.00	12.00	0.160	0.3400	001024	0.79748	1.5645	0331	2884	0.530217	
	0.20	0.40	0.180	0.6724	0.069183	3911170	2850510	02630	15777	0.145311	
	0.40	0.80	0.180	0.6724	6724	49196	3210181	2150543	2218	17892	0.90273
	1.00	1.20	0.180	0.6724	035933	2618821	1757858	1896	16183	0.548384	
	1.50	2.00	0.180	0.6724	020270	1748177	11723208	1284	13822	0.183285	
	2.00	3.00	0.180	0.6724	011181	1119031	7474748	1587	0578	0.003430	
	3.00	6.00	0.180	0.6724	006945	777085	520371	0833	8815	0.000233	
	6.00	12.00	0.180	0.6724	003318	437090	392499	0576	6651	0.000002	
	0.20	0.40	0.200	0.6724	0.008539	148708	0.9218	0.0209	2071	0.000007	
	0.40	0.80	0.200	0.6724	0.008539	148708	0.9218	0.0209	2071	0.000007	
	1.00	1.20	0.200	0.6724	0.008539	148708	0.9218	0.0209	2071	0.000007	
	1.50	2.00	0.200	0.6724	0.008539	148708	0.9218	0.0209	2071	0.000007	
	2.00	3.00	0.200	0.6724	0.008539	148708	0.9218	0.0209	2071	0.000007	
	3.00	6.00	0.200	0.6724	0.008539	148708	0.9218	0.0209	2071	0.000007	
	6.00	12.00	0.200	0.6724	0.008539	148708	0.9218	0.0209	2071	0.000007	
	0.20	0.40	0.220	0.6724	0.008539	148708	0.9218	0.0209	2071	0.000007	
	0.40	0.80	0.220	0.6724	0.008539	148708	0.9218	0.0209	2071	0.000007	
	1.00	1.20	0.220	0.6724	0.008539	148708	0.9218	0.0209	2071	0.000007	
	1.50	2.00	0.220	0.6724	0.008539	148708	0.9218	0.0209	2071	0.000007	
	2.00	3.00	0.220	0.6724	0.008539	148708	0.9218	0.0209	2071	0.000007	
	3.00	6.00	0.220	0.6724	0.008539	148708	0.9218	0.0209	2071	0.000007	
	6.00	12.00	0.220	0.6724	0.008539	148708	0.9218	0.0209	2071	0.000007	
	0.20	0.40	0.240	0.6724	0.008539	148708	0.9218	0.0209	2071	0.000007	
	0.40	0.80	0.240	0.6724	0.008539	148708	0.9218	0.0209	2071	0.000007	
	1.00	1.20	0.240	0.6724	0.008539	148708	0.9218	0.0209	2071	0.000007	
	1.50	2.00	0.240	0.6724	0.008539	148708	0.9218	0.0209	2071	0.000007	
	2.00	3.00	0.240	0.6724	0.008539	148708	0.9218	0.0209	2071	0.000007	
	3.00	6.00	0.240	0.6724	0.008539	148708	0.9218	0.0209	2071	0.000007	
	6.00	12.00	0.240	0.6724	0.008539	148708	0.9218	0.0209	2071	0.000007	
	0.20	0.40	0.260	0.6724	0.008539	148708	0.9218	0.0209	2071	0.000007	
	0.40	0.80	0.260	0.6724	0.008539	148708	0.9218	0.0209	2071	0.000007	
	1.00	1.20	0.260	0.6724	0.008539	148708	0.9218	0.0209	2071	0.000007	
	1.50	2.00	0.260	0.6724	0.008539	148708	0.9218	0.0209	2071	0.000007	
	2.00	3.00	0.260	0.6724	0.008539	148708	0.9218	0.0209	2071	0.000007	
	3.00	6.00	0.260	0.6724	0.008539	148708	0.9218	0.0209	2071	0.000007	
	6.00	12.00	0.260	0.6724	0.008539	148708	0.9218	0.0209	2071	0.000007	
	0.20	0.40	0.280	0.6724	0.008539	148708	0.9218	0.0209	2071	0.000007	
	0.40	0.80	0.280	0.6724	0.008539	148708	0.9218	0.0209	2071	0.000007	
	1.00	1.20	0.280	0.6724	0.008539	148708	0.9218	0.0209	2071	0.000007	
	1.50	2.00	0.280	0.6724	0.008539	148708	0.9218	0.0209	2071	0.000007	
	2.00	3.00	0.280	0.6724	0.008539	148708	0.9218	0.0209	2071	0.000007	
	3.00	6.00	0.280	0.6724	0.008539	148708	0.9218	0.0209	2071	0.000007	
	6.00	12.00	0.280	0.6724	0.008539	148708	0.9218	0.0209	2071	0.000007	
	0.20	0.40	0.300	0.6724	0.008539	148708	0.9218	0.0209	2071	0.000007	
	0.40	0.80	0.300	0.6724	0.008539	148708	0.9218	0.0209	2071	0.000007	
	1.00	1.20	0.300	0.6724	0.008539	148708	0.9218	0.0209	2071	0.000007	
	1.50	2.00	0.300	0.6724	0.008539	148708	0.9218	0.0209	2071	0.000007	
	2.00	3.00	0.300	0.6724	0.008539	148708	0				

TABLE I. - Continued. TURBULENCE VELOCITY AND SCALE RATIOS

$$V_1^2 = \frac{(q_1^2)^C}{(q_1^2)^A} N, V_2^2 = \frac{(q_2^2)^C}{(q_2^2)^A} N_B = 0.05$$



N	K	MK	μ_C	i_1	V_1^2	V_2^2	$\frac{1}{3}(V_1^2 + 2V_2^2)$	V_1	V_2	$\frac{(L_1)^C}{(L_1)^A}$	$\frac{(L_2)^C}{(L_2)^A}$
3	0.20	0.60	0.023	0.464	0.540040	0.506067	0.517391	0.7349	0.7114	2.585687	0.6795
3	.40	1.20	.023	.464	.179071	.298411	.358631	.4232	.5463	2.332176	.8533
3	.60	1.80	.023	.464	.062658	.191382	.148474	.2503	.4375	1.969100	.9845
3	1.00	3.00	.023	.464	.0106829	.090657	.064048	.1041	.3011	1.3335	
3	1.50	4.50	.023	.464	.003090	.043429	.0299829	.0556	.2084	1.08468	1.2119
3	2.00	6.00	.023	.464	.001602	.0024431	.016821	.0400	.1563	0.082965	1.2467
3	3.00	9.00	.023	.464	.000655	.010061	.00627	.0256	.1003	0.000001	1.2771
3	0.20	0.60	0.040	0.800	0.414559	0.609296	0.544384	0.439	0.7806	1.134084	0.7786
3	.40	1.20	.040	.800	.150915	.414814	.3865	.6441	.931719	1.0579	
3	.60	1.80	.040	.800	.057959	.290588	.213058	.2408	.5391	.716850	1.1174
3	1.00	3.00	.040	.800	.010863	.149045	.108945	.1042	.3861	.313094	1.1888
3	1.50	4.50	.040	.800	.002433	.073531	.049838	.0493	.2712	.046378	1.3335
3	2.00	6.00	.040	.800	.000948	.0417282	.028130	.0308	.2043	.001686	1.3581
3	3.00	9.00	.040	.800	.000297	.017244	.011595	.0179	.1313	0.000000	1.3842
3	0.20	0.60	0.060	0.1300	0.334881	0.774595	0.627824	0.5782	0.8801	0.625219	1.1468
3	.40	1.20	.060	1.200	.138245	.557192	.417843	.3718	.7465	.458149	1.1806
3	.60	1.80	.060	1.200	.061227	.403982	.389731	.3474	.6356	.301609	1.2048
3	1.00	3.00	.060	1.200	.014901	.214731	.148121	.1221	.4634	.101467	1.2633
3	1.50	4.50	.060	1.200	.003837	.107935	.073836	.0619	.3285	.013076	1.2597
3	2.00	6.00	.060	1.200	.001410	.061748	.041635	.0375	.2485	.000504	1.2743
3	3.00	9.00	.060	1.200	.000348	.025715	.017859	.0187	.1604	0.000000	1.2909
3	0.20	0.60	0.100	0.2000	0.233820	1.159982	0.851261	0.4835	1.0770	0.322197	1.3715
3	.40	1.20	.100	2.000	.114535	.854734	.608001	.3384	.9245	.196781	1.3778
3	.60	1.80	.100	2.000	.060266	.630013	.440097	.2455	.7937	.110453	1.3887
3	1.00	3.00	.100	2.000	.019742	.341681	.234368	.1405	.5845	.027607	1.3900
3	1.50	4.50	.100	2.000	.006456	.174120	.118232	.0804	.4173	.008801	1.3965
3	2.00	6.00	.100	2.000	.002674	.100394	.067821	.0517	.3169	.000096	1.3013
3	3.00	9.00	.100	2.000	.000700	.048144	.028389	.0265	.2053	0.000000	1.3077
3	0.20	0.60	0.140	0.2795	0.171388	1.370760	1.104303	0.4140	1.8533	0.284697	1.3070
3	.40	1.20	.140	2.795	.0911893	1.161718	.805110	.3031	1.0778	.125338	1.3086
3	.60	1.80	.140	2.795	.058607	.858724	.590010	.2294	.9267	.064181	1.3100
3	1.00	3.00	.140	2.795	.019738	.467611	.318320	.1405	.6838	.014115	1.3121
3	1.50	4.50	.140	2.795	.007263	.239110	.161828	.0852	.4890	.001273	1.3148
3	2.00	6.00	.140	2.795	.003261	.138196	.093818	.0571	.3717	.000040	1.3159
3	3.00	9.00	.140	2.795	.000943	.058187	.039106	.0307	.2412	0.000000	1.3184
3	0.20	0.60	0.180	0.3589	0.130623	1.984489	1.366534	0.3614	1.4087	0.178804	1.3200
3	.40	1.20	.180	3.589	.073861	1.648924	.1003903	.2718	.12120	.094578	1.3305
3	.60	1.80	.180	3.589	.044337	.1086540	.739139	.2106	.10484	.046545	1.3310
3	1.00	3.00	.180	3.589	.017917	.592291	.400833	.1339	.7696	.009430	1.3317
3	1.50	4.50	.180	3.589	.007045	.303168	.204461	.0839	.5506	.000796	1.3325
3	2.00	6.00	.180	3.589	.003323	.175357	.118018	.0576	.4188	.000000	1.3331
3	3.00	9.00	.180	3.589	.001027	.071919	.049682	.0380	.2719	0.000000	1.3343
3	0.20	0.60	0.240	0.6724	0.058380	3.388875	2.378623	0.2411	1.4087	0.178804	1.3311
3	.40	1.20	.240	6.724	.035932	2.680464	.1758954	.1896	.16188	.0553386	1.3311
3	.60	1.80	.240	6.724	.023271	.1958945	.130035	.1525	.139285	.085866	1.3311
3	1.00	3.00	.240	6.724	.010561	.1057512	.708529	.1028	.10884	.004558	1.3312
3	1.50	4.50	.240	6.724	.004615	.541593	.362600	.0679	.7359	.000346	1.3312
3	2.00	6.00	.240	6.724	.002363	.313411	.209728	.0486	.5598	.0000010	1.3312
3	3.00	9.00	.240	6.724	.000826	.132212	.088417	.0287	.3636	0.000000	1.3312
3	0.20	0.60	0.500	0.9761	0.033565	4.089388	3.171447	0.1838	2.1930	0.094079	1.3325
3	.40	1.20	.500	9.761	.021424	3.561311	2.381348	.1464	1.8871	.044083	1.3326
3	.60	1.80	.500	9.761	.014238	2.635133	1.761508	.1193	1.6833	.019596	1.3325
3	1.00	3.00	.500	9.761	.006716	1.437254	.960408	.0819	1.1989	.003408	1.3326
3	1.50	4.50	.500	9.761	.003040	.736096	.491744	.0551	.8580	.000249	1.3326
3	2.00	6.00	.500	9.761	.001601	.425979	.284520	.0400	.6587	.0000007	1.3326
3	3.00	9.00	.500	9.761	.000585	.179708	.120000	.0242	.4839	0.000000	1.3326
3	0.20	0.60	1.000	1.8262	0.012142	6.440788	4.397906	0.0108	2.5379	0.074309	1.3332
3	.40	1.20	1.000	1.8262	.008001	.4769367	.318245	.0084	2.1839	.033785	1.3332
3	.60	1.80	1.000	1.8262	.005453	.3529023	.2354499	.0738	1.8786	.014620	1.3332
3	1.00	3.00	1.000	1.8262	.002667	.1928408	.1284095	.0516	1.3874	.003447	1.3332
3	1.50	4.50	1.000	1.8262	.001248	.985804	.657619	.0353	.9929	.000174	1.3332
3	2.00	6.00	1.000	1.8262	.000675	.570488	.380550	.0260	.7553	.0000005	1.3332
3	3.00	9.00	1.000	1.8262	.000857	.240674	.160535	.0160	.4906	0.000000	1.3332
3	0.20	0.60	2.000	2.9822	0.004836	5.475824	3.632859	0.0838	2.3400	0.069981	1.3332
3	.40	1.20	2.000	2.9822	.003211	4.054817	2.704744	.0678	2.0137	.031508	1.3332
3	.60	1.80	2.000	2.9822	.002800	.2091175	.1394850	.0567	1.7321	.013584	1.3332
3	1.00	3.00	2.000	2.9822	.001065	.1140575	.760745	.0329	1.0680	.002256	1.3332
3	1.50	4.50	2.000	2.9822	.000511	.584153	.389606	.0226	.7643	.000159	1.3332
3	2.00	6.00	2.000	2.9822	.000278	.318052	.1885460	.0167	.5814	.0000004	1.3332
3	3.00	9.00	2.000	2.9822	.000107	.1426126	.093026	.0103	.2776	0.000000	1.3332
3	0.20	0.60	3.000	3.5866	0.003408	1.3810242	1.015051	0.0857	1.833	0.075878	1.3331
3	.40	1.20	3.000	3.5866	.002045	.1126308	.751554	.0452	1.0613	.034216	1.3331
3	.60	1.80	3.000	3.5866	.001392	.6333395	.556060	.0373	.9129	.014851	1.3331
3	1.00	3.000	3.000	3.5866	.000680	.454553	.303262	.0261	.6742	.0024490	1.3331
3	1.50	4.50	3.000	3.5866	.000318	.232802	.155307	.0178	.4825	.000177	1.3331
3	2.00	6.00	3.000	3.5866	.000171	.134724	.089873	.0131	.3670	.000005	1.3331
3	3.00	9.00	3.000	3.5866	.000063	.036836	.077933	.0082	.2384	0.000000	1.3331
3	0.20	0.60	5.000	4.0835	0.001897	2.527763	2.072475	0.0436	0.567	0.095180	1.3325
3	.40	1.20	5.000	4.0835	.001209	.190872	.127651	.0348	.4369	.044644	1.3325
3	.60	1.80	5.000	4.0835	.000802	.141232	.094422	.0283	.3758	.019878	1.3325
3	1.00	3.00	5.000	4.0835	.000378	.077031	.051480	.0194	.2775	.003456	1.3325
3	1.50	4.50	5.000	4.0835	.000171	.039452	.026358	.0131	.1986	.0002854	1.3325
3	2.00	6.00	5.000	4.0835	.000090	.022831	.015250	.0095	.1511	.000007	1.3325
3	3.00	9.00	5.000	4.0835	.000033	.009632	.006432	.0057	.0281	0.000000	1.3325
3	0.20	0.60	7.000	4.2611	0.001544	0.61987	0.41772	0.0367	0.3490	0.123896	1.3301
3	.40	1.20	7.000	4.2611	.000820	.045899	.030873	.0286	.2148	.060441	1.3302
3	.										

TABLE I. - Concluded. TURBULENCE VELOCITY AND SCALE RATIOS

$$v_1^2 = \frac{(\overline{q_1^2})^c}{(\overline{q_1^2})^A}, v_2^2 = \frac{(\overline{q_2^2})^c}{(\overline{q_2^2})^A}, M_B = 0.05$$



N	K	M _X	M _C	t ₁	v ₁ ²	v ₂ ²	$\frac{1}{3}(v_1^2 + 2v_2^2)$	v ₁	v ₂	$\frac{(L_1)^c}{(L_1)^A}$	$\frac{(L_2)^c}{(L_2)^A}$
4	0.20	0.80	0.023	0.464	0.372531	0.419630	0.403930	0.6104	0.6478	2.511752	0.7415
4	.40	1.60	.023	0.464	0.088571	0.20316	0.176401	0.2976	0.4694	2.118971	.9461
4	.60	2.40	.023	0.464	0.024446	1.297283	0.094631	1.564	3.5602	1.506345	1.0754
4	1.00	4.00	.023	0.464	0.004133	0.502064	0.036087	0.643	2.2882	3.16765	1.1940
4	1.50	6.00	.023	0.464	0.001340	0.020415	0.014057	0.366	1.429	.010418	1.8478
4	2.00	8.00	.023	0.464	0.000687	0.009659	0.006648	0.093	0.000076	1.2719	
4	3.00	12.00	.023	0.464	0.000196	0.003004	0.002068	0.140	0.548	0.000000	1.2939
4	0.20	0.80	0.040	0.800	0.294622	0.533282	0.454089	0.5488	0.7306	1.069313	1.0045
4	.40	1.60	.040	0.800	0.0792895	0.326488	0.244090	0.2816	0.5714	0.794642	1.1003
4	.60	2.40	.040	0.800	0.028570	0.207318	0.147735	1.690	4.553	4.33953	1.1596
4	1.00	4.00	.040	0.800	0.003558	0.0767652	0.059621	0.596	2.8961	1.23891	1.2823
4	1.50	6.00	.040	0.800	0.001634	0.034873	0.023793	0.404	1.867	0.02877	1.2589
4	2.00	8.00	.040	0.800	0.000291	0.016564	0.011139	0.171	1.287	0.000055	1.2788
4	3.00	12.00	.040	0.800	0.000807	0.005156	0.003507	0.144	0.718	0.000000	1.2992
4	0.20	0.80	0.060	1.800	0.247292	0.693267	0.544608	0.4973	0.8286	0.566333	1.1594
4	.40	1.60	.060	1.800	0.079644	0.449581	0.326269	0.2882	0.6705	0.351702	1.1977
4	.60	2.40	.060	1.800	0.0289065	0.294652	0.206123	1.705	5.42	1.89625	1.2823
4	1.00	4.00	.060	1.800	0.005464	0.126129	0.084241	0.739	3.580	0.35861	1.2534
4	1.50	6.00	.060	1.800	0.001149	0.051638	0.034808	0.339	2.827	0.001818	1.2744
4	2.00	8.00	.060	1.800	0.000361	0.024658	0.016559	0.190	1.572	0.000020	1.2870
4	3.00	12.00	.060	1.800	0.000970	0.007718	0.005169	0.083	0.879	0.000000	1.3011
4	0.20	0.80	0.100	2.000	0.183255	1.047693	0.759380	0.4875	1.0236	0.276830	1.3738
4	.40	1.60	.100	2.000	0.074048	0.972804	0.698885	0.721	0.815	1.363556	1.8818
4	.60	2.40	.100	2.000	0.035989	0.649998	0.521198	0.833	4.619	0.59130	1.2867
4	1.00	4.00	.100	2.000	0.008663	0.059572	0.040202	0.931	4.538	0.008154	1.2845
4	1.50	6.00	.100	2.000	0.002214	0.039723	0.026719	0.471	1.898	0.000340	1.3011
4	2.00	8.00	.100	2.000	0.000747	0.040349	0.027149	0.273	2.009	0.000004	1.3059
4	3.00	12.00	.100	2.000	0.000141	0.013706	0.008518	0.119	1.127	0.000000	1.3121
4	0.20	0.80	0.140	2.795	0.238086	1.420634	0.993118	0.5108	1.1519	0.186881	1.3076
4	.40	1.60	.140	2.795	0.0629288	0.956311	0.654517	0.708	0.9716	0.882020	1.3095
4	.60	2.40	.140	2.795	0.031611	0.635245	0.434034	0.778	0.7970	0.382127	1.3111
4	1.00	4.00	.140	2.795	0.009446	0.282570	0.191528	0.978	5.316	0.003823	1.3135
4	1.50	6.00	.140	2.795	0.002721	0.115987	0.077965	0.582	1.400	0.000142	1.3158
4	2.00	8.00	.140	2.795	0.000996	0.055665	0.037442	0.316	2.359	0.000001	1.3176
4	3.00	12.00	.140	2.795	0.000307	0.017577	0.01787	0.144	1.326	0.000000	1.3803
4	0.20	0.80	0.180	3.589	0.107175	1.795354	1.233287	0.3874	1.3599	0.146030	1.3802
4	.40	1.60	.180	3.589	0.0528254	1.202174	0.818668	0.2886	1.0964	0.59904	1.3808
4	.60	2.40	.180	3.589	0.0277670	0.804234	0.545410	1.666	0.8968	0.882187	1.3814
4	1.00	4.00	.180	3.589	0.008997	0.358159	0.241772	0.948	5.985	0.02434	1.3283
4	1.50	6.00	.180	3.589	0.0036685	0.146665	0.098672	0.518	3.893	0.000087	1.3831
4	2.00	8.00	.180	3.589	0.001072	0.070690	0.047484	0.327	2.659	0.000001	1.3838
4	3.00	12.00	.180	3.589	0.000240	0.02347	0.014978	0.155	1.495	0.000000	1.3850
4	0.20	0.80	0.340	6.724	0.049196	1.202019	2.151078	0.2818	1.7894	0.906358	1.3311
4	.40	1.60	.340	6.724	0.0267690	2.145072	1.438978	1.637	1.4646	0.332991	1.3311
4	.60	2.40	.340	6.724	0.015537	1.435571	0.962236	1.246	1.1982	0.11394	1.3311
4	1.00	4.00	.340	6.724	0.005717	0.639715	0.428383	0.756	7.998	0.01091	1.3313
4	1.50	6.00	.340	6.724	0.001981	0.262123	0.175409	0.445	5.120	0.000034	1.3313
4	2.00	8.00	.340	6.724	0.000837	0.126404	0.084549	0.289	3.555	0.000000	1.3313
4	3.00	12.00	.340	6.724	0.000215	0.039293	0.026733	0.147	3.000	0.000000	1.3314
4	0.20	0.80	0.500	9.761	0.028736	4.351619	2.910658	0.1695	2.0861	0.736357	1.3325
4	.40	1.60	.500	9.761	0.0162624	2.915262	1.948929	1.275	1.7074	0.26085	1.3325
4	.60	2.40	.500	9.761	0.009712	1.951048	1.303936	0.985	1.3968	0.08575	1.3325
4	1.00	4.00	.500	9.761	0.003726	0.869446	0.580873	0.610	9.324	0.000795	1.3326
4	1.50	6.00	.500	9.761	0.001342	0.356268	0.237959	0.366	5.969	0.000024	1.3326
4	2.00	8.00	.500	9.761	0.000585	0.171810	0.114735	0.242	4.145	0.000000	1.3326
4	3.00	12.00	.500	9.761	0.000158	0.054361	0.036293	0.126	2.372	0.000000	1.3326
4	0.20	0.80	1.000	18.362	0.010515	5.82744	3.888668	0.1223	3.4141	0.57497	1.3328
4	.40	1.60	1.000	18.362	0.006181	1.904175	2.604843	0.786	1.9759	0.19565	1.3333
4	.60	2.40	1.000	18.362	0.003795	2.612189	1.743191	0.616	1.6164	0.062669	1.3333
4	1.00	4.00	1.000	18.362	0.001504	1.164390	0.776761	0.388	1.0791	0.005633	1.3333
4	1.50	6.00	1.000	18.362	0.000565	0.317129	0.318275	0.338	6.907	0.000016	1.3333
4	2.00	8.00	1.000	18.362	0.000284	0.230097	0.153483	0.159	4.797	0.000000	1.3333
4	3.00	12.00	1.000	18.362	0.000072	0.072804	0.048560	0.085	2.698	0.000000	1.3333
4	0.20	0.80	1.500	24.920	0.005017	4.954627	2.105060	0.0776	2.2829	0.539623	1.3333
4	.40	1.60	1.500	24.920	0.003566	1.219249	2.214021	0.597	1.8819	0.183099	1.3333
4	.60	2.40	1.500	24.920	0.0020203	2.2211425	1.481684	0.469	1.1904	0.057999	1.3333
4	1.00	4.00	1.500	24.920	0.0008867	0.989948	0.660257	0.898	3.950	0.005148	1.3333
4	1.50	6.00	1.500	24.920	0.0003534	0.405646	0.270542	0.183	6.369	0.000048	1.3333
4	2.00	8.00	1.500	24.920	0.0001534	0.195624	0.130466	0.123	1.4283	0.000000	1.3333
4	3.00	12.00	1.500	24.920	0.0000423	0.061926	0.042429	0.066	2.6408	0.000000	1.3333
4	0.20	0.80	2.000	29.8282	0.0004290	4.453316	2.2043611	0.0476	1.8583	0.539270	1.3325
4	.40	1.60	2.000	29.8282	0.002490	2.1313477	1.543148	0.397	1.5810	0.182124	1.3325
4	.60	2.40	2.000	29.8282	0.001538	1.548307	1.032777	0.392	1.2443	0.058000	1.3325
4	1.00	4.00	2.000	29.8282	0.000619	0.689977	0.460191	0.895	0.8306	0.000513	1.3325
4	1.50	6.00	2.000	29.8282	0.000233	1.0882730	0.188564	0.153	5.317	0.000015	1.3325
4	2.00	8.00	2.000	29.8282	0.0001058	1.36348	0.090933	0.103	1.693	0.000000	1.3325
4	3.00	12.00	2.000	29.8282	0.000018	0.17193	0.011468	0.043	1.311	0.000000	1.3325
4	0.20	0.80	3.000	3.5866	0.0003690	1.376249	0.918396	0.0519	1.1731	0.58876	1.3333
4	.40	1.60	3.000	3.5866	0.001578	0.918198	0.615185	0.397	0.962	0.19867	1.3333
4	.60	2.40	3.000	3.5866	0.000968	0.617046	0.416868	0.311	0.785	0.06374	1.3333
4	1.00	4.00	3.000	3.5866	0.000386	0.27497					

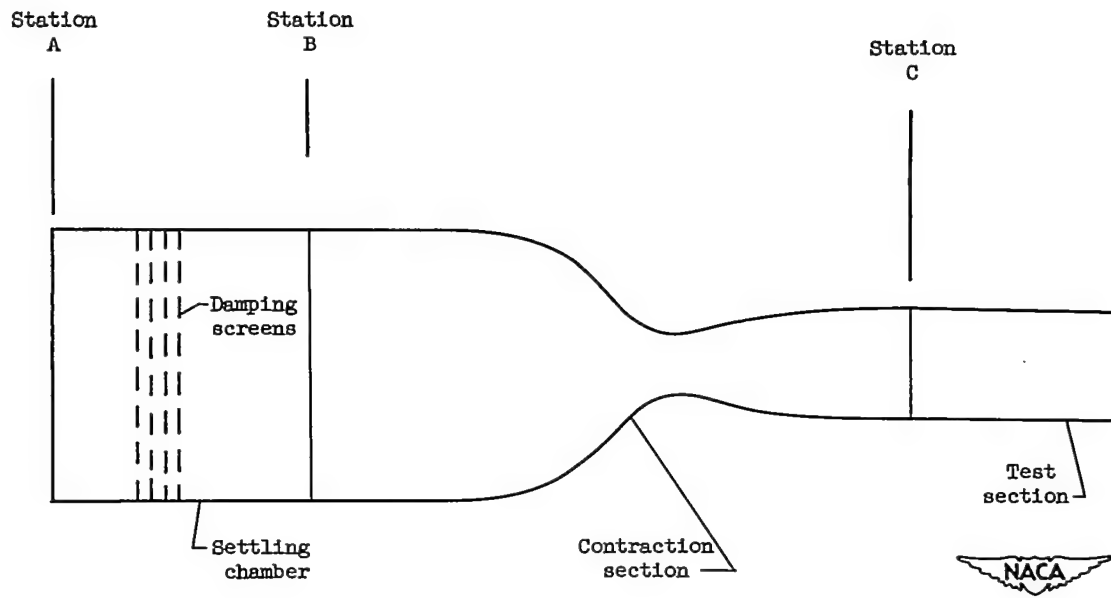


Figure 1. - Configuration treated in analysis.

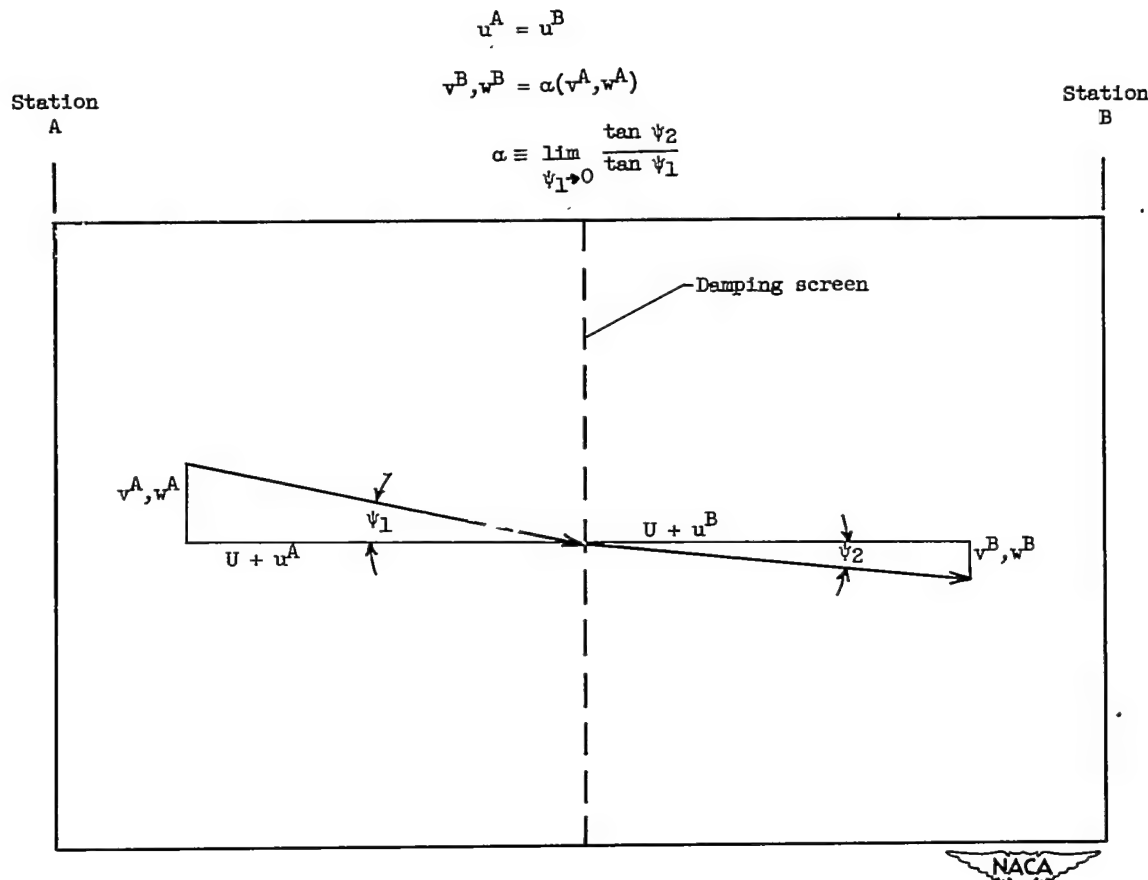


Figure 2. - Action of damping screen on components of combined turbulent and induced velocities at screen.

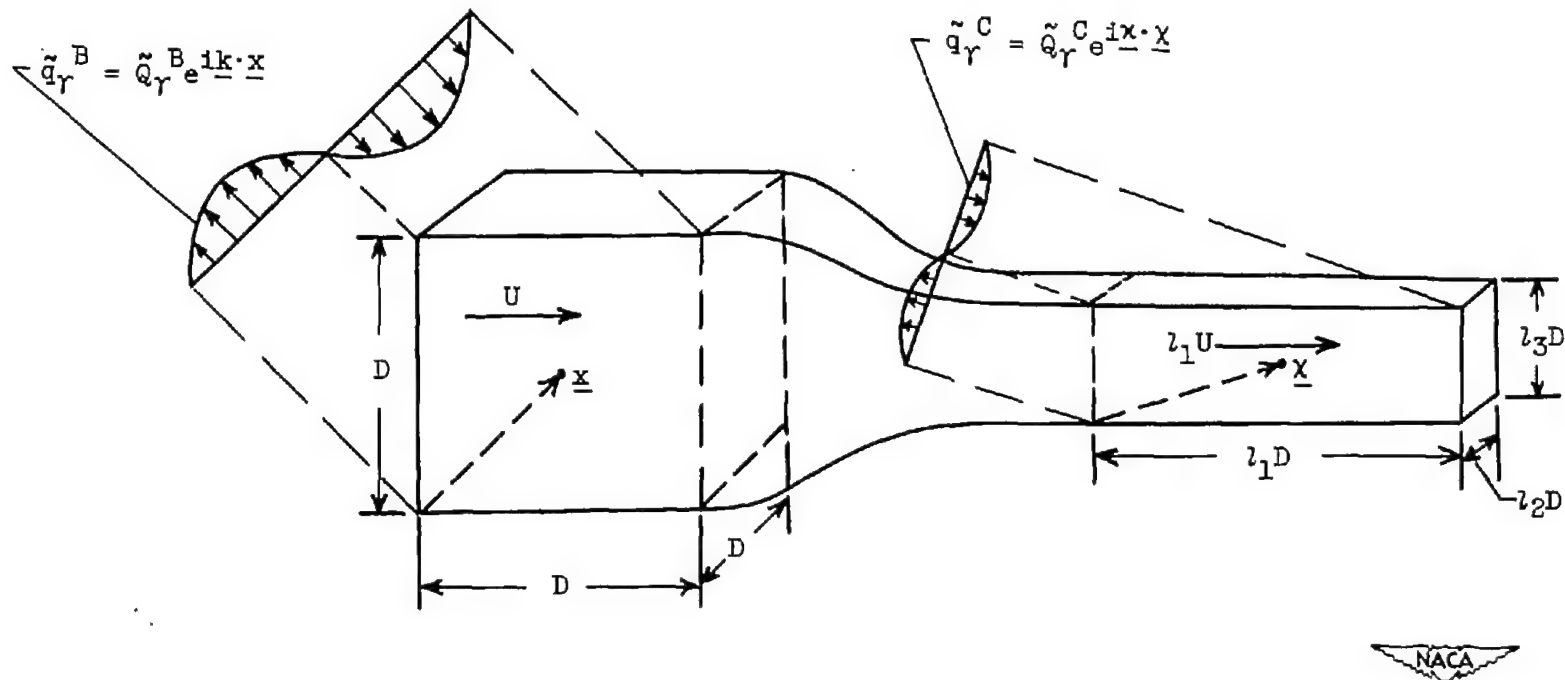
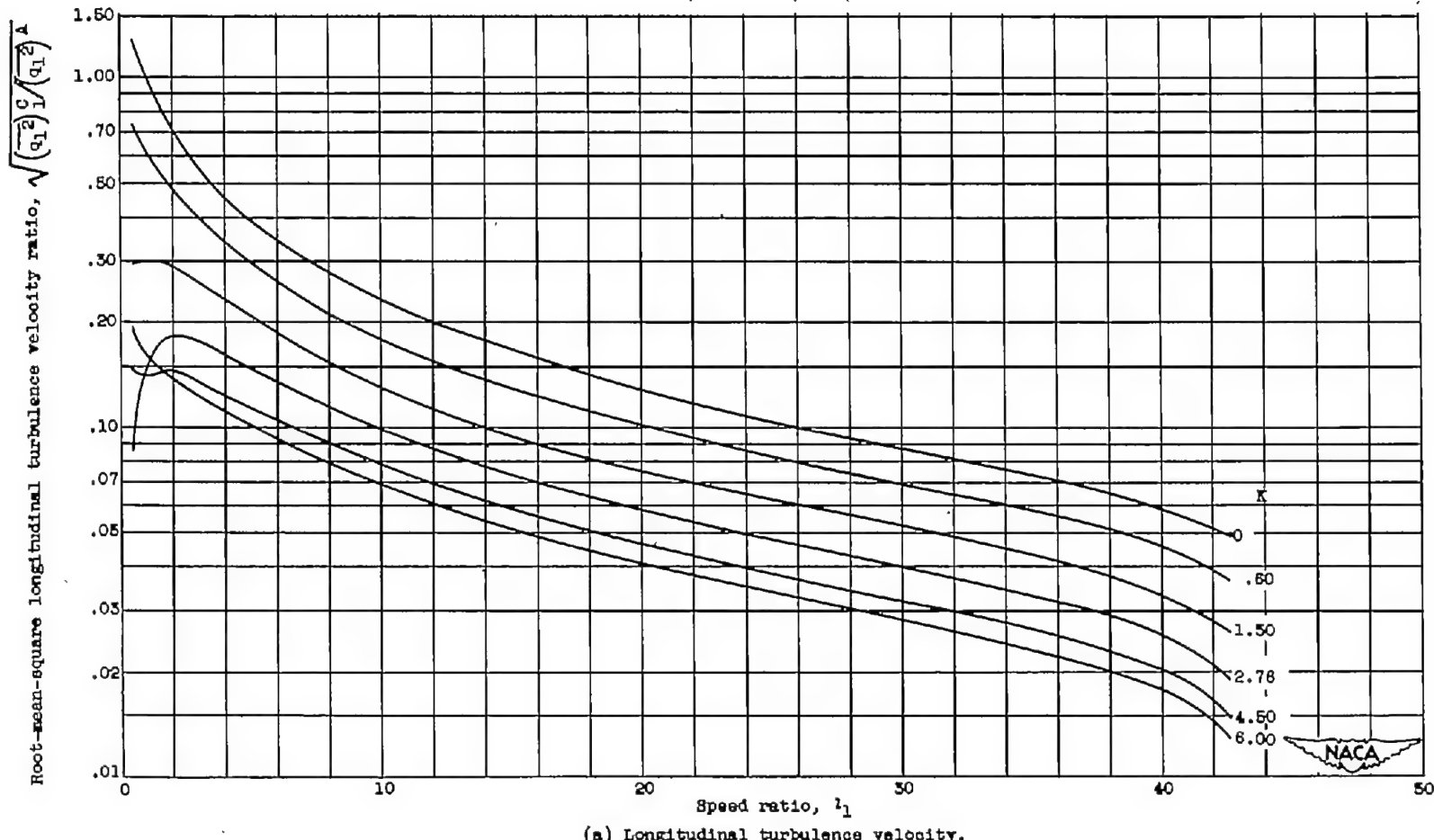
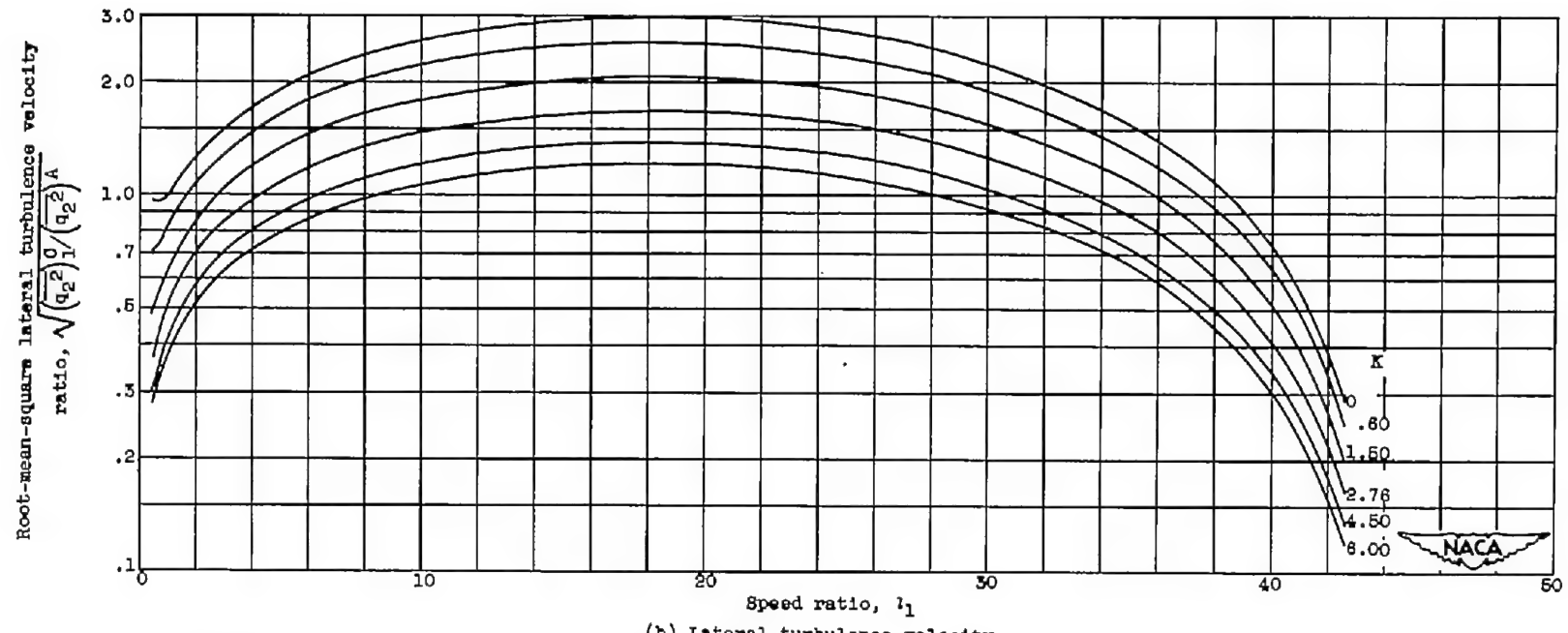


Figure 3. - Typical fluid-element- and plane-wave distortions resulting from stream convergence.



(a) Longitudinal turbulence velocity.

Figure 4. - Variation of root-mean-square turbulence velocity ratio with speed ratio (M_B of 0.05) and screen pressure-drop coefficient K in absence of turbulence decay for single-screen-axisymmetric-contraction configurations with upstream isotropic turbulence.



(b) Lateral turbulence velocity.

Figure 4. - Concluded. Variation of root-mean-square turbulence velocity ratio with speed ratio (M_B of 0.05) and screen pressure-drop coefficient K in absence of turbulence decay for single-screen-axisymmetric-contraction configurations with upstream isotropic turbulence.

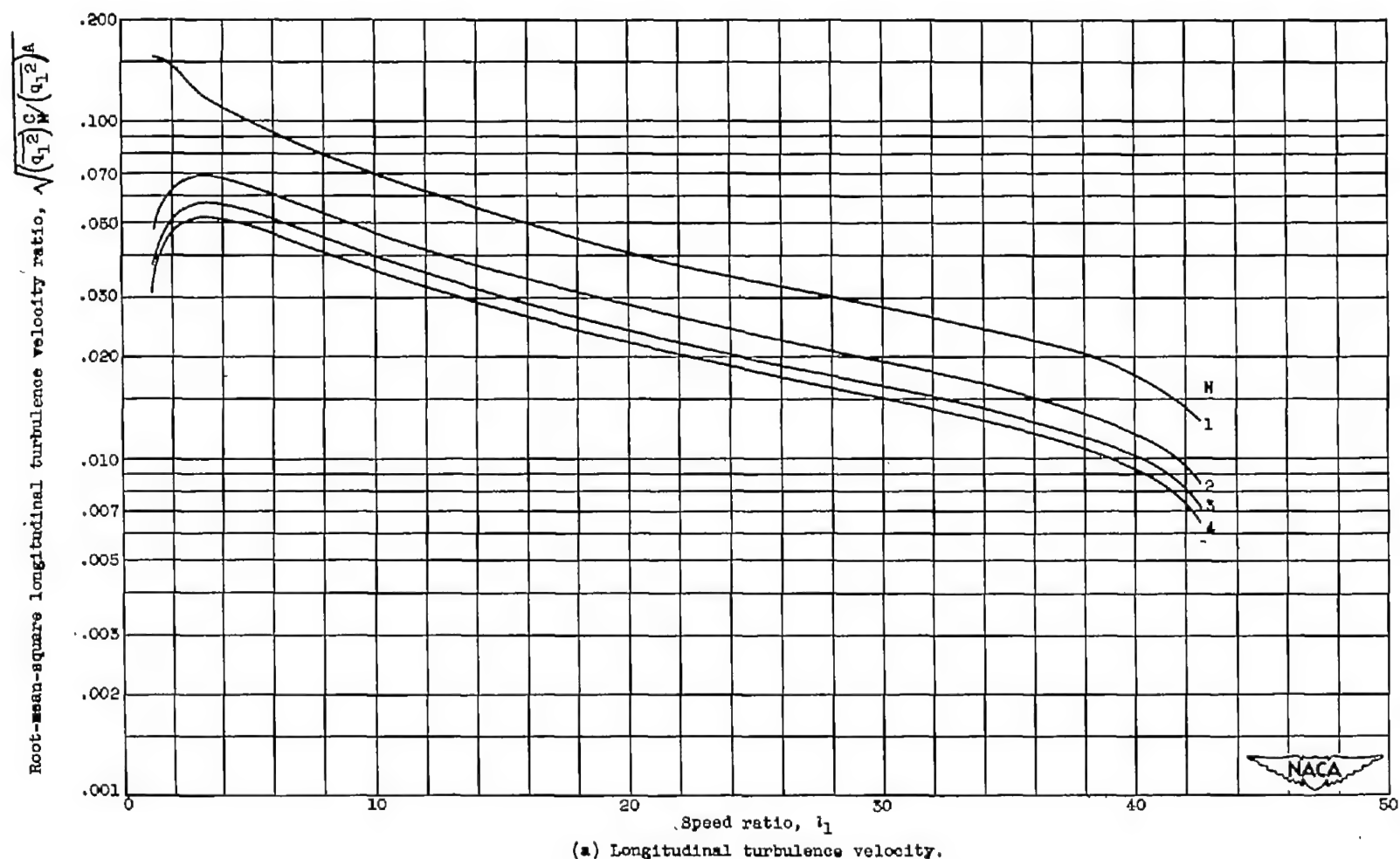


Figure 5. - Effect of multiple screens N and speed ratio (N_B of 0.05) on root-mean-square turbulence velocity ratio in absence of turbulence decay for screen-axisymmetric-contraction configurations with upstream isotropic turbulence and constant screen losses. Over-all screen pressure-drop coefficient, NK , 8.

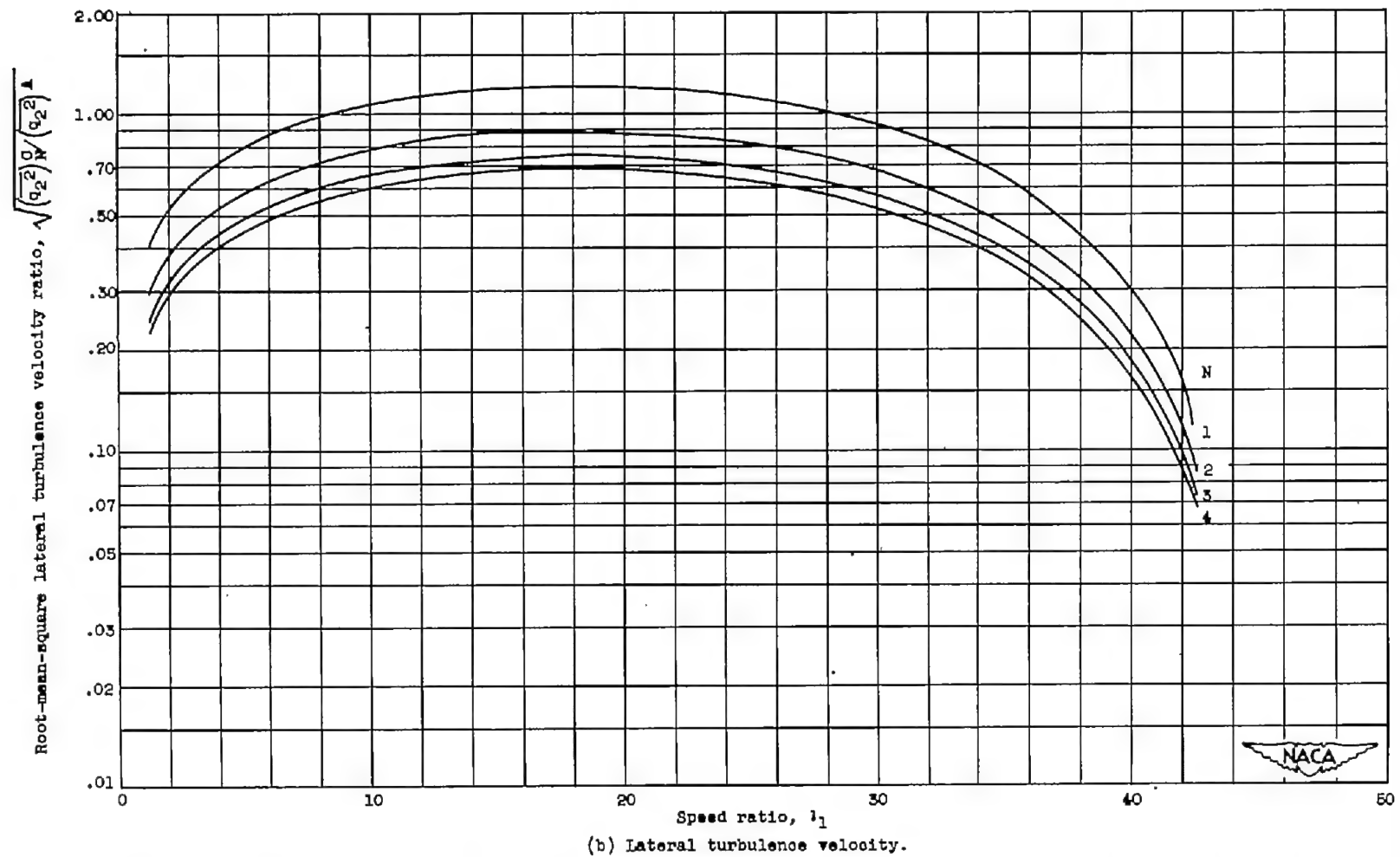


Figure 5. - Concluded. Effect of multiple screens N and speed ratio (M_B of 0.05) on root-mean-square turbulence velocity ratio in absence of turbulence decay for screen-axisymmetric-contraction configurations with upstream isotropic turbulence and constant screen losses. Over-all screen pressure-drop coefficient, MK , 6.

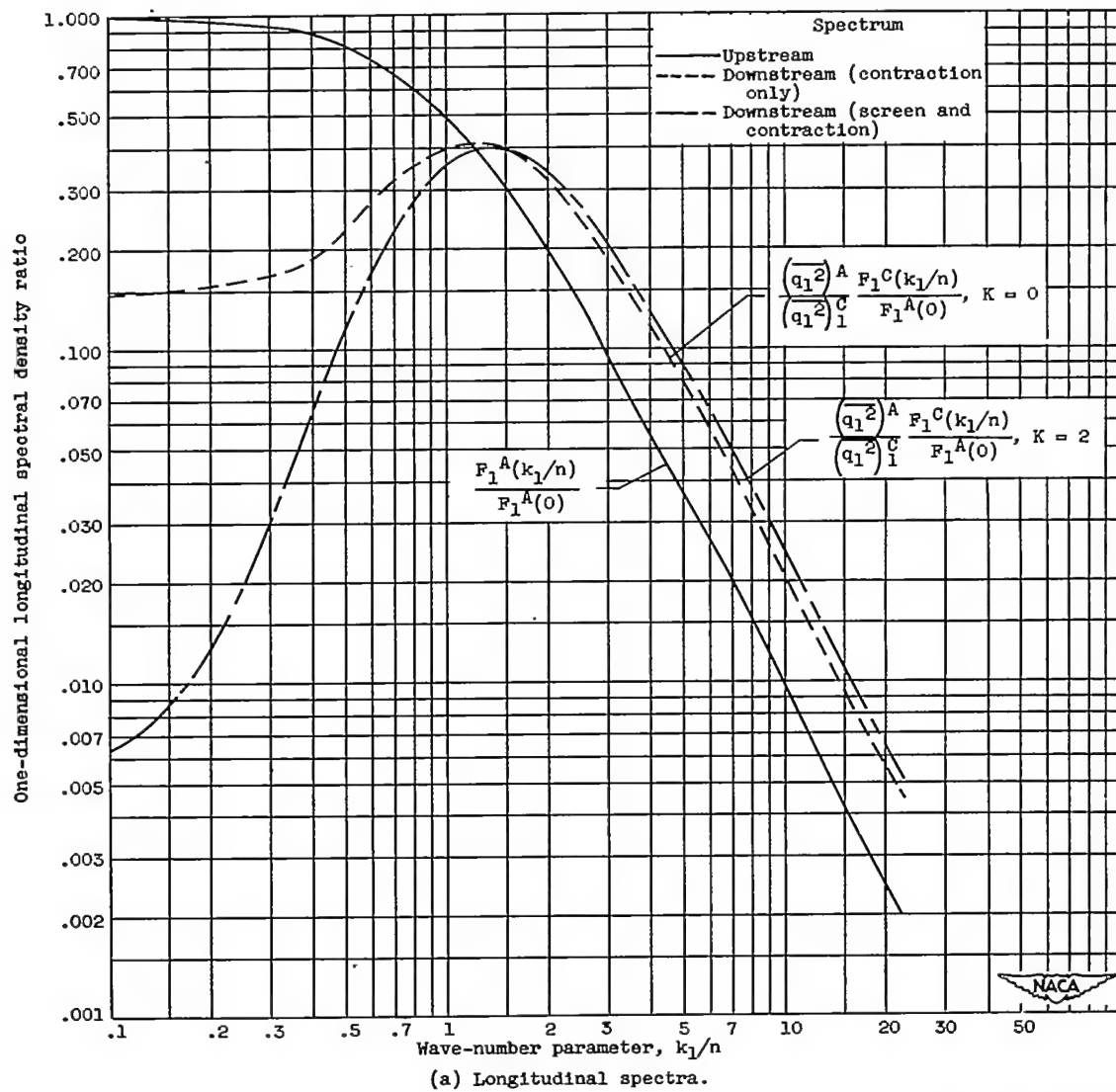


Figure 6. - Comparison of one-dimensional spectra in absence of turbulence decay for contraction and for single-screen-contraction configurations for upstream isotropic turbulence having amplitude function $G(k) = H(k^2 + n^2)^{-3}$. M_B , 0.05; M_C , 2.00; l_1 , 29.822.

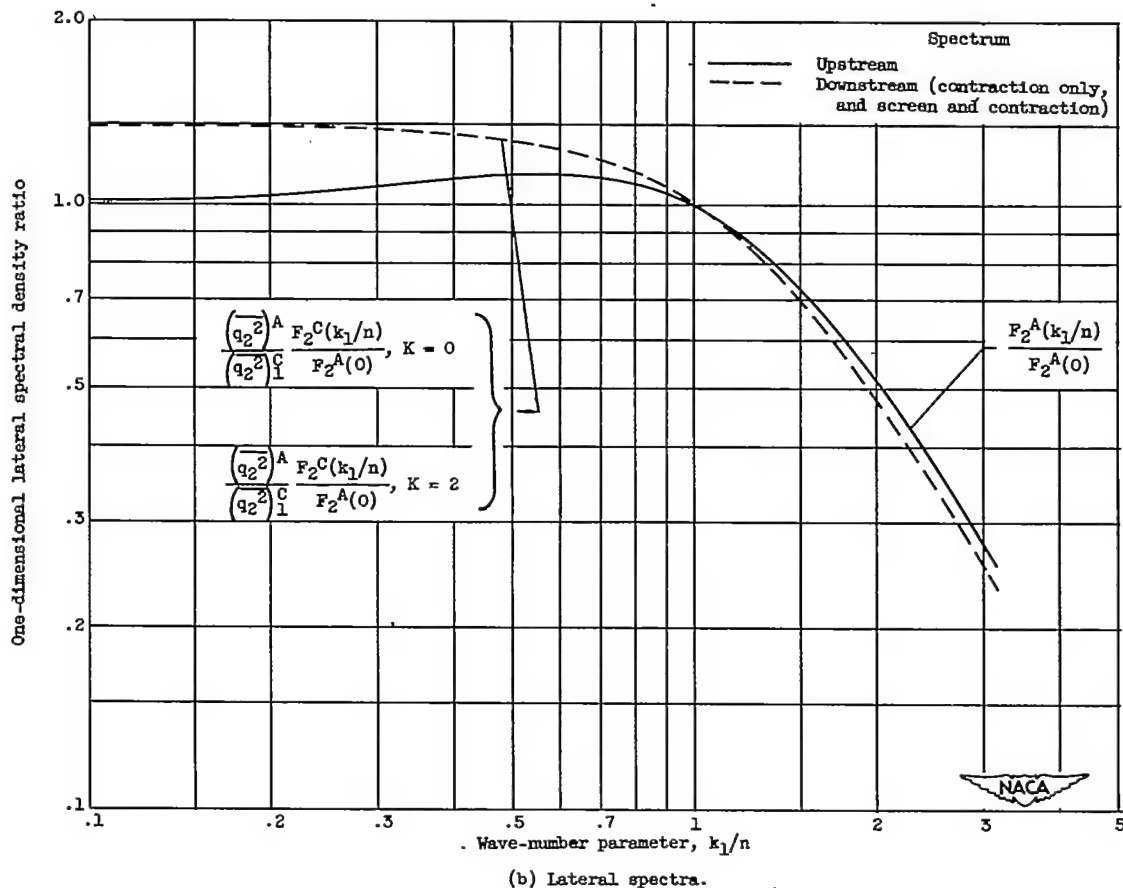


Figure 6. - Concluded. Comparison of one-dimensional spectra in absence of turbulence decay for contraction and for single-screen-contraction configurations for upstream isotropic turbulence having amplitude function $G(k) = H(k^2 + n^2)^{-3}$. M_B , 0.05; M_C , 2.00; l_1 , 29.822.

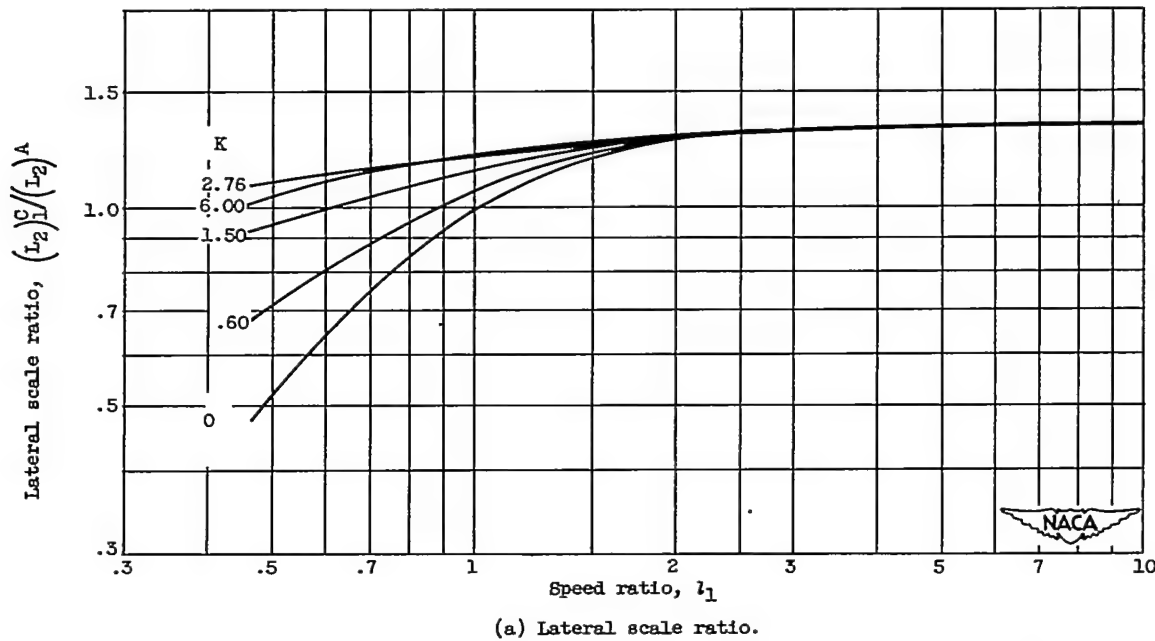


Figure 7. - Variation of scale ratio with speed ratio (M_B of 0.05) and screen pressure-drop coefficient K in absence of turbulence decay for single-screen-axisymmetric-contraction configurations with upstream isotropic turbulence.

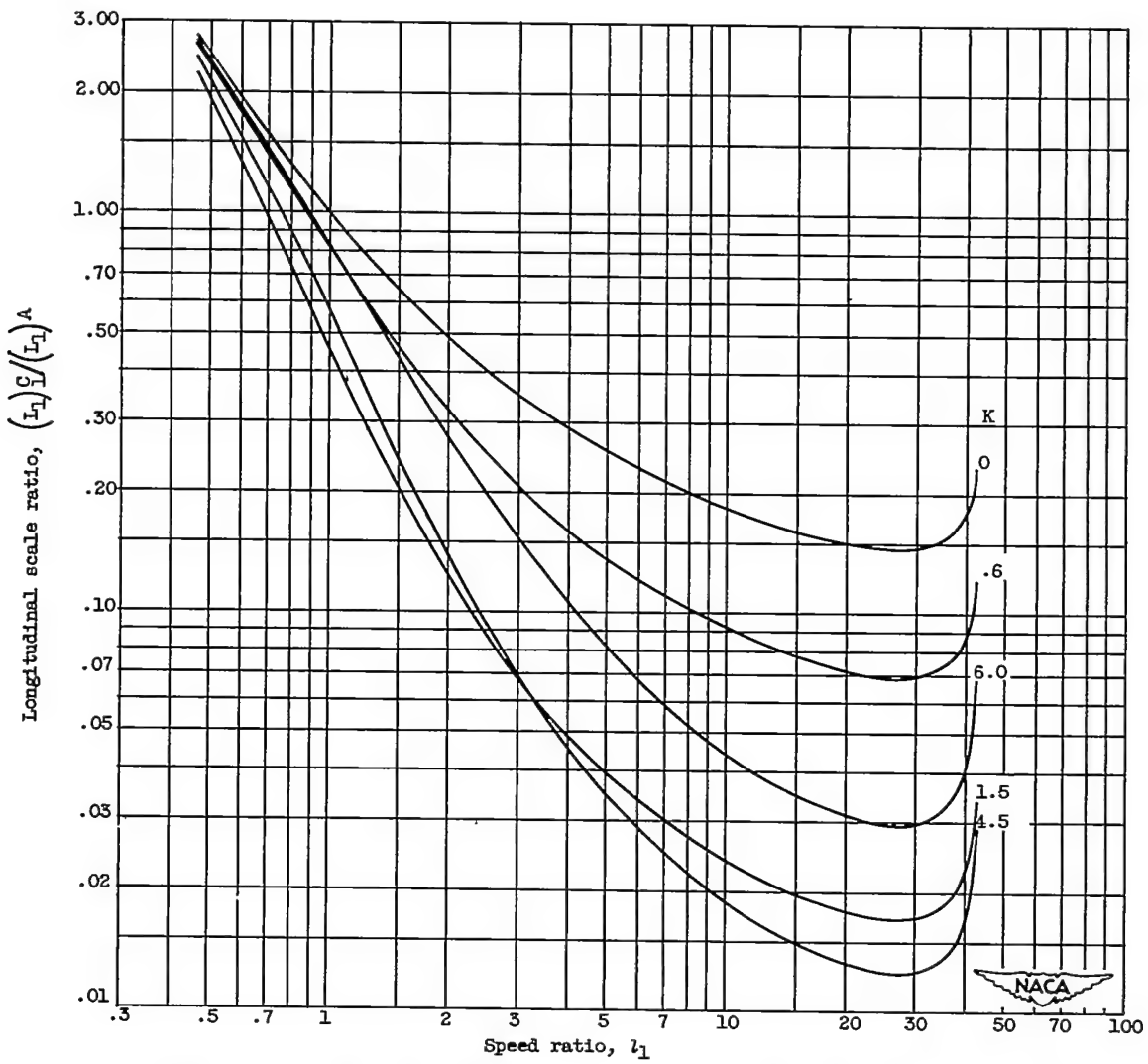
(b) Longitudinal scale ratio. Longitudinal scale ratio equals zero for $K = 2.76$.

Figure 7. - Concluded. Variation of scale ratio with speed ratio (M_B of 0.05) and screen pressure-drop coefficient K in absence of turbulence decay for single-screen-axisymmetric-contraction configurations with upstream isotropic turbulence.

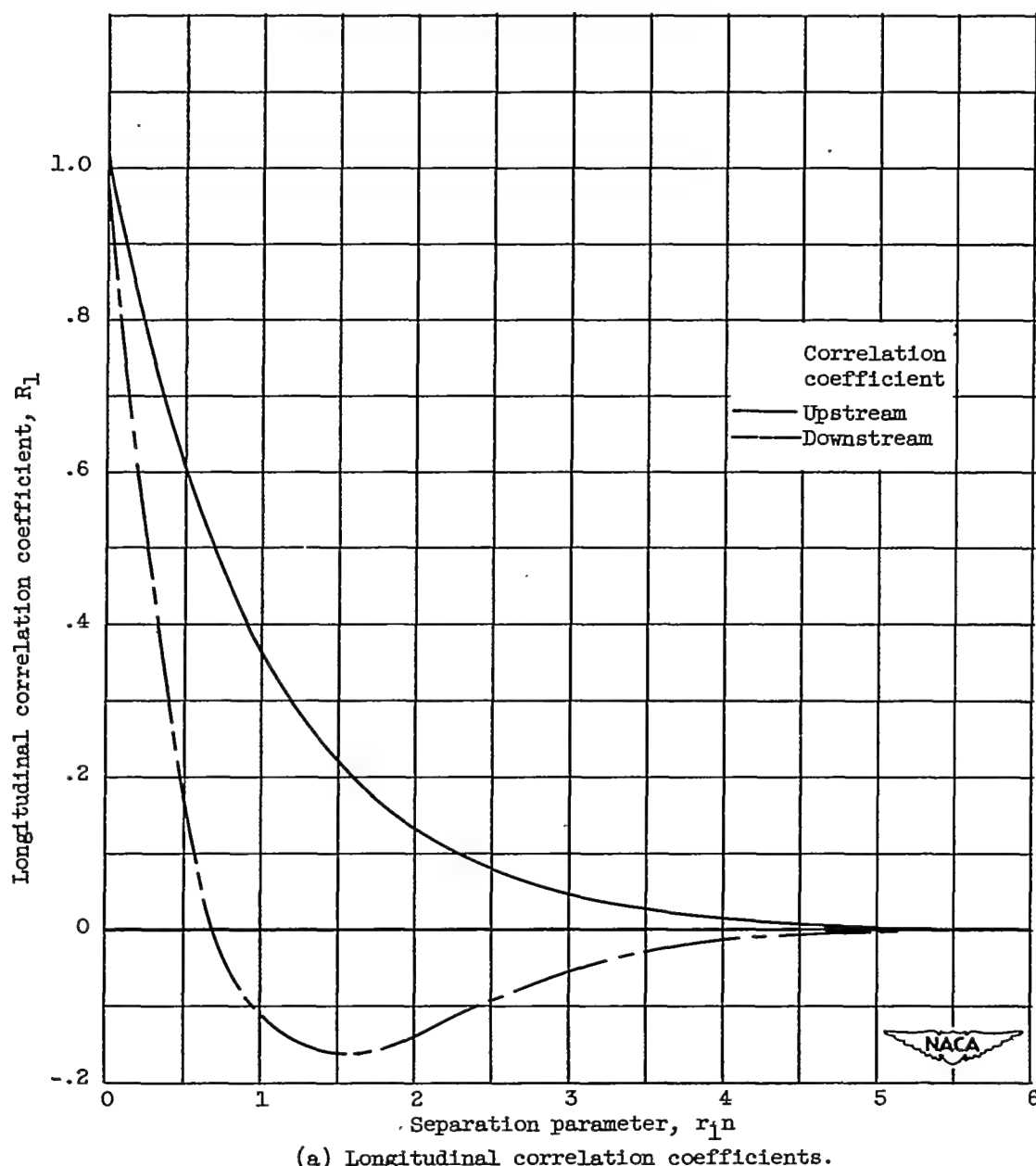
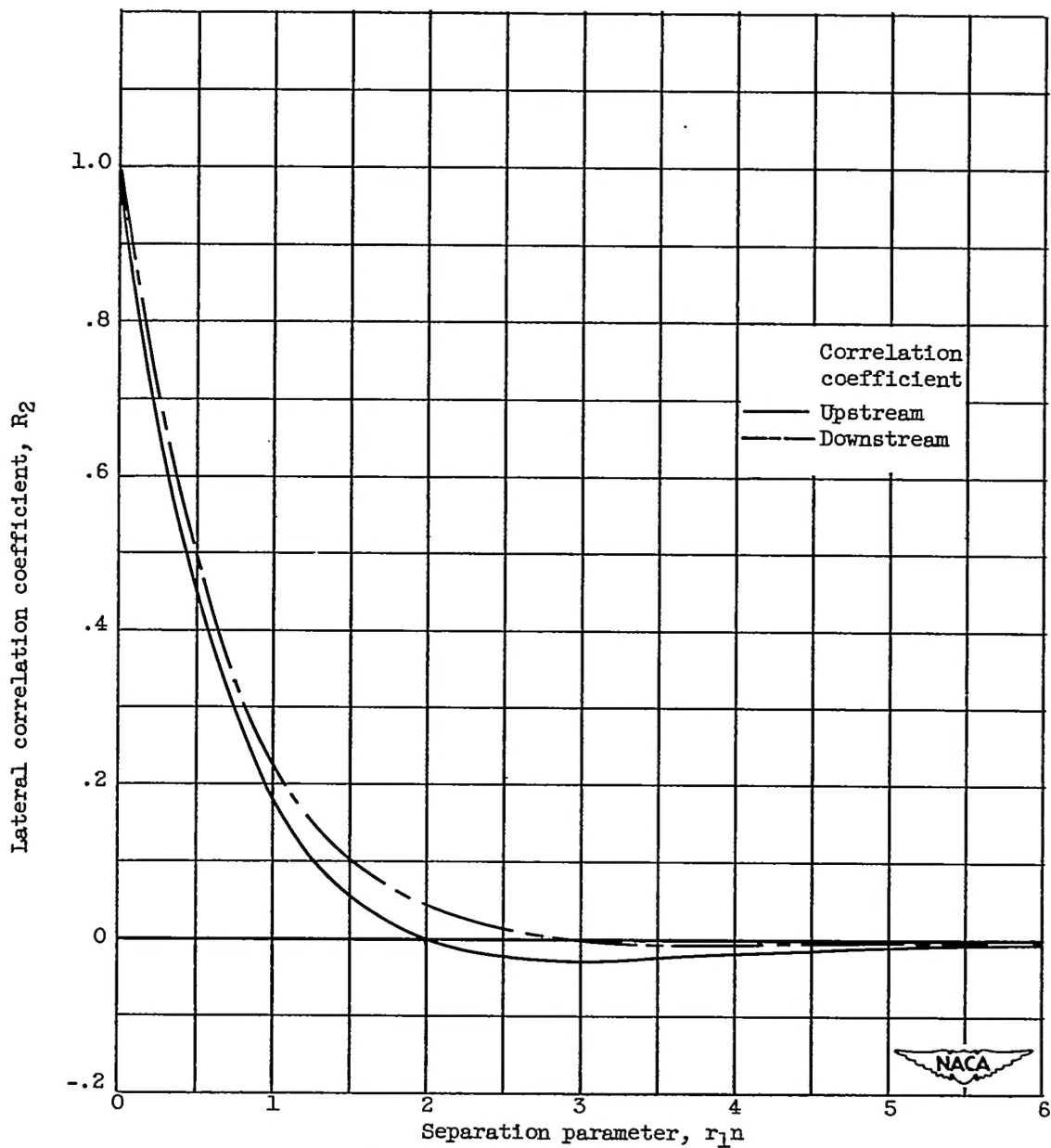


Figure 8. - Comparison of correlation coefficients in absence of decay for a screen-contraction configuration ($M_B = 0.05$, $M_C = 2.00$, $K = 2$, $N = 1$) with upstream isotropic turbulence having amplitude function $G(k) = H(k^2 + n^2)^{-3}$.



(b) Lateral correlation coefficients.

Figure 8. - Concluded. Comparison of correlation coefficients in absence of decay for a screen-contraction configuration ($M_B = 0.05$, $M_C = 2.00$, $K = 2$, $N = 1$) with upstream isotropic turbulence having amplitude function $G(k) = H(k^2 + n^2)^{-3}$.

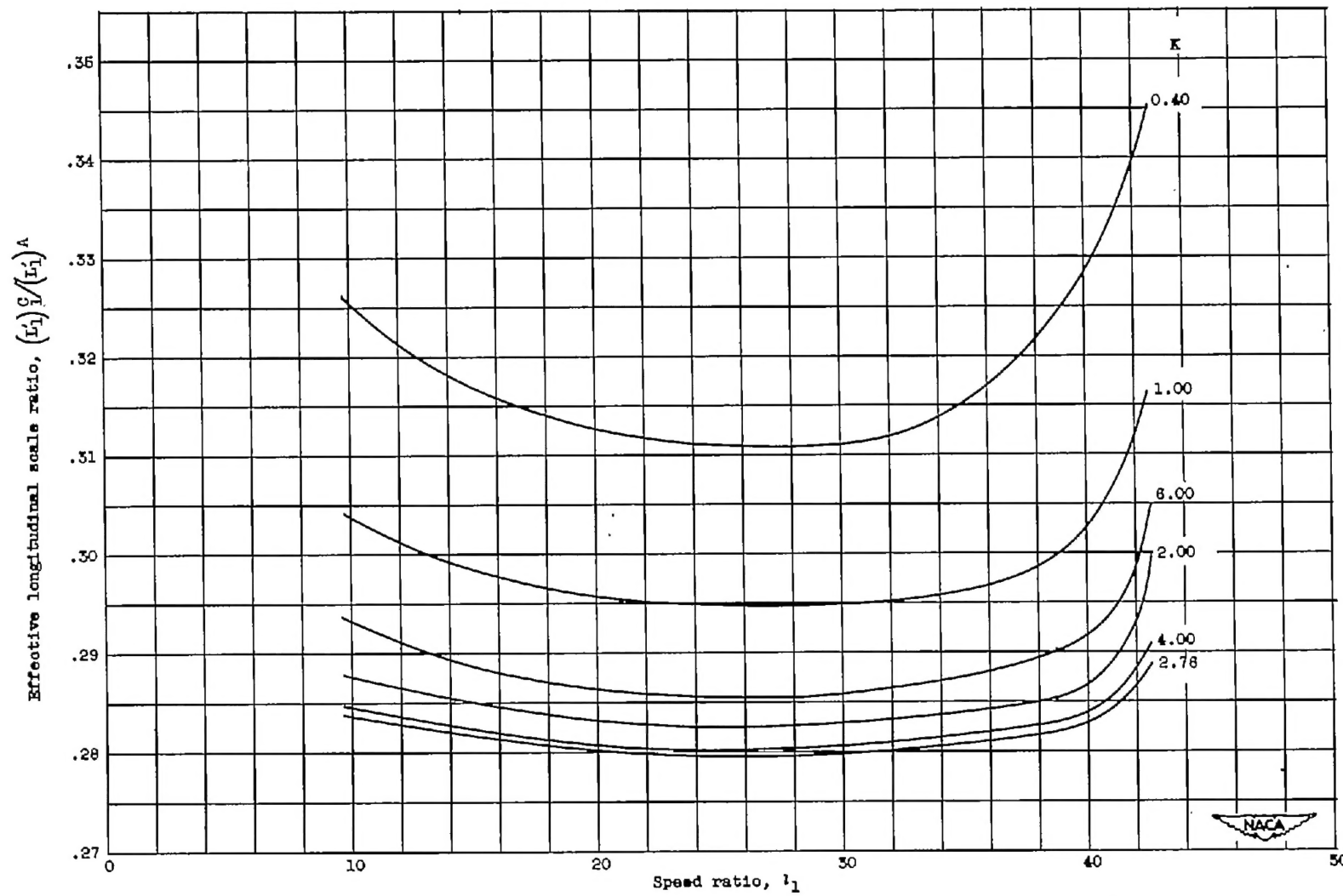


Figure 9. - Variation of effective longitudinal scale ratio in absence of turbulence decay with speed ratio (M_B of 0.05) and screen pressure-drop coefficient K for single-screen-axisymmetric-contraction configuration with upstream isotropic turbulence having amplitude function $G(k) = H(k^2 + n^2)^{-3}$.

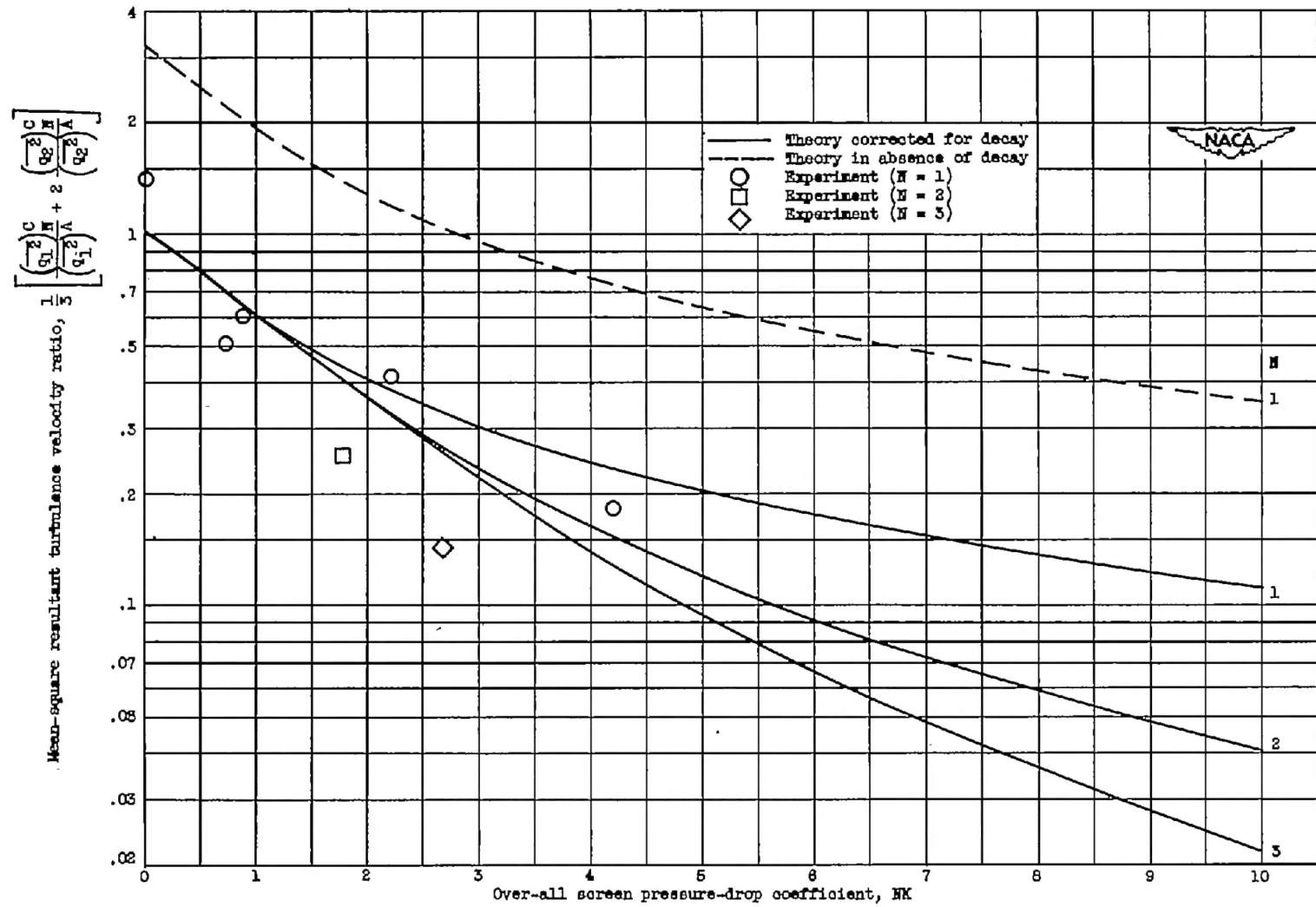


Figure 10. - Comparison of theoretical mean-square resultant turbulence velocity ratios corrected for decay with experiment of reference 1. Speed ratio $M_B = 0.06$, $M_C = 0.34$; M screens in series; upstream isotropic turbulence; scale L_2^A , 0.06 foot (estimated).

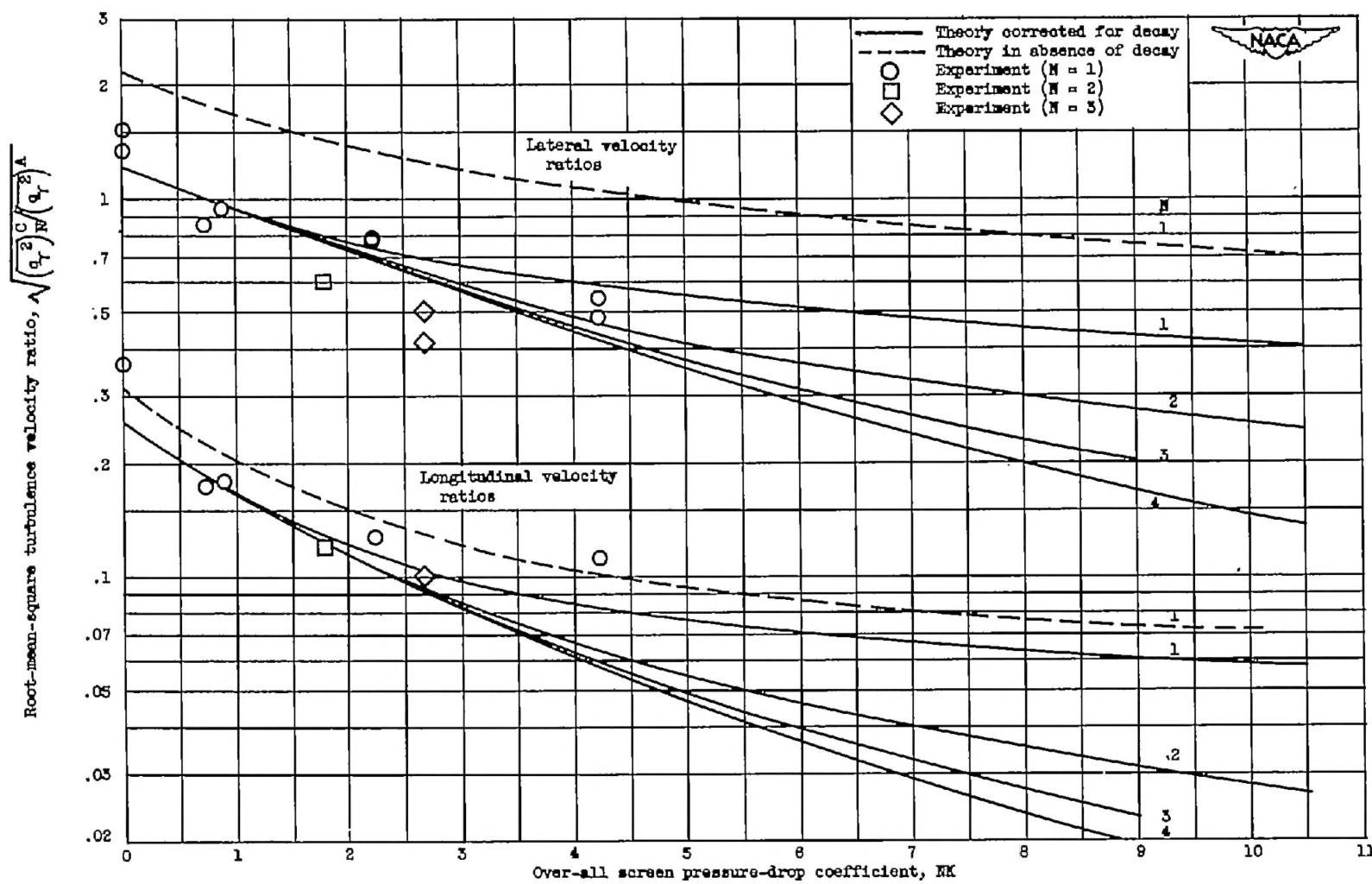


Figure 11. - Comparison of theoretical root-mean-square longitudinal and lateral turbulence velocity ratios corrected for decay with experiment of reference 1. Speed ratio l_1 , 8.7 ($M_B = 0.05$, $M_C = 0.34$); N screens in series; upstream isotropic turbulence; scale L_2^A , 0.05 foot (estimated).